Improving Airport Runway Braking Analysis through Innovative Modeling

by

Cheng Zhang

A thesis
presented to the University of Waterloo
in fulfillment of the
thesis requirement for the degree of
Master of Applied Science
in
Civil Engineering

Waterloo, Ontario, Canada, 2014

AUTHOR'S DECLARATION

I hereby declare that I am the sole author of this thesis. This is a true copy of the thesis, including any required final revisions, as accepted by my examiners.

I understand that my thesis may be made electronically available to the public.

Abstract

Landing excursion accidents have become a major concern over recent decades regarding airline and airport safety. Available runway friction has a significant impact on aircraft landing performance. This is especially noted when aircraft are landing on wet or otherwise contaminated runways due to the reduced braking action, which has been well documented since the dawn of the jet aircraft age. The objective of this thesis is to develop a tool to help make recommendations for airports that are subjected to diverse weather conditions.

In order to model an aircraft's real landing performance, a mechanistic-empirical aircraft deceleration equation was developed. This equation contains all of the major forces that contribute to aircraft braking, and is calibrated and validated using digital flight data from dry runway aircraft landings. Digital flight data from a Boeing 737-700, runway pavement condition monitoring data, and weather data was collected. Finally, a Boeing 737-700 case study was conducted.

As a result, it is able to back calculate the braking friction coefficient from the developed equation and evaluate the impact of wet and contaminated runways on aircraft braking performance. A study of a Boeing 737-700 aircraft landing performance on runways under different conditions was conducted.

A mechanistic-empirical landing distance model is established based on the mechanistic-empirical deceleration equation, in order to accurately calculate the required landing distance. When developing the landing distance model, the following characteristics are considered: pilot settings (TLA, spoiler position, and flap position configurations), aircraft operational characteristics (touchdown speed and weight), the runway friction condition, and aircraft braking system characteristics. A Boeing 737-700 real data case study was conducted and a comparison was made with the Boeing 737 Quick Reference Handbook reference landing distance. The results indicate the model offers an accurate prediction of aircraft landing distance.

Finally, future applications of this thesis are introduced. The potential of the development of a runway assessment, evaluation, and reporting framework was proposed. Opportunities of applying this thesis in on-board landing distance calculation, quick exit taxiway design and airport operation optimization, and fuel consumption reduction were presented. Moreover, the development of the Braking Availability Tester was discussed.

Acknowledgements

I first would like to express my sincere gratitude to my supervisor, Dr. Susan Tighe from the Civil and Environmental Engineering Department at the University of Waterloo. Her guidance, support, and motivation not only help me in pursuing my master study but also my future career as an engineer.

I would also like to express my sincere appreciation to Prof. Soo Jeon and Prof. HJ Kwon from the Mechanical and Mechatronics Engineering Department at the University of Waterloo for their valuable support in this project.

I would also acknowledge the data acquiring support of the WestJet Airline, Waterloo International Airport. I gratefully acknowledge Team Eagle of their great support. I enjoyed working in a wonderful environment with all these experienced leaders in aviation industry. Special thanks to Dave Roger, Currie Russell, Janine Maurice, Paul Cudmore, Steve McKeown, Arnie Beck, Peter Kleinschmidt, and Rick Thibodeau for comments and technical supports.

I would like to thank my colleagues in the CPATT the co-op students that participated in this research. Doubra Ambaiowei, Laura Bland, Mohab El-Hakim, Marcelo Gonzales, Amin Hamdi, Federico Irali, Gulfam Jannat, Aleks Kivi, Andrew Northmore, Aleli Osorio, Daniel Pickel, Sonia Rahman, Xiomara Sanchez, Magdy Shaheen, and Haolin Zhang, I would like to thank you all for your support, help, and collaboration in my research.

I would like to thank my family. Mom and dad, thank you for bringing me to this wonderful world and teaching me everything. Jingru, thank you for always standing by me. I love you all forever. I also would like to thank all my friends both in China and Canada for their support.

Dedication

To My Family

Table of Contents

List of Figures

List of Tables

List of Equations

Chapter 1
Introduction

1.1 Background

On April 12, 2007, a Pinnacle Airlines flight Bombardier/Canadair Regional Jet (CRJ) CL600-2B19 ran off the runway at Cherry Capital Airport during its landing. As a consequence, the forward lower fuselage, including the nose gear well area, was substantially damaged (NTSB, 2008). According to the National Transportation Safety Board (NTSB), the probable contributing factor to this accident was inefficient braking action due to a contaminated runway and the deteriorating weather (NTSB, 2008). The accident demonstrates the significance of runway braking performance analysis and prediction especially under severe runway conditions.

On December 8, 2005, a Southwest Airline Boeing 737-7H4 slid off the runway at the Chicago-Midway Airport during its landing in a snowstorm. The aircraft ran into an off-airport street after it rolled through a blast fence and an airport perimeter fence (NTSB, 2007). Finally, it stopped after hitting two cars, which resulted in a child being killed. One passenger in the vehicle was severely injured and three passengers in the vehicle along with 103 airplane occupants, including 2 pilots, received minor injuries. In addition, the airplane received considerable damage (NTSB, 2007). According to NTSB's investigation, one of the contributing reasons for this accident was that the on-board performance computer provided little safety margin for the landing distance. The accident report also indicated that the accident could have been prevented if the pilots had used maximum reverse thrust properly after touchdown and continued using the maximum reverse setting until the aircraft reached a full stop (NTSB, 2007). The accident and the investigation indicate that a variety of factors that affect aircraft stopping capability should be considered during landing distance prediction, including reverse thrust configurations.

"A runway excursion occurs when an aircraft on the runway surface leaves the end (overrun) or the side (veer-off) of the runway surface. Runway excursions can occur on takeoff or landing (Transport Canada, 2012)." Runway excursion has remained the most common accident/incident in the past few years. Figure 1.1 shows the percentage of runway excursion accidents of all accidents according to International Air Transport Association (IATA). It indicates runway excursions contribute to nearly a quarter of all the accidents and no trends show an obvious decrease (IATA, 2009; IATA, 2011; IATA, 2012a; IATA, 2012b). In addition, from 1998 to 2007, over half of the accidents, a third of the

fatal accidents, and nearly a quarter of all the fatalities happened in the aircraft landing phase, which takes approximately only 4% of the entire flight time on average (Xiaoyan, 2009). Landing overrun happens when an aircraft cannot stop before it reaches the end of the runway during landing (Transport Canada, 2012). It should be note that landing overrun is one of the most frequent accident/incident (Pasindu, Fwa, & Ong, 2011). The best way to prevent landing overrun is to better understand aircraft braking performance and accurately calculate landing distance, which are very significance for airport operators and airline pilots.

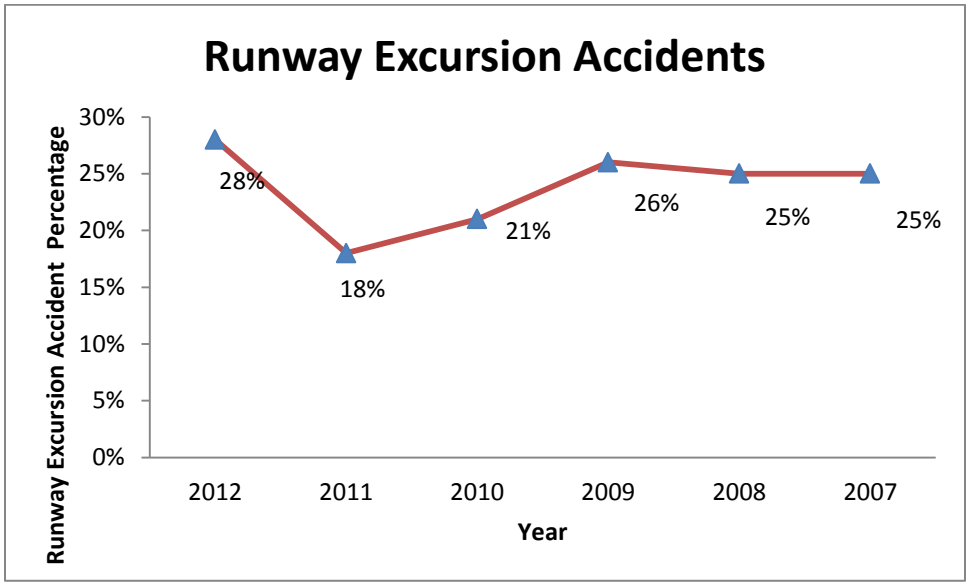

Figure 1.1 Runway Excursion Accidents

The digital flight data and runway condition monitoring data provide the opportunity to analyze the real-time performance of an aircraft during landing. With the help of such data, innovative modeling, which incorporates a variety of factors, should be conducted to have an in-depth insight into aircraft landing performance.

1.2 Scopes and Objectives

During aircraft landing, there are three portions: approach, flare, and braking. Approach distance starts from the runway threshold to the place where the initiation of flare happens; flare distance is the distance the aircraft travels during its flare segment; and braking distance is the distance the aircraft travels from when the braking application is applied to the place where the aircraft's speed reduces to a certain value to ensure a safe turnoff (Warren, Wahi, Amberg, Straub, & Attri, 1974). Braking

distance is the essential component of the entire landing distance among these three landing segments (Pasindu et al., 2011) and it also has the largest variance with different runway conditions. Therefore, this research will focus on modeling and analyzing aircraft braking on runway pavements under different conditions. The applicable airport runways of this research include all classes of civil or non-military airport runway, including international, regional, and local airports, with asphalt or concrete runway pavements.

The objectives of this thesis are:

- Study aircraft landing performance and build a mechanistic-empirical (M-E) aircraft deceleration equation;
- Analyze runway pavement braking performance, especially wet and contaminated runway pavement braking actions, based on the calibrated aircraft landing deceleration equation;
- Develop a landing distance model which can provide an accurate prediction of aircraft landing distance under different runway conditions to help airlines and airport operators mitigate the risk of runway overrun; and
- Propose future potential applications of the M-E aircraft deceleration equations and the M-E landing distance model to the aviation industry.

1.3 Methodology

The overall methodology of this thesis is shown in Figure 1.2. First, a literature review was conducted to identify aircraft landing distance influence factors. Based on aircraft landing distance influence factors, a M-E aircraft deceleration equation was built. This equation contains all of the essential contributing forces during aircraft braking and was calibrated using digital flight data from dry runway aircraft landings. With the help of this equation, evaluation of the impact of wet and contaminated runways on aircraft braking, regarding braking actions and limitations, was conducted. Based on the calibrated deceleration equation and aircraft braking system characteristics, a landing distance model was developed. This research was conducted by the University of Waterloo collaborating with WestJet Airline, Waterloo International Airport, and Team-Eagle. Digital flight data provided by a WestJet Boeing 737-700, runway pavement condition monitoring data from Waterloo International Airport, and weather data from the University Weather Station and Environment Canada were collected for this research. Finally, future applications, conclusions, and

recommendations regarding runway condition assessment and reporting were provided based on all the research findings.

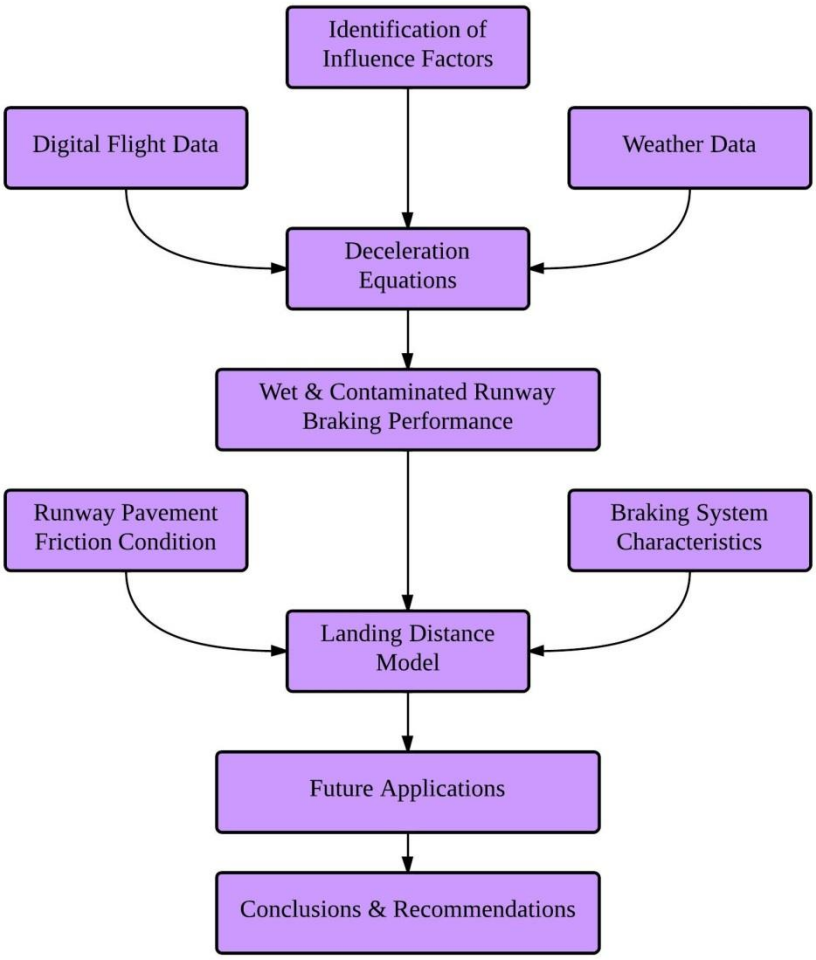

Figure 1.2 Research Methodology

1.4 Organization of This Thesis

This thesis consists of seven chapters, along with figures, equations and tables demonstrating the data and supporting the information.

Chapter 1 provides an overview of the entire research including a brief background, scope and objectives, the overall methodology, and the organization of the thesis.

Chapter 2 presents the literature review of this research and identifies the room for further improvement.

Chapter 3 presents the M-E aircraft deceleration equation including the development and a Boeing 737-700 case study.

Chapter 4 discusses aircraft braking performance under wet and contaminated runway conditions.

Chapter 5 presents the M-E landing distance model including the establishment of the model and a Boeing 737-700 case study.

Chapter 6 discusses the potential applications of the methods developed in this thesis.

Chapter 7 concludes current findings, highlights the major contributions of this research, provides some recommendations based on the research results, and discusses future work.

Chapter 2
Literature Review

In order to obtain a comprehensive understanding of airport runway braking performance, reviews of aircraft landing performance influence factors, pavement surface parameters, wet runways, contaminated runways, and aircraft landing distance calculations are conducted in this chapter. Furthermore, this chapter also provides a summary of current findings and the main gaps.

2.1 Landing Performance Influence Factors

There is a variety of influence factors, which have impacts on aircraft landing performance. In order to identify the influence factors, it is important to have an understanding of a good landing. According to Van Es (2005), a good landing has a stable approach in term of passing runway threshold at proper speed and height. After approach, the aircraft starts a flare without any rapid movements and ends by a positive touchdown without any floating. Braking actions including aerodynamic braking (spoilers, flaps, and reverse thrust if applicable) apply immediately after touchdown and remain stable (Van Es, 2005). During this process, the major landing performance influence factors from a civil engineering perspective are pavement surface characteristics, aircraft characteristics (influenced by aircraft tire type, inflation pressure, braking system, operation characteristics, etc.), environmental factors, and driving behavior of the pilots.

2.2 Pavement Surface Characteristics

2.2.1 Friction and Pavement Textures

Pavement friction is one of the most important pavement characteristics, which is related to pavement surface texture. “Pavement surface texture is defined as the deviations of the pavement surface from a true planar surface (Hall et al., 2009).” Based on the wavelength, the surface texture of a pavement can be categorized into three levels:

- Micro-texture (Wavelength<0.02 in);
- Macro-texture (Wavelength=0.02 to 2 in);
- Mega-texture (Wavelength=2 to 20 in); and

Wavelengths longer than 20 in are defined as roughness or unevenness (Hall et al., 2009).

Friction is mainly provided by micro-texture and macro-texture, which contribute to the adhesion friction and the hysteresis friction (Hall et al., 2009). The micro-texture is influenced by the aggregate mineralogy, the interaction with traffic and surrounding environment, and the pavement conditions (TAC, 2013). If the speed of the passing vehicle is low, the friction between the tires and the pavement surface is mainly produced by micro-texture. However, as the speed increases, the macro-texture contributes more to friction as well as water drainage (Hall et al., 2009).

2.2.2 Pavement Friction

Pavement friction evaluation or skid-resistant evaluation is often thought of primarily as safety insurance regarding airport pavement management and safe operations. It is necessary to assess a current existing pavement's skid-resistant capability of operating aircrafts with a variety of weights and aerodynamic performance. This is especially needed for runways with severe weather conditions. The friction evaluation of airport pavements is also a significant part of an airport pavement management system. With the help of friction evaluation for an existing pavement, decisions of maintenance or rehabilitation can be made. A lot of research has been done by different agencies and governments. Pavement evaluation methods of Transport Canada, Federal Aviation Administration (FAA), and International Civil Aviation Organization (ICAO) are introduced.

Transport Canada

All airports in Canada serving turbojet aircrafts are required to take friction measurements because of the high speed and weight landings (Transport Canada, 2004). The Surface Friction Tester (SFT) is selected as the standard friction measuring device determining the standard runway coefficient of friction. Friction measuring results from continuous friction measuring equipment (CFME) other than SFT are required to be correlated to comparable results obtained from SFT. The correlation should be done by the owners or operators of the non-standard friction devices. The frequency and timing of friction measurements should provide reliable information to take associated action specified in Table 2-1 and should be determined by the airport operators. Table 2-1 is made based on 9.4 of TP312 4th Edition, and all the Coefficient of Friction (COF) is based on the results from a SFT. Transport Canada aerodrome safety circular also provides the situation when the frequency should be increased and the test conditions (Transport Canada, 2004).

The aerodrome safety circular (2004) also demonstrates an example of friction testing using an alternative device—the GripTester. The GripTester is a lightweight trailer device. It can be carried by

passenger vehicles with a water supply tank, because of its relatively light weight and small size. An equation is built to correlate the GripTester results to SFT results. The correlation is identified by a series of parallel tests conducted by both GripTester and SFT (Transport Canada, 2004).

Table 2-1 Transport Canada Airfield Pavement Runway Friction Standards (Transport Canada, 2004)

Corrective Action To Restore Runway Surface Friction	Coefficient of Friction (COF) Numbers as Measured With a Surface Friction Tester
	When The "Runway Average COF" Is Less Than
Shall Be Planned	0.60
Shall Be Taken	0.50
	When A "Runway 100 Metre Section Average COF" Is Less Than
Shall Be Planned	0.50 (Treaded Tire) 0.40 (Smooth Tire)
Shall Be Taken	0.30

Federal Aviation Administration

The FAA has developed an advisory circular, AC-150-5320-12c, for airport pavement surface friction measurement, construction, and maintenance. In the circular, it defines the minimum friction survey frequency with a table, which is developed based on “an average mix of turbojet aircraft operating on any particular runway” (FAA, 1997). According to the number of “daily minimum turbojet aircraft landings per runway end”, the minimum frequency can be as high as once per week, and can be as low as yearly (FAA, 1997). It should be noted that the frequency should be adjusted if necessary due to the accumulated operations to ensure the airport operators have enough information to detect unsafe friction conditions and take corrective actions. Furthermore, an outline of survey without CFME is provided by the FAA. It points out that visual inspections are important to identify pavement drainage conditions, groove deteriorations, and structural deficiencies. The advisory circular also recommends visual checks and friction surveys during rainfalls (FAA, 1997).

The FAA developed a table of the standard friction values based on National Aeronautics and Space Administration (NASA)'s Wallops Flight Facility. Table 2-2 defines the three standard friction values: minimum operation friction coefficient, maintenance planning friction coefficient, and new designed or constructed friction coefficient. Different friction values measured by different FAA qualified CFME at the speed of 40 and 60 mph (65 and 95 km/h) for the three standard level are provided in Table 2-2 (FAA, 1997).

Table 2-2 Friction Level Classification for Runway Pavement Surfaces (FAA, 1997)

	40 mph			60 mph		
	Minimum	Maintenance Planning	New Design/ Construction	Minimum	Maintenance Planning	New Design/ Construction
Mu Meter	.42	.52	.72	.26	.38	.66
Dynatest Consulting, Inc. Runway Friction Tester	.50	.60	.82	.41	.54	.72
Airport Equipment Co. Skiddometer	.50	.60	.82	.34	.47	.74
Airport Surface Friction Tester	.50	.60	.82	.34	.47	.74
Airport Technology USA Safegate Friction Tester	.50	.60	.82	.34	.47	.74
Findlay, Irvine, Ltd. Griptester Friction Meter	.43	.53	.74	.24	.36	.64
Tatra Friction Tester	.48	.57	.76	.42	.52	.67
Norsemeter RUNAR (operated at fixed 16% slip)	.45	.52	.69	.32	.42	.63

International Civil Aviation Organization

ICAO Airport Services Manual Part 2 stipulates that the friction values should be measured and reported (ICAO, 2002). According to the recommendations of ICAO, existing runways, new designed runways and overlay runways should be tested by CFME, not only for the sake of consistency of all airports, but also for facility comparison. ICAO recommends six friction testers: Mu-meter Trailer, Skiddometer Trailer, Surface Friction Tester Vehicle, Runway Friction Tester Vehicle, TATRA Friction Tester Vehicle, and Griptester Trailer (ICAO, 2002). Similarly to FAA, ICAO defined three friction levels: a design level, a maintenance friction level, and a minimum friction level. A design level is the minimum friction a new constructed or resurfaced airport runway should have; a maintenance friction level is the boundary of whether maintenance should be done, and a minimum friction level is the minimum operating friction condition. The tests are also under the same speeds as

FAA regulations (65km/h and 95km/h). The associated information is shown in Table 2-3. The manual also points out that the friction condition varies due to the frequency of operations and rubber deposits, so the entire length of the runway should be measured (ICAO, 2002).

Table 2-3 Runway Surface Condition Levels (ICAO, 2002)

Test equipment	Test tire		Test speed (km/h)	Test water depth (mm)	Design objective for new surface	Maintenance planning level	Minimum friction level
	Type	Pressure (kPa)					
(1)	(2)		(3)	(4)	(5)	(6)	(7)
Mu-meter Trailer	A	70	65	1.0	0.72	0.52	0.42
	A	70	95	1.0	0.66	0.38	0.26
Skiddometer Trailer	B	210	65	1.0	0.82	0.60	0.50
	B	210	95	1.0	0.74	0.47	0.34
Surface Friction	B	210	65	1.0	0.82	0.60	0.50
Tester Vehicle	B	210	95	1.0	0.74	0.47	0.34
Runway Friction	B	210	65	1.0	0.82	0.60	0.50
Tester Vehicle	B	210	95	1.0	0.74	0.54	0.41
TATRA Friction	B	210	65	1.0	0.76	0.57	0.48
Tester Vehicle	B	210	95	1.0	0.67	0.52	0.42
RUNAR	B	210	65	1.0	0.69	0.52	0.45
Trailer	B	210	95	1.0	0.63	0.42	0.32
GRIPTESTER	C	140	65	1.0	0.74	0.53	0.43
Trailer	C	140	95	1.0	0.64	0.36	0.24

It should be noted that the FAA and ICAO have similar regulations about runway friction levels. Friction values are all provided with the given speed and type of the testing device. This is likely caused by the fact that under different speeds, the friction values are different and the different CFMEs have different testing results. For the same condition, the higher the speed is, the lower the friction test results are. In addition, when the speed increases, the variance of different devices' results increases.

2.2.3 Airport Pavement Condition Reporting

In order to provide reliable and consistent reporting of aircraft runway pavement, a uniform description of runway conditions has been developed in terms of estimated braking actions. Three levels are introduced: good, medium, and poor. It should be noted that, if good braking action is reported with the presence of snow or ice, the runway is not expected to be the same condition as a

clean dry runway; however, the runway surface should still provide enough friction for braking and directional control (ICAO, 2004).

Transport Canada requires airports in Canada, which operate turbo-jet-powered or turbo-propeller-powered aircrafts, to report a Canadian Runway Friction Index (CRFI). CRFI will be discussed later in this chapter (Transport Canada, 2014a).

Runways can be categorized by its surface condition as well. The following definitions are given by Transportation Canada (Transport Canada, 1999a).

- Contaminated Runway: "A contaminated runway has standing water, slush, snow, compacted snow, ice or frost covering more than 25% of the required length and width of its surface."
- Dry Runway: "A dry runway is neither 'wet' nor 'contaminated'."
- Wet Runway: "A wet runway is covered with sufficient moisture to cause it to appear reflective, but is not 'contaminated'."

2.3 Wet Runways

Studies on wet runway have been conducted since the 1960s. Walter B. Horne (1975) studied the influence that atmosphere, pavement, tire, aircraft, and pilot parameters combination have on aircraft stopping control under wet runway pavement conditions. He pointed out that the available tire/ground friction coefficient is the major factor that influences the stopping and directional control ability. The available tire/ground friction coefficient is a result of the combination of the depth of water present on the runway and the aircraft ground speed. He also pointed out that, for a wet runway, good runway interfacial drainage ability will result in an available tire-ground friction coefficient approaching that of a dry runway. However, high rainfall rate and/or poor runway interfacial drainage ability will result in a drastic drop in available tire-ground friction coefficient, especially when the aircraft is travelling at a high ground speed. The study also discussed hydroplaning and its influence factors, which will be discuss late in this chapter (Horne, 1975).

Transport Canada developed a report which aimed to summarize wet runway friction background information and the assessment of aircraft operations on wet runways (Comfort, 2001). The report points out that factors, such as speed, slip ratio, hydroplaning occurrences, water film depth, pavement texture, tire pressure, and the presence of contaminants, affect wet runway friction.

Comfort (2001) had the same theory as Horne (1975). He states that available tire-ground friction coefficient is the key factor that influences aircraft wet runway pavement performance, and the coefficient is determined by the runway water depth and tire-pavement drainage capability.

Since both studies have similar result, it is necessary to discuss all factors together (Comfort, 2001; Horne, 1975; Yager, 1983). As a result, Figure 2.1 presents a summary of factors affecting aircraft wet runway performance.

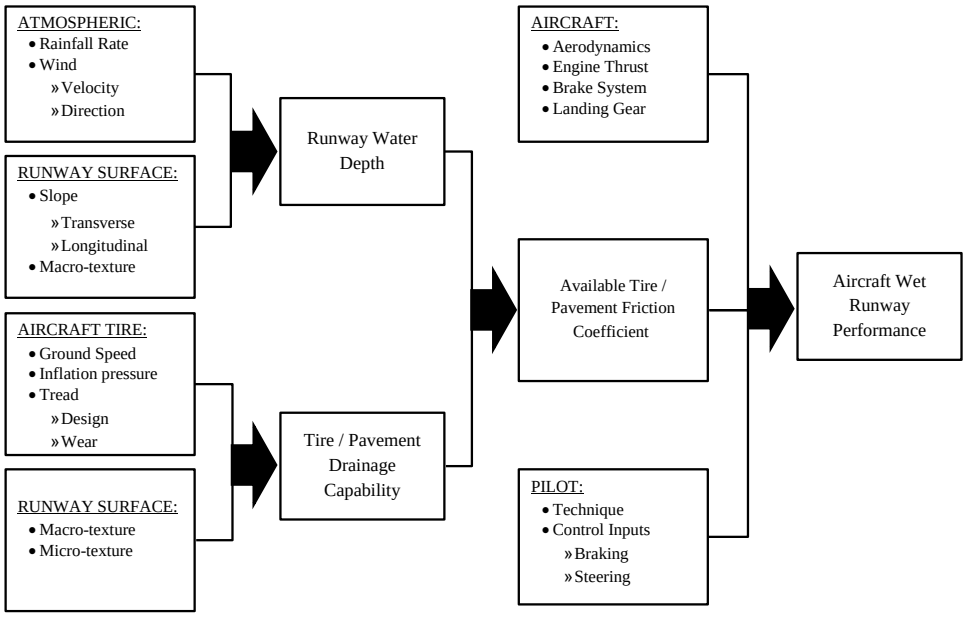

Figure 2.1 Factors Affecting Aircraft Wet Runway Performance (Comfort, 2001)

A study of SFT test results over time was also conducted by Comfort (2001). The long term friction observation indicates that the friction value decreases over time. In addition, it is found that the runway average friction coefficient and the low 100m section friction coefficient for large international airports are lower than that for smaller airports. The possible reason for this fact is that the large airports have more air traffic, which will result in a loss of texture, rubber deposits, and engine byproducts deposits. Studies on short time airport runway friction coefficient changes were conducted as well, which pointed out that friction coefficient can be greatly variable in a short time. Studies found that a rainfall can wash up the accumulated contaminants and dust on the runway (Transport Canada, 1989). The washing will result in an increase in friction value after the rainfall, and this increase can be up to 0.25. However, it should be noted that during the rainfall the friction coefficient will still decrease because of the wet condition, and the biggest drop in friction might

happen at the beginning of the rainfall if contaminants are built up on the runway surface (Comfort, 2001). Due to the variance in friction over time, real-time runway friction condition should be provided to the pilots to ensure safe aircraft ground operations.

2.3.1 Wet Runway Braking

The impacts of pavement texture on wet runway braking had been conducted in the 1960s by NASA (Leland, Yager, & Joyner, 1968) and antiskid braking system and aircraft tire-tread wear were also studied by NASA in 1960s to 1970s (Leland, 1965; Tanner & Stubbs, 1977).

The study by Leland, et al. (1968) pointed out that a reliable runway might provide insufficient friction for a landing when the runway surface is damp or flooded with water even if the runway can satisfy aircraft landing conditions when it is dry. Several influence factors play important roles in aircraft braking performance including the ground speed, the tire tread pattern types, the inflation pressure, the water depth, and the runway surface texture. Tests were done on different runways from smooth surface to rough surface using three different kinds of aircraft tires with different treads. The results indicated that four kinds of pavement: smooth concrete, textured concrete, small-aggregate asphalt, and large aggregated asphalt surfaces pavement have similar braking friction coefficients when the surface is dry. The damp surfaces were created by wetting the pavement with water and then removed all the standing water. With the presence of water, braking friction coefficients vary largely between different runway surfaces. Results showed that for the two asphalt pavements, approximately 25% drop in friction occurs; texture concrete pavement have a larger drop up to 50%; and there is a vast drop for smooth concrete pavement which results in a very poor braking friction coefficient lower than 0.1. Flooded runways (runways with a water depth of 0.25mm to 0.51mm) tests also illustrated that different pavement surfaces have different results under the same wet condition. For large-aggregate asphalt surface, the standing water caused a greatest decrease in friction. All the test speeds were under the hydroplaning speed, so it is assumed that hydroplaning did not occur. All results indicated that the braking friction coefficient decreases with the increase of the ground speed (Leland et al., 1968).

2.3.2 Hydroplaning

When a water film presents on the runway pavement surface, and a rolling tire passes along the water film, the tire squeezes the water. The water film generated hydrodynamic lift forces because of the squeezing. When the speed researches a critical speed, the hydrodynamic force lifts the aircraft and

separates the tire from the ground surface. There are two types of hydroplaning, viscous hydroplaning and dynamic hydroplaning (Van Es, 2001).

NASA Technical Note written by Walter Horne and Robert Dreber in 1963 (Horne & Dreher, 1963) investigated pneumatic tire hydroplaning. It indicates that the minimum hydroplaning speed (*Vp*) is mainly affected by the aircraft's tire inflation pressure. It also listed several other factors, such as landing-gear wheel arrangement, vertical load, and pavement surface characteristics; however, they all have negligible affects. A hydroplaning speed equation is developed as the result of the study, which is given as Equation (2-1) (Horne & Dreher, 1963).

$$V_p = 9\sqrt{p} \quad \textbf{(2-1)}$$

where: V_p is the hydroplaning speed in knots, and p is the tire inflation pressure in psi (Horne & Dreher, 1963).

With the research of hydroplaning went deeper, a study at the National Aerospace Laboratory (NLR) in the Netherlands, undertaken by Van Es (2001), pointed out that modern tires have lower hydroplaning speeds than previously assumed. The study focuses on different types of aircraft tires and compares the predicted hydroplaning speed with the NASA equation, and then provides a modified hydroplaning speed equation for modern aircraft tire (Van Es, 2001).

$$V_p = 6\sqrt{p} \quad \textbf{(2-2)}$$

where: V_p is the hydroplaning speed in knots, and p is the tire inflation pressure in psi (Van Es, 2001).

2.4 Contaminated Runways

Operating on contaminated runways is a critical safety concern for air transportation. After "the Munich Disaster" in 1958, which is regarded as the first major accident related to runway contaminants, its safety concern was realized. Since then, research on contaminated runways has been conducted and has continued. Although a vast amount of research has been done and published, contaminated runway accident/incident is still one of the most frequent air transportation accident/incident causes (Van Es, Roelen, Kruijsen, & Giesberts, 2001). In general, the presence of contaminants will reduce runway friction condition. Furthermore, different types of contaminants will have different impact on runway friction, and will be discussed later according to CRFI in this chapter.

2.4.1 Contaminated Runway Braking

Klein-Paste (2012) studied commercial aircraft braking performance during winter operations on contaminated runways. In his study, data from 24,928 landings at two airports in Norway during winter of 2008 to 2010 was collected for analysis. The Boeing Airplane Braking Performance Model is used to calculate the aircraft braking coefficient. Among all of the landings, 885 landings are found with limited stopping capability, which occupies 3.6% of all the observed data. Klein-Paste also studied the relationship between airplane braking coefficient and a variety of factors including the type of contaminants, the depth of contaminants, the spatial coverage, and the temperature. At Tromsø Airport, 67% of all the landings were operated under contaminated runways, and a significant high percentage (21.1%) of friction limited landings occurred. The possible reason for this high percentage is that aggressive braking was used due to the runway length. Findings regarding commercial airplanes braking coefficients of this research are summarized as follows (Klein-Paste et al., 2012):

- With the same or similar reported contaminated conditions, the aircraft braking coefficient can be dramatically variable. It is likely because the reported contaminated conditions only reflect the contaminated type, depth and spatial coverage, but many other factors also affect aircraft braking performance.
- Although a great variability exists, aircraft braking coefficient still depends on the type of contaminants and the spatial coverage. In general, runways with dry snow have a greater braking coefficient than wet snow.
- No significant correlation is found between the runway temperature and the average aircraft braking coefficient.

2.4.2 Canadian Runway Friction Index

In order to have a better understanding of runway friction and establish a universal means of defining runway friction, a Joint Winter Runway Friction Measurement Program (JWRFMP) was conditioned. Transport Canada and NASA started JWRFMP in 1995 with the cooperation of other North American and European organizations. An International Runway Friction Index (IRFI) was developed with the help of the American Society for Testing and Materials (ASTM) (Transport Canada, 1999b).

CRFI is developed under JWRFMP to expend the application of runway friction index in terms of aircraft landing distance prediction. Before the development of CRFI, James Brake Index (JBI) was

used in Canada which is based on the James Brake Decelerometer (JBD). In order to address the problems of the JBI, CRFI was developed and applied in Canada. CRFI is an index that refracts a runway's friction condition. A series of tables and charts are developed based on CRFI values and are used by Canadian airports to calculate the required landing distance (Croll, Bastuan, Martin, & Carson, 2002).

A total of eight aircrafts in six different types including a NRC Falcon 20, NASA B737 and B757, FAA and First Air B727, deHavilland and Nav Canada Dash 8, and a Fairchild Dornier DU328 turboprop, were used to collect braking data. Two hundreds seventy five full braking tests are conducted on runways with more than 70 contaminated conditions. With the testing data, a study of aircraft landing distance prediction has been conducted and CRFI Tables of Recommended Landing Distance were developed (Croll et al., 2002).

To measure CRFI, a decelerometer is mounted in a test vehicle measuring decelerating force with brake applied. The results of the decelerometer are evaluated from 0 to 1. During testing, the brakes on the testing vehicle are applied at 300m (1000ft) intervals along the runway centreline within 10m (30ft). The reason why testing is carried out at these location is that most of the aircrafts are operating at this given location. After the testing, an average number of testing results is reported as the CRFI. When CRFI equals to 1, it means the runway has an equivalent theoretical maximum decelerating capability as a dry runway, and 0 means the runway has an extremely slippery surface for decelerating. A CRFI of 0.8 or above is expected for a bare and dry runway. Table 2-4 and Table 2-5 are CRFI Tables of Recommended Landing Distance provided by Transport Canada. Table 2-4 is referred as CRFI Table 1, and Table 2-5 is referred as CRFI Table 2 (Transport Canada, 2014b).

CRFI recommended landing distances tables for reverse thrust landing and no reverse thrust landing are developed based on a 95 percent confidence level. It means that for 20 landings, 19 landing will be properly operated by using the recommended landing distances tables conservatively (Transport Canada, 2014b).

It should be noted that the recommended landing distance provided by Table 2-4 and Table 2-5 is the landing distance from approaching with standard pilot techniques (Transport Canada, 2014b). The recommended landing distance is based on "a stabilized approach at V_{ref} using a glideslope of 3° to 50ft or lower, a firm touchdown, minimum delay to nose lowering, minimum delay time to deployment of ground lift dump devices and application of brakes and discing and/or reverse thrust, and sustained maximum antiskid braking until stopped (Transport Canada, 2014b)".

Table 2-4 CRFI Table 1 (Transport Canada, 2014b)

Reported Canadian Runway Friction Index (CRFI)														
Landing Distance (Feet) Bare and Dry	0.60	0.55	0.50	0.45	0.40	0.35	0.30	0.27	0.25	0.22	0.20	0.18	Landing Field Length (Feet) Bare and Dry	Landing Field Length (Feet) Bare and Dry
Unfactored	Recommended Landing Distances (no Discing/Reverse Thrust)												60% Factor	70% Factor
1 800	3 120	3 200	3 300	3 410	3 540	3 700	3 900	4 040	4 150	4 330	4 470	4 620	3 000	2 571
2 000	3 480	3 580	3 690	3 830	3 980	4 170	4 410	4 570	4 700	4 910	5 070	5 250	3 333	2 857
2 200	3 720	3 830	3 960	4 110	4 280	4 500	4 750	4 940	5 080	5 310	5 490	5 700	3 667	3 143
2 400	4 100	4 230	4 370	4 540	4 740	4 980	5 260	5 470	5 620	5 880	6 080	6 300	4 000	3 429
2 600	4 450	4 590	4 750	4 940	5 160	5 420	5 740	5 960	6 130	6 410	6 630	6 870	4 333	3 714
2 800	4 760	4 910	5 090	5 290	5 530	5 810	6 150	6 390	6 570	6 880	7 110	7 360	4 667	4 000
3 000	5 070	5 240	5 430	5 650	5 910	6 220	6 590	6 860	7 060	7 390	7 640	7 920	5 000	4 286
3 200	5 450	5 630	5 840	6 090	6 370	6 720	7 130	7 420	7 640	8 010	8 290	8 600	5 333	4 571
3 400	5 740	5 940	6 170	6 430	6 740	7 110	7 550	7 870	8 100	8 500	8 800	9 130	5 667	4 857
3 600	6 050	6 260	6 500	6 780	7 120	7 510	7 990	8 330	8 580	9 000	9 320	9 680	6 000	5 143
3 800	6 340	6 570	6 830	7 130	7 480	7 900	8 410	8 770	9 040	9 490	9 840	10 220	6 333	5 429
4 000	6 550	6 780	7 050	7 370	7 730	8 170	8 700	9 080	9 360	9 830	10 180	10 580	6 667	5 714

Table 2-5 CRFI Table 2 (Transport Canada, 2014b)

Reported Canadian Runway Friction Index (CRFI)														
Landing Distance (Feet) Bare and Dry	0.60	0.55	0.50	0.45	0.40	0.35	0.30	0.27	0.25	0.22	0.20	0.18	Landing Field Length (Feet) Bare and Dry	Landing Field Length (Feet) Bare and Dry
Unfactored	Recommended Landing Distances (Discing/Reverse Thrust)												60% Factor	70% Factor
1 200	2 000	2 040	2 080	2 120	2 170	2 220	2 280	2 340	2 380	2 440	2 490	2 540	2 000	1 714
1 400	2 340	2 390	2 440	2 500	2 580	2 660	2 750	2 820	2 870	2 950	3 010	3 080	2 333	2 000
1 600	2 670	2 730	2 800	2 880	2 970	3 070	3 190	3 280	3 360	3 460	3 540	3 630	2 667	2 286
1 800	3 010	3 080	3 160	3 250	3 350	3 480	3 630	3 730	3 810	3 930	4 030	4 130	3 000	2 571
2 000	3 340	3 420	3 520	3 620	3 740	3 880	4 050	4 170	4 260	4 400	4 510	4 630	3 333	2 857
2 200	3 570	3 660	3 760	3 880	4 020	4 170	4 360	4 490	4 590	4 750	4 870	5 000	3 667	3 143
2 400	3 900	4 000	4 110	4 230	4 380	4 550	4 750	4 880	4 980	5 150	5 270	5 410	4 000	3 429
2 600	4 200	4 300	4 420	4 560	4 710	4 890	5 100	5 240	5 350	5 520	5 650	5 790	4 333	3 714
2 800	4 460	4 570	4 700	4 840	5 000	5 190	5 410	5 560	5 670	5 850	5 980	6 130	4 667	4 000
3 000	4 740	4 860	5 000	5 160	5 340	5 550	5 790	5 950	6 070	6 270	6 420	6 580	5 000	4 286
3 200	5 080	5 220	5 370	5 550	5 740	5 970	6 240	6 420	6 560	6 770	6 940	7 110	5 333	4 571
3 400	5 350	5 500	5 660	5 850	6 060	6 310	6 590	6 790	6 930	7 170	7 340	7 530	5 667	4 857
3 600	5 620	5 780	5 960	6 160	6 390	6 650	6 960	7 170	7 320	7 570	7 750	7 950	6 000	5 143
3 800	5 890	6 060	6 250	6 460	6 700	6 980	7 310	7 540	7 700	7 970	8 160	8 380	6 333	5 429
4 000	6 070	6 250	6 440	6 660	6 910	7 210	7 540	7 780	7 950	8 220	8 430	8 650	6 667	5 714

Headwind and crosswind are also considered when using the CRFI. Figure 2.2 provides the information to address crosswind and headwind with the vertical lines indicating the reported CRFI and its corresponding maximum crosswind. An example is demonstrated in Figure 2.2, which indicates a runway that has a wind heading 40 ° off the runway with a crosswind component of 13 knots requires a minimum CRFI of 0.35. Therefore, runways with a CRFI lower than 0.35 will lead to unstable directional control, uncontrollable drifting or yawing (Transport Canada, 2014b).

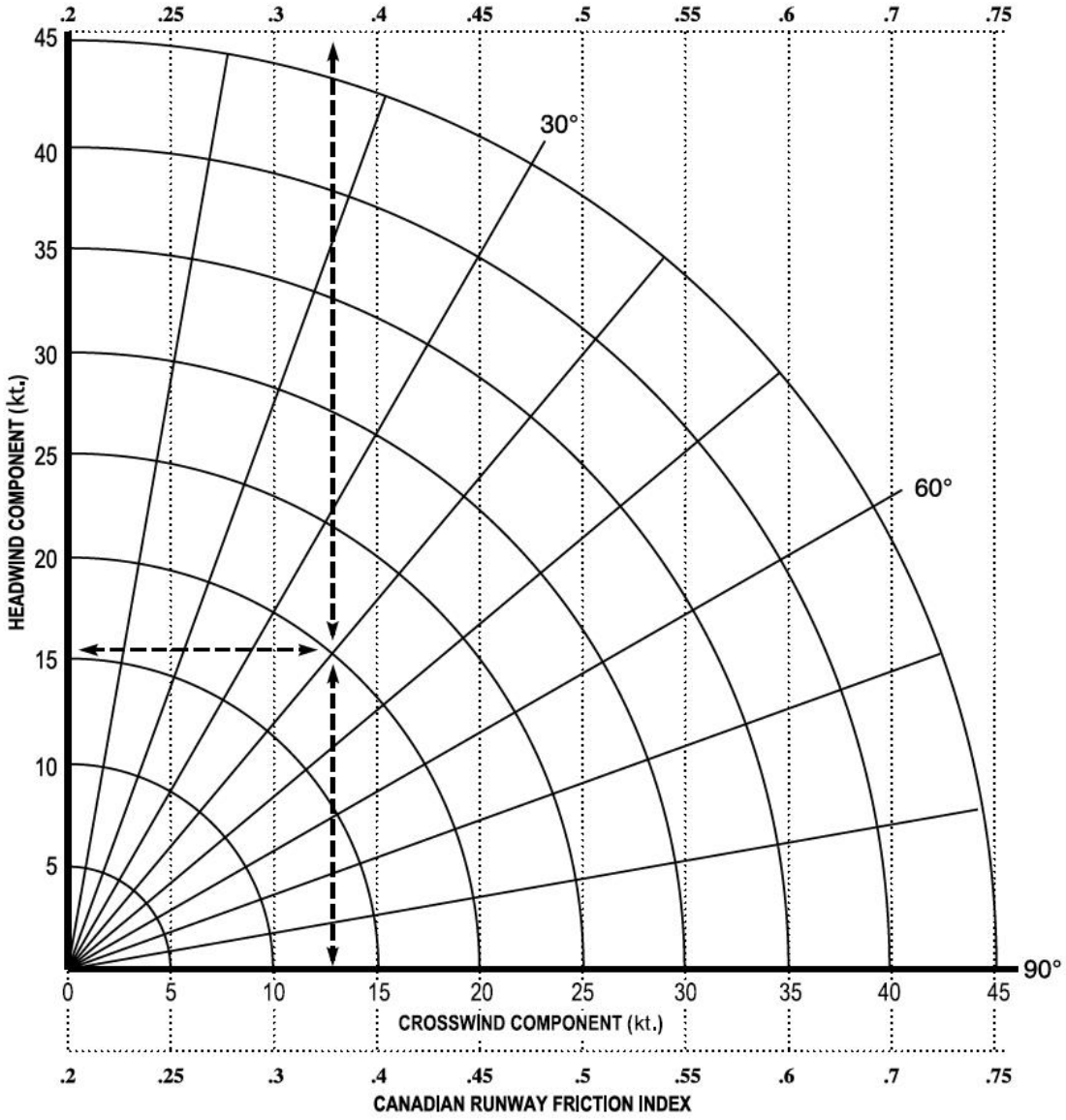

Figure 2.2 Crosswind Limits for CRFI (Transport Canada, 2014b)

Transport Canada also provides ranges of CRFI with different surface contaminated types. CRFI information for loose snow on packed snow, loose snow on ice, loose snow on pavement, sanded packed snow, bare packed snow, sanded ice, and bare ice are provided in Figure 2.3. According to Transport Canada, CRFI depends on surface type and have no correlation with surface temperature; however, an exception for melting point temperature exists, which will result in a water film and more severe slippery condition. It should be noted that the provided range of CRFI in Figure 2.3 is temperature independent (Transport Canada, 2014b).

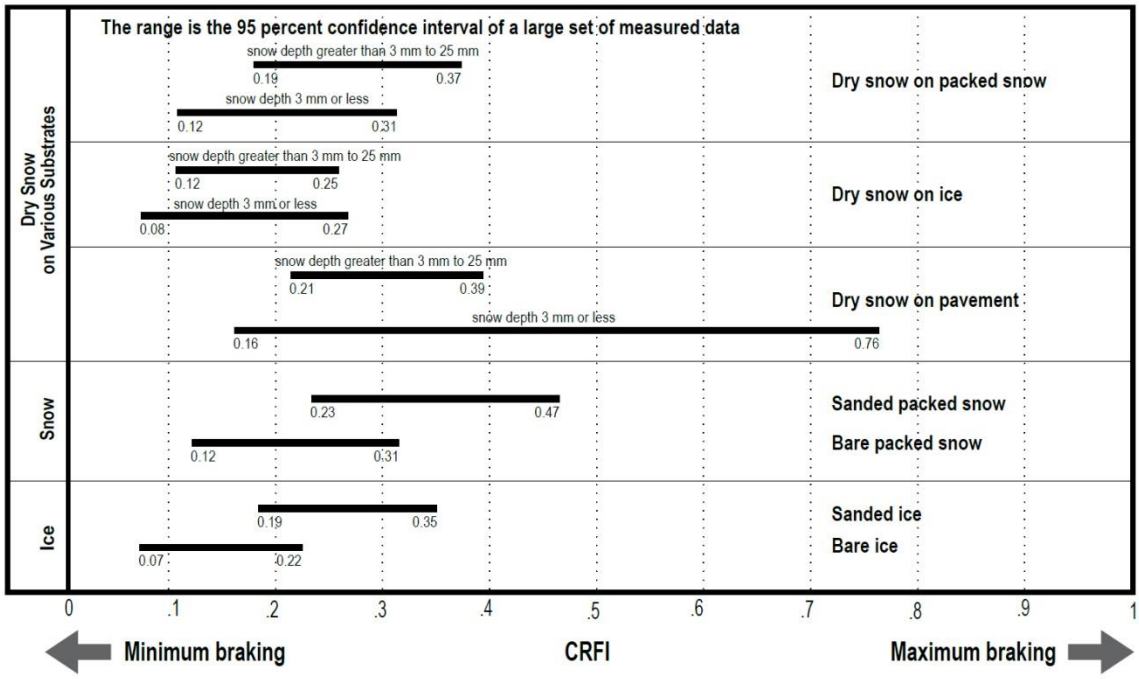

Figure 2.3 Expected Range of CRFI by Surface Type (Transport Canada, 2014b)

Figure 2.3 indicates that the majority of surface types have a CRFI range of approximately 0.2. However, the largest range of 0.6 occurs for dry snow on pavement with a depth of 3mm or less. This is likely related to the fact that a thin layer of snow is extremely non-uniform. Therefore, the CRFI can be as high as a value similar to a dry pavement and as low as packed snow (Transport Canada, 2014b).

The results show bare ice has the most severe condition followed by dry snow on ice. Thick layers of dry snow (snow depth greater than 3 mm to 25 mm) on packed snow and on pavement have similar CRFIs. This is likely related to the fact that the thick snow layer separates the tire and the support surfaces. Compared to a bare and dry condition with a CRFI of 0.8 or above, contaminated runways

have a much lower CRFI, which indicates that winter contaminants deteriorate runway braking performance significantly. Transport Canada also provides a minimum CRFI and a maximum CRFI for each condition, which is provided in Table 2-6 (Transport Canada, 2014b).

Table 2-6 Minimum and Maximum CRFIs for Various Surfaces (Transport Canada, 2014b)

SURFACE	LOWER CFRI LIMIT	UPPER CRFI LIMIT
Bare Ice	No Limit	0.3
Bare Packed Snow	0.1	0.4
Sanded Ice	0.1	0.4
Sanded Packed Snow	0.1	0.5
Dry Snow on Ice (depth 3 mm or less)	No Limit	0.4
Dry Snow on Ice (depth 3 to 25 mm)	No Limit	0.4
Dry Snow on Packed Snow (depth 3 mm or less)	0.1	0.4
Dry Snow on Packed Snow (depth 3 to 25 mm)	0.1	0.4
Dry Snow on Pavement (depth 3 mm or less)	0.1	Dry Pavement
Dry Snow on Pavement (depth 3 mm to 25 mm)	0.1	Dry Pavement

2.5 Landing Distance Calculation

Among the three landing distance portions, braking distance is the main component of the entire landing distance (Pasindu et al., 2011) and has the largest variance due to different weather and runway conditions. Landing distance studies have been done by aircraft manufacturers, government agencies, and researchers. In this thesis, Boeing landing distances chart, Airbus Runway Overrun Prevention System, CRFI, combat traction report, and several related researches are reviewed.

In order to provide pilots a reference of required landing distance, Boeing provides a landing distance chart for each type of aircraft. For example, the 737 Flight Crew Operations Manual-Quick Reference Handbook (737QRH) provides the Normal Configuration Landing Distances Chart (NCLDC) and the Non-Normal Configuration Landing Distances Chart. For normal configuration landing distance calculation, NCLDC considers landing distance influence factors including braking methods, weight, airport altitudes, runway slope, temperature, wind speed, velocity-reference, reverse thrust, flap configurations, and reported braking actions (The Boeing Company, 2013). However, reported braking actions are not well defined in the manual and may vary from different airport operators. In addition, conditions of no reverse thrust, one-engine reverse thrust, and two-engine reverse thrust are considered but the actual amount of reverse thrust applied is not considered. In order to calculate a more accurate required landing distance, braking actions need to be quantified and the actual amount of reverse thrust should be considered.

Airbus introduced its Runway Overrun Prevention System (ROPS) to reduce runway excursion risk on its fleet. ROPS calculates real-time aircraft landing distance and remaining landing distance during landing and compares them (Airbus, 2010; Chapman, 2013). However, ROPS is an option only available for some of Airbus aircrafts, which makes it an incomplete solution for airlines.

Transport Canada introduced the CRFI to evaluate runway pavement friction condition. Two tables of reference landing distances are developed based on CRFI, including a series of CRFI values to estimate the required landing distance. The CRFI-Table 1 is used when reverse thrust is not available and the CRFI-Table 2 is used when reverse thrust is applied. The CRFI method is mainly used for winter operations; therefore, the table was calibrated using winter aircraft landing data (Transport Canada, 2014b). However, the specific application requirement also becomes one of the main limitations of this method. To calculate the required landing distance, the CRFI method needs the required landing distance on dry pavement as a reference, which is not available if landing at an airport for the first time. Therefore, it is not applicable if the dry pavement landing distance is not provided as a reference. In addition, this approach only considers runway condition and reverse thrust (Transport Canada, 2014b). Other landing distance significant influence factors, such as touchdown speed, air density, aircraft weight, and aircraft aerodynamic configurations, should be considered.

In the Combat Traction Report developed by Boeing Commercial Airplane Company, NASA, United States Air Force, and FAA, two tasks are conducted: the identification of stopping distance significant influence factors and the development of a runway performance prediction method. The Boeing brake control simulator was used for the analysis. Five parameters were chosen: peak available ground friction, drag device effectiveness, braking application speed, air density, and engine idle thrust. By using Buckingham's π theorem, a prediction model is developed (Wahi, 1977; Warren et al., 1974).

$$(\pi_1) = C_\alpha(\pi_2)^{C_1}(\pi_3)^{C_2}, (\pi_4)^{C_3} \quad \textbf{(2-3)}$$

Where: $\pi_1 = sg/v^2$; $\pi_2 = \mu$; $\pi_3 = C_L/C_D$; $\pi_4 = \rho v^6/Feg^2$; s=braking stopping distance; g=acceleration caused by gravity (Warren et al., 1974)

The Combat Traction Report used 727-200, 737 advanced, 747-200, C-141A, and F-4E to calibrate the model. The aircraft models are not widely used in airlines nowadays and may differ from new jet aircrafts. Also, pilot settings are not considered in the Combat Traction Report (Wahi, 1977; Warren et al., 1974).

With the development of computer technology, finite element analysis has been used to calculate aircraft braking distance. Pasindu et al. (2011) did some studies on skid resistance evaluation based on finite element analysis. In their study, Skid Number is determined by the Finite Element Simulation Model to calculate the braking distance. However, reverse thrust is not studied, and the tire is assumed to be locked which is not the real scenario for modern jet aircraft which has an antiskid braking system.

Puvrez (1965) studied statistical information of several parameters including approach gradient, threshold height, threshold speed, touchdown speed, coefficient of braking friction, time of initiation of the controls, and aerodynamic drag to establish a distribution of landing distance (Puvrez, 1965). However, the established distribution of landing distance is for Short Take-Off and Landing (STOL) aircraft.

Van Es et al. (2010) from the National Aerospace Laboratory Air Transport Safety Institute developed a report which proposes several ground distance calculation methods and variants using actual landing data. However, the braking characteristics during ground roll including auto-brake settings, brake pressure, weather, and runway characteristics are not investigated and are recommended in future study (Van Es, Van der Geest, Cheng, & Hackler, 2010).

2.6 Summary

Landing performance influence factors and pavement surface parameters were reviewed in this chapter. Among all the parameters, runway friction is the key characteristic related to aircraft landing performance. A lot of research on airport pavement friction has been done by different government agencies. Pavement evaluation methods of Transport Canada, FAA, and ICAO are introduced in this thesis. The key findings are summarized as:

- Friction is the major factor that influences the stopping and directional control ability.
- Runway friction measurement results vary from different measuring devices.
- Runway friction is speed dependent. With the increase of the speed, the available maximum friction decreases.

Then, reviews on wet runways were conducted including wet runway influence factors, wet runway aircraft braking, and hydroplaning. The key findings are summarized as:

- Speed, slip ratio, hydroplaning, water film depth, pavement texture, tire pressure, and the presence of contaminants have impacts on wet runway friction.
- Friction coefficient can be greatly variable in a short time due to rainfall and presence of contaminants.
- With the presence of water, braking friction coefficients vary largely between different runway surfaces.
- Even if a runway is able to provide friction support for aircraft landing when it is dry, the runway might provide insufficient friction when the runway surface is damp or flooded with water.
- Hydroplaning speed is a function of tire inflation pressure, and equation for modern aircraft tires has been identified.

Relative information on contaminated runways is discussed regarding contaminated runway braking and the Canadian state-of-art practice of the CRFI. The key findings are summarized as:

- Winter contaminants have a significant influence on runway braking performance.
- For the same or similar reported contaminated condition, the CRFIs can be in a wide range.
- Friction coefficient varies greatly if measured with different measuring devices.

Landing distance calculation methods including manufacturer recommendations, government agency reports, and other research from different institutions have been discussed. The key findings are summarized as:

- The current landing distance calculation methods are not universally applicable.
- The current landing distance calculation methods do not consider an accurate amount of reverse thrust and pilot settings.

According to the findings of past studies, the gaps in the current aviation industry regarding runway braking performance are summarized as follows:

- A tool that evaluates runway friction based on aircraft measurements. Since runway friction measurement results vary from one CFME device to another and differ from

different speeds, a method that can evaluate runway friction based on aircraft measurement is required to provide a uniform evaluation.

- An evaluation method of aircraft braking performance on wet and contaminated runways using digital flight data. Runway friction can be very variable for wet and contaminated runway and most of the analysis is based on CFME results. Therefore, an analysis of aircraft braking performance based on flight data is needed.
- An aircraft landing distance calculation method which considers a variety of influence factors. According to the review of current landing distance calculations, it should be noted that a study of landing distance prediction method which integrates pilot settings, an accurate amount of reverse thrust, antiskid braking system performance, and provides a wide application of aircrafts and airport runways is missing from the body of existing research.

Chapter 3
Mechanistic-Empirical Aircraft Deceleration Equation

An M-E aircraft deceleration equation is established in this chapter with the overall purpose of creating a tool that models aircraft landing performance based on aircraft measurements. A Boeing 737 case study is conducted, and the associated validation result for each flight is provided in Appendix A.

This chapter is based on a paper peer-reviewed by Transportation Research Board and presented at the 94th Transportation Research Board Annual Meeting, Washington D.C., U.S.A., 12-16 January, 2014 (Zhang, Tighe, Jeon, & Kwon, 2014).

3.1 Methodology

The overall methodology used in developing the M-E deceleration equation is provided in Figure 3.1. First, an aircraft force and moment analysis was conducted. The force and moment analysis contains major factors that contribute to deceleration during aircraft braking. Then, based on the analysis, the mechanistic deceleration equation for each kind of force is identified. Finally, an entire aircraft deceleration was built by combining all the mechanistic deceleration equations. In the entire aircraft deceleration equation, there is an aircraft characteristic adjustment coefficient for each force. They were calibrated by regression using 75% of the data. After calibration, the equation was validated using the rest of the data.

3.2 Identification of Influence Factors

Figure 3.2 depicts the free body diagram of an aircraft during landing (not to scale) (Zhang et al., 2014). Aircrafts use a combination of aerodynamic braking and runway surface braking to reduce their speed. Due to the high touchdown speed and the application of spoilers and flaps, aerodynamic drag force is critical in modeling aircraft landing. Reverse thrust is another significant and typical method to help aircraft decelerate. Runway surface friction is essential for aircraft landings. Finally, the slope of the runway also contributes, positively or negatively, to aircraft deceleration due to gravity.

In summary, four forces are the major deceleration factors: aerodynamic drag force, engine thrust/reverse thrust, friction force, and the parallel component of gravity generated by the slope of the runway.

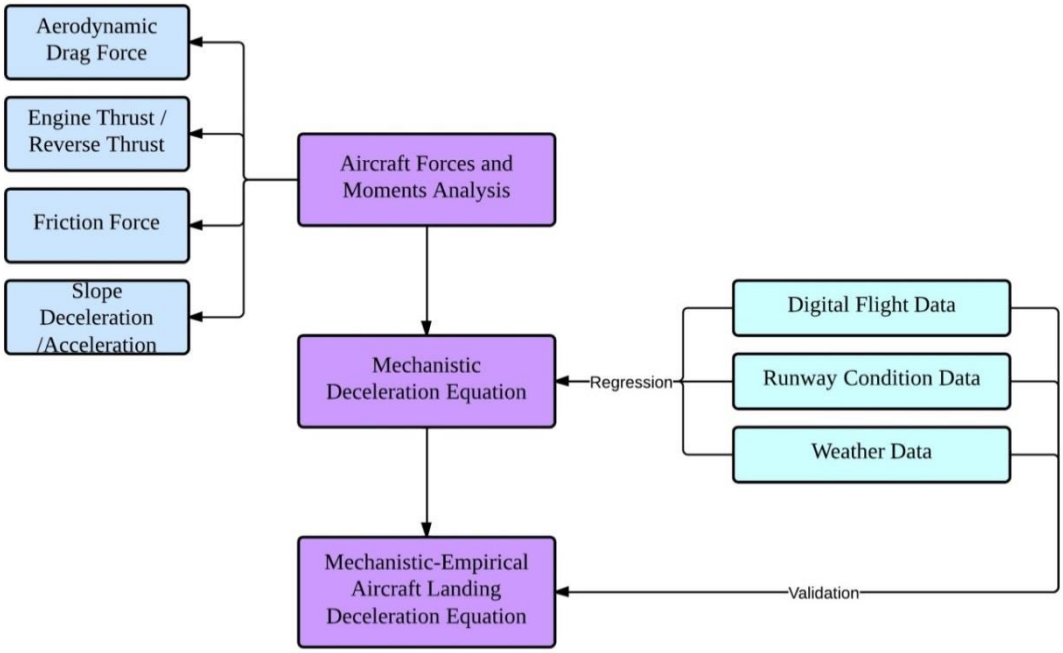

Figure 3.1 Deceleration Equation Methodology

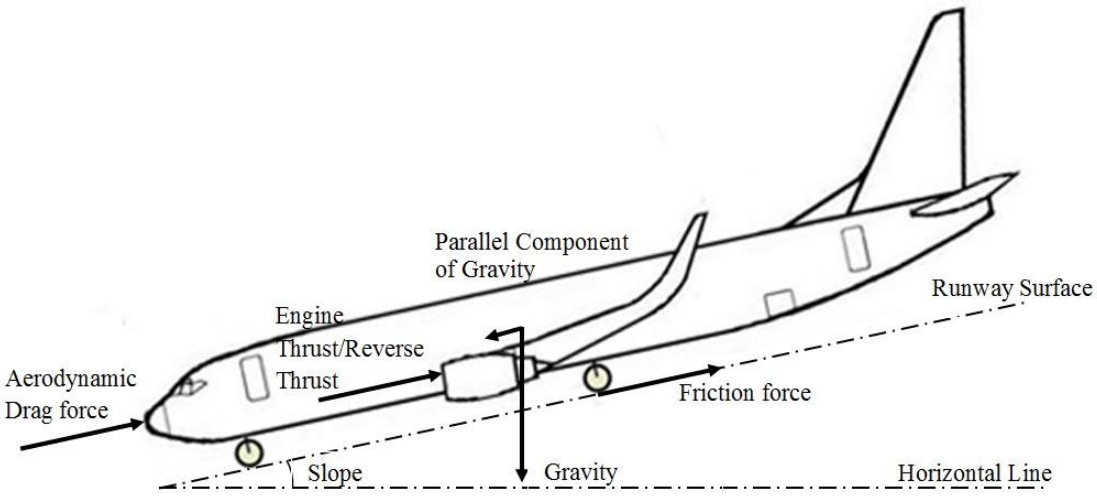

Figure 3.2 Aircraft Forces and Moments (Zhang et al., 2014)

According to the force balance, the entire aircraft force equation can be described as:

$$ma = D + T + F + S \quad \textbf{(3-1)}$$

where:

m: The weight of the aircraft, kg;

a: The deceleration/acceleration of the aircraft, m/s^2;

D: Aerodynamic drag force, N;

T: Thrust/reverse thrust, N;

F: Friction force, N; and

S: Component of gravity parallel to the runway, N.

3.3 Deceleration Equations

3.3.1 Aerodynamic Drag Force Equation

The generation of the aerodynamic drag force is caused by the pressure distribution and shear stress distribution on the body of the aircraft. According to an analysis based on physic principles, the aircraft aerodynamic drag force is a function of the air density, the aircraft wing area, the aircraft velocity in the freestream, and the aerodynamic drag coefficient (Anderson, 2001). The aerodynamic drag force coefficient varies from one given geometric body shape to another. The flaps and spoilers change the geometric body shape of the aircraft, which changes the aerodynamic drag force coefficient. The aerodynamic drag force equation is given as:

$$D = \frac{1}{2}\rho_{air} S_{wing} V^2 C_{Dg} \quad \textbf{(3-2)}$$

where:

ρ_{air}: Air density, kg/m^3;

S_{wing}: The aircraft reference area, m^2;

V: Aircraft velocity in the freestream, m/s; and

C_{Dg}: The drag coefficient of the aircraft (Anderson, 2001).

3.3.2 Engine Thrust/Reverse Thrust Equations

The engine generates thrust and reverse thrust to control the longitudinal velocity during landing. Furthermore, the engine thrust and reverse thrust are controlled by the thrust lever that is identified as its indicated angle setting, which is referred to as the Thrust Lever Angle (TLA). The thrust or reverse thrust in use (PT) can be reflected by TLA, and the relationship can be simplified as linear (Shepler, 2010). The relative equations are identified as Equation (3-3) and (3-4). The percent thrust in use and the TLA relationship is determined by regression using digital flight data.

$$PT = f(TLA) = \eta \cdot TLA + \theta \quad \textbf{(3-3)}$$

$$T = \alpha \cdot PT = \alpha \cdot f(TLA) \quad \textbf{(3-4)}$$

where:

α: Thrust force coefficient;

T: Thrust, kN;

PT: Percent thrust in use, %; and

η, θ: Percent thrust in use and TLA relationship coefficient (Zhang et al., 2014).

3.3.3 Friction Force Equations

The friction force is generated by the interaction between a rolling pneumatic tire and the runway pavement surface when braking is applied. The friction force consists of two parts: the rolling resistance force and the braking slip force (Hall et al., 2009). The friction force is controlled by the braking pressure applied which is an output of the aircraft braking system. In this study, it is assumed that the deformation of the pneumatic tire is always symmetric. As a result, during aircraft braking, landing gears have braking force, rolling resistance force, braking slip force, ground force, and gravity. The forces and moments of a landing gear wheel during braking are shown in Figure 3.3.

The analysis indicates that the total friction force (rolling resistance force and braking slip force) is a linear function of the applied braking pressure (Zhang et al., 2014).

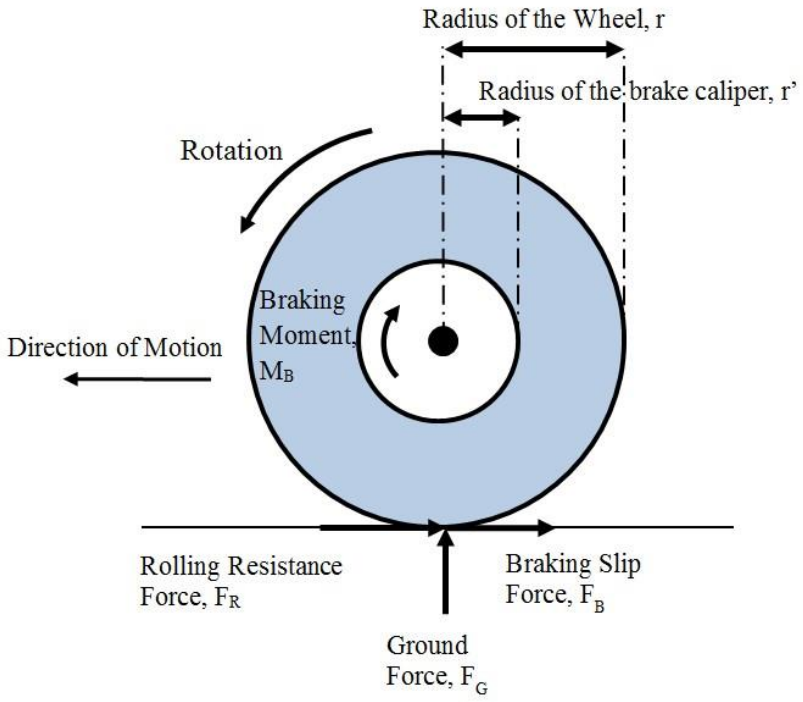

Figure 3.3 A Braked Wheel on A Bare and Dry Pavement (Andresen & Wambold, 1999)

$$M_B - F_B \cdot r - F_R \cdot r = 0 \quad \textbf{(3-5)}$$

$$M_B = \int_o^{r'} \mu \cdot BP \cdot 2\pi r \cdot r \cdot dr = \frac{4\pi r'^3}{3} BP \quad \textbf{(3-6)}$$

$$F = F_B + F_R = \frac{M_B}{r} = \frac{4\pi r'^3}{3r} BP \quad \textbf{(3-7)}$$

where:

M_B: Braking moment, N·m;

BP: Braking pressure, kPa;

r: The radius of the landing gear wheel, m;

r': The radius of the brake caliper, m;

μ: The friction coefficient of the brake caliper;

F: Total friction force

F_B: Braking slip force, N;

F_R: Rolling resistance force, N; and

F_G: Ground force, N (Zhang et al., 2014).

3.3.4 Slope Deceleration/Acceleration Equation

According to Figure 3.2, a component of gravity that is parallel to the runway pavement surface generated by the slope of the runway also has an impaction, positively or negatively, on aircraft decelerating. The force for this component of gravity is given as:

$$S = mg \cdot \sin\varphi \tag{3-8}$$

where:

φ: The slope of the runway, degree.

3.3.5 Deceleration Equations Calibration

According to Equation (3-1) to (3-8), the variables are: the TLA for each engine, the braking pressure, the velocity, and the air density; other than these, the values are constant. The values of the aircraft wing area, the drag coefficient of the aircraft, the radius of the landing gear wheel, the friction coefficient of the brake caliper, and the radius of the brake caliper differ from one aircraft to another. For a given flap and spoiler configurations, the aerodynamic drag force is a function of air density, square of velocity, and an aircraft aerodynamic drag force adjustment coefficient. Flap and spoiler configurations affect the body shape of the aircraft, resulting in a difference in pressure distribution and shear stress distribution. Therefore, the aircraft aerodynamic drag force adjustment coefficient varies in different configurations and should be calibrated according to different flap and spoiler configurations respectively. According to Equation (3-4), engine thrust and reverse thrust force for each engine is identified as a function of TLA and aircraft engine thrust/reverse thrust adjustment coefficients. According to Equation (3-7), the friction force is described as a function of braking pressure and an aircraft friction force adjustment coefficient. The aircraft friction force adjustment coefficient should be determined for each landing gear braking caliper, respectively.

$$\begin{cases} D = a_1 \cdot \rho_{air} V^2 \\ T = a_2 \cdot [f(TLA_1) + \cdots + f(TLA_{nE})] \\ F = a_{3_1} \cdot BP_1 + \cdots + a_{3_{nW}} \cdot BP_n \end{cases} \tag{3-9}$$

$$a = a_1 \cdot \frac{\rho_{air} V^2}{m} + a_2 \left\{ \frac{f(TLA_1)}{m} + \cdots + \frac{f\left(TLA_{n_E}\right)}{m} \right\} + \left\{ a_{3_1} \cdot \frac{BP_1}{m} + \cdots + a_{3_{n_w}} \cdot \frac{BP_{n_w}}{m} \right\} + g \cdot \sin\varphi$$

(3-10)

where:

n_E: Engine numbers;

n_W: Landing gear wheel numbers;

a_1: Aircraft aerodynamic drag force adjustment coefficient;

a_2: Aircraft engine thrust/reverse thrust adjustment coefficient; and

$a_{3_1} - a_{3_{n_w}}$: Aircraft friction force adjustment coefficients for each landing gear calipers.

3.4 Boeing 737-700 Real Data Case Study

After the establishment of the deceleration equation, a Boeing 737-700 real data case study was conducted.

3.4.1 Data Collection

The sources of the data used in this study are shown in Table 3-1.

Table 3-1 Sources of Data

Data Type	Sources of Data
Flight Data	• Digital Flight Data Recorder installed in a WestJet Boeing 737-700 aircraft
Runway Data	• Waterloo International Airport runway monitoring system.
Weather Data	• The University of Waterloo's Weather Station • Environment Canada

Digital Flight Data

The parameters obtained from a WestJet Boeing 737-700 are provided in Table 3-2. The WestJet Boeing 737-700 is equipped with blended winglets, which improve the aerodynamic performance and handling characteristics of the aircraft. The WestJet Boeing 737-700 has two GE/Snecma CFM56-7B turbofan engines with reverse thrust capability. The aircraft has a maximum takeoff weight of approximately 70,080 kg (WestJet, 2014).

Table 3-2 Digital Flight Data Parameter List

Parameters	Definitions	Unit
FLIGHT_PHASE	Flight phase	
RALTC	Radar altitude	feet
IAS	Indicated air speed (calibrated)	knot
GSC	Ground speed	knot
SPD_BRK_HDL	Speed brake handle	deg
AIR_GND	Air/ground	Yes/No
LDGLR	Left landing gear position	Yes/No
LDGNOS	Nose landing gear position	Yes/No
LDGR	Right landing gear position	Yes/No
BRK_PR_MNALT_L	Left wheel brake pressure, main or alternate	psi
BRK_PR_MNALT_R	Right wheel brake pressure, main or alternate	psi
HEAD	Heading	deg
HEAD_MAG	Magnetic heading	deg
LATG	G force loading along the lateral axis of the aircraft	g
LONG	G force loading along the longitudinal axis of the aircraft	g
VRTG	G force loading along the vertical axis of the aircraft	g
DRIFT	Drift	deg
WIN_DIR	Wind direction	deg
WIN_SPDR	Wind speed	knot
LATP	Latitude	deg
LONP	Longitude	deg
TLA1C	Reverse thrust information for engine 1	Yes/No
TLA2C	Reverse thrust information for engine 2	Yes/No
BRK_SEL_MN_ALT	Brake select, main or alternate	Yes/No
SPOIL_POS_NO10	No 10 spoiler position	deg
SPOIL_POS_NO3	No 3 spoiler position	deg
SPOIL_POS4_R	No 4 spoiler position	deg
SPOIL_POS9_R	No 9 spoiler position	deg
AOAL	Angle of attack lift	deg
AOAR	Angle of attack right	deg
FLAP1	Flap 1 position	deg
FLAP2	Flap 2 position	deg
CK_GW	Weight of the aircraft	t
GW	Weight of the aircraft	lb
AUTO_BRK	Auto braking	Yes/No
ASPD_BRK_EXT	Aerodynamic speed braking	Yes/No
TLA1	Thrust lever angle for number 1 engine	deg
TLA2	Thrust lever angle for number 2 engine	deg
N11	Thrust in use for engine 1	%
N11C	Thrust in use for engine 1	%
N12	Thrust in use for engine 2	%
N12C	Thrust in use for engine 2	%

Runway Data

The Region of Waterloo International Airport (YKF) is located in the triangle bordered by the cities of Cambridge, Kitchener, and Waterloo, and is a fully equipped, certified airport facility classified airport (YKF, 2014). Two runways are operating at the Region of Waterloo International Airport: Runway 08-26 and Runway 14-32, which are shown in Figure 3.4. Runway 08-26 is the primary runway. The elevation is 1055 feet above sea level, and the local time is UTC-5 (-4 during day-light savings time). Runway condition descriptions are reordered every several hours depending on the weather conditions (YKF, 2014). Runway condition data for Runway 08-26 is collected daily from the Waterloo International Airport runway monitoring system.

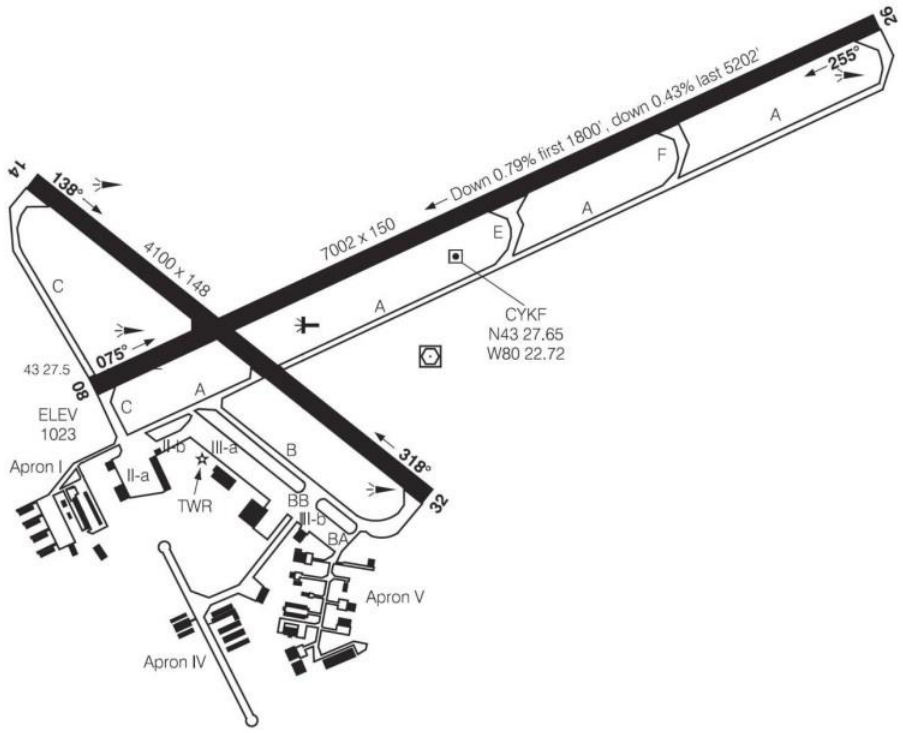

Figure 3.4 Waterloo International Airport Map (YKF, 2014)

Weather Data

GeoNor gauge value, relative humidity, air temperature, and barometric pressure information from the University of Waterloo weather station were collected to determine the precipitation and the air density.

Radar maps of Canadian Historical Weather Radar-Exeter (Environment Canada, 2014) were collected to help determine the precipitation condition when there was a gap between the aircraft landing time and the runway condition description reported time.

The parameters of radar altitude, flight phase, left landing gear position, right landing gear position, and nose landing gear position are used to determine the position of the aircraft and when the aircraft touches down. Spoiler positions and flap positions are used to ensure the aircraft applied the same aerodynamic braking configurations. Auto braking and aerodynamic speed braking information are used to determine the braking configurations of the aircraft. The G force loading along the longitudinal axis of the aircraft is used to determine the deceleration of the aircraft. The angle of attack (AOA) is used to determine the lift coefficient of the aircraft. Heading information is used to identify landing approach direction. Wind speed and wind direction are used to calculate the headwind and the crosswind. Aircraft velocity in the freestream is a function of the aircraft ground speed and the headwind. Since the slope of Runway 08-26 is not uniform, latitude and longitude information is used to determine the slope of the given location.

The runway condition is determined by the following mechanisms:

- If the runway condition descriptions before and after landing time are both “Bare and Dry”, and the time slot between these two descriptions is less than 2 hours, the runway is determined to be “Bare and Dry”.
- If the runway condition descriptions before and after the landing time are both “Bare and Wet” and the time slot between these two descriptions is less than 2 hours, the runway is determined to be wet.
- If the closest runway condition description before the landing time is “Bare and Wet” and the time slot between the description and the landing time is less than 1 hours, the runway condition is determined to be wet.
- If the runway condition description before the landing time is “Bare and Dry” and the runway condition description after the landing time is “Bare and Wet”, the weather data from the University of Waterloo weather station and Environment Canada is used to determine if a rainfall happened prior to or during landing. The runway condition is based on the descriptions before and after landing, and the rainfall data.

- If the runway condition descriptions before and after the landing time both record the presence of winter contaminants and the time slot between these two descriptions is less than 4 hours, the runway is determined to be contaminated.
- If the closest runway condition description before the landing time records the presence of winter contaminants and the time slot between the description and the landing time is less than 1 hours, the runway condition is determined to be contaminated.
- If the runway condition descriptions before and after the landing time are different and the time slot between these two descriptions is more than 24 hours, this data is deleted from the database.

Example:

Table 3-3 Pavement Condition Determination Example

	Report Type	Runway Condition	Time
Case 1	Before Landing	Bare & Wet 100%	8 min before Landing
	After Landing	Bare & Dry 100%	4 hours after landing
Case 2	Before Landing	Bare & Dry 100%	5 hours before landing
	After Landing	Bare & Wet 100%	5 hours after landing

Case 1: The runway is determined to be wet.

Case 2: Weather data from the University of Waterloo weather station and Environment Canada are required. The GeoNor gauge value did not change during the five hours prior to landing, which indicate no rainfall occurred. The radar map is given as Figure 3.5 and during the five hours prior to landing there was not rainfall recorded. Therefore, the runway condition is determined to be "Bare and Dry 100%".

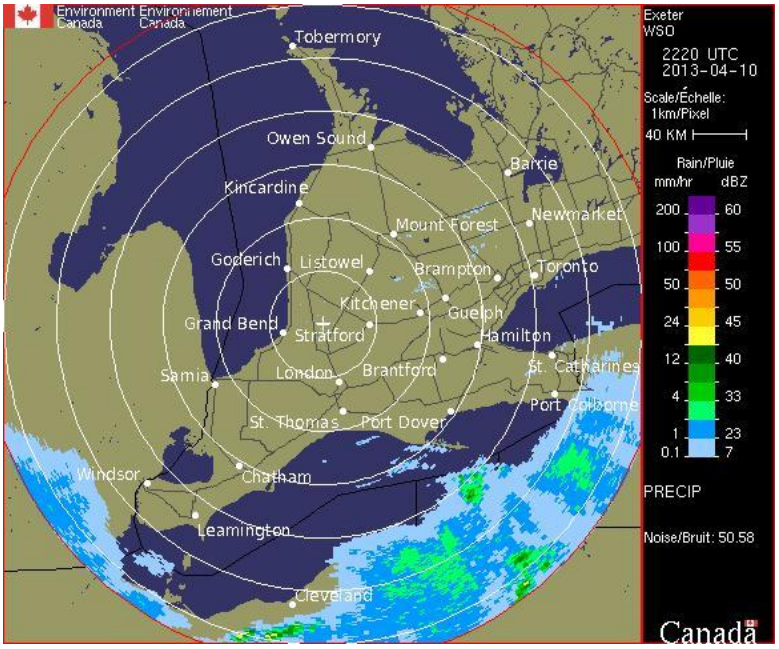

Figure 3.5 Radar Map for Pavement Condition Determination (Environment Canada, 2014)

Finally, data from 56 clear dry runway landings, 21 wet runway landings, and 11 contaminated runway landings was collect. For all data, flap position is 30 degrees and spoiler position is 40 degrees. Twenty eight dry runway landings' data is used to calibrate and validate the M-E deceleration equation and the remaining data is used to analyze aircraft landing performance in Chapter 4.

3.4.2 Boeing 737-700 Deceleration Equations

Engine power is used to identify the relationship between TLA and percent thrust in use. Figure 3.6 illustrates the relationship between TLA and thrust in use. If the value of percent thrust in use is negative, it illustrates that reverse thrust has been applied.

The point distribution is discrete because of the lag of engine fans. When TLA switches from one angle to another, the aircraft system changes the input of the engine, including fuel supply and engine temperature. The engine fans need a short time to decelerate or accelerate their speed, and the engine power is influenced by the engine temperatures that also have a lag. The lag becomes larger during the switch from idle to reverse thrust. The lag of decelerate/accelerate and temperature transition cause the box-shape distribution of the data points.

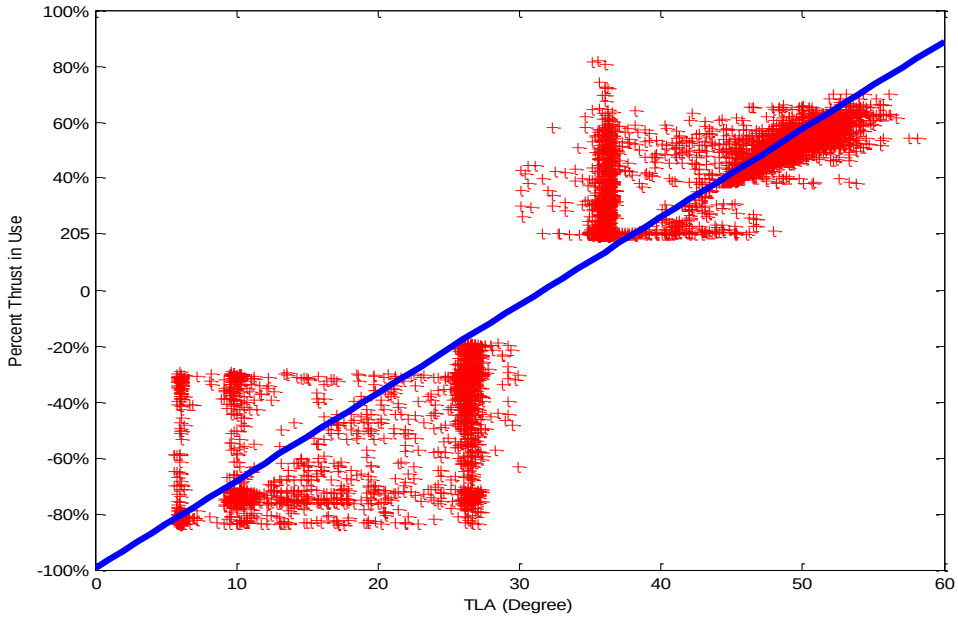

Figure 3.6 Engine in Use vs TLA

Seventy five percent randomly elected data points from 28 flights are used to calibrate the model and the remaining 25% of the data is used to validate the calibrated model. When PT equals to 1, it means the engine uses its full power. After regression, the relationship between the engine power in use and TLA can be described as:

$$T = \alpha \cdot PT = 0.031 \cdot (TLA) - 0.995 \quad \textbf{(3-11)}$$

Based on Equation (3-10) using linear regression, the M-E deceleration equation for Boeing 737-700 is:

$$a = 0.002 \cdot \frac{\rho_{air} V^2}{m} - 56.38 \left\{ \frac{f(TLA_1)}{m} + \frac{f(TLA_2)}{m} \right\} + \left\{ 0.072 \cdot \frac{BP_1}{m} + 0.070 \cdot \frac{BP_2}{m} \right\} + g \cdot \sin\varphi \quad \textbf{(3-12)}$$

The M-E equations for each force are given as follows.

$$\begin{cases} D = 0.002 \cdot \rho_{air} V^2 \\ T = -56.38[(TLA_1) + (TLA_2)] \\ F = 0.072 \cdot BP_1 + 0.070 \cdot BP_2 \end{cases} \quad \textbf{(3-13)}$$

The coefficient of determination (R Square) of the model is 0.967, which indicates a good correlation between the statistic model and the observed data. The analysis of variance (ANOVA) is used to analyze the differences between statistical models and the given data. The ANOVA results indicate that the model has a mean square error of 0.11. The Significance F equals to 0, which means the model is statistically sound and significant. According to the statistic results for each coefficient, the standard errors are all very small. The p-values are all infinite small, and the largest value of the four coefficients is 9.8×10^{-24}; therefore, all the factors are statistically significant. The statistic results of the regression are given in Table 3-4.

Figure 3.7 is the residual case order plot. A total of 573 data points are used for regression, and 30 data points are shown in red, which indicate that the residual is larger than expected in 95% confidence. The 30 data points are regarded as outliers. The residual case order plot indicates the regression fits the initial data well.

Table 3-4 Statistic Results

Regression Statistics	
Multiple R	0.984
R Square	0.967
Adjusted R Square	0.965
Standard Error	0.335
Observations	573

ANOVA					
	df	*SS*	*MS*	*F*	*Significance F*
Regression	4	1898.686	474.672	4224.978	0
Residual	569	63.927	0.112		
Total	573	1962.613			

	Coefficients	***Standard Error***	***t Stat***	***P-value***	***Lower 95%***	***Upper 95%***
Intercept	0	#N/A	#N/A	#N/A	#N/A	#N/A
Drag	0.0020	0.0002	10.5106	9.8E-24	0.002	0.002
Thrust	-56.3768	3.0362	-18.5682	1.6E-60	-62.340	-50.413
Friction-Left	0.0718	0.0060	11.9842	1.15E-29	0.060	0.084
Friction-Right	0.0697	0.0065	10.7417	1.24E-24	0.057	0.082

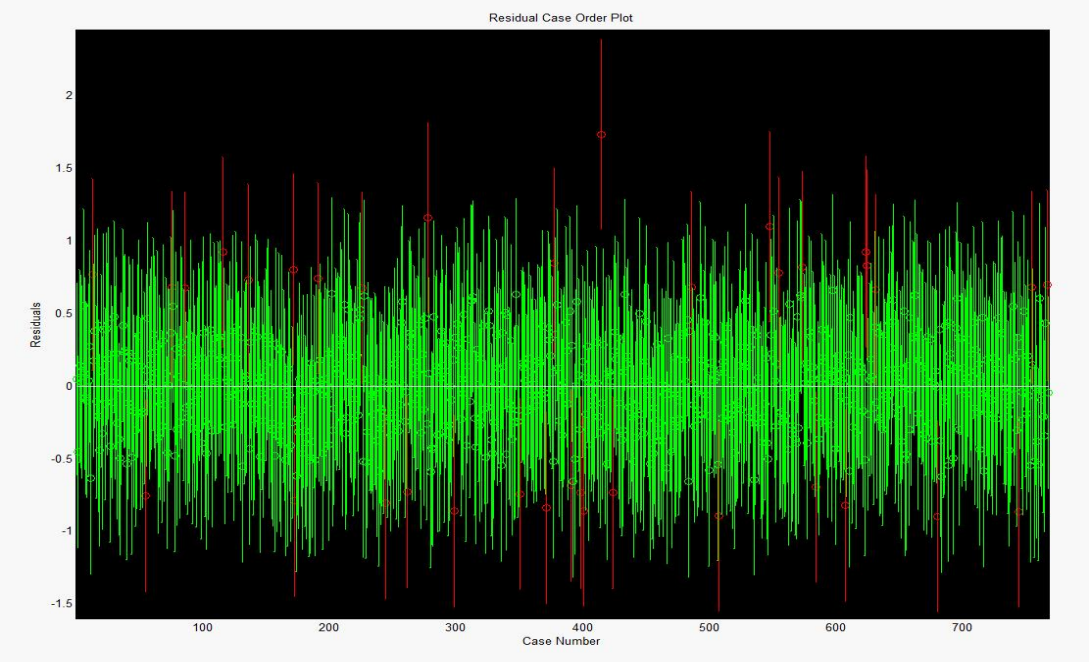

Figure 3.7 Residual Case Order Plot

Figure 3.8 demonstrates the validation of the model. The validation results indicate that the predicted data have a mean square error of 0.11. The statistical analysis is given in Table 3-5. The model is shown to match the observed data for this Boeing 737-700 aircraft.

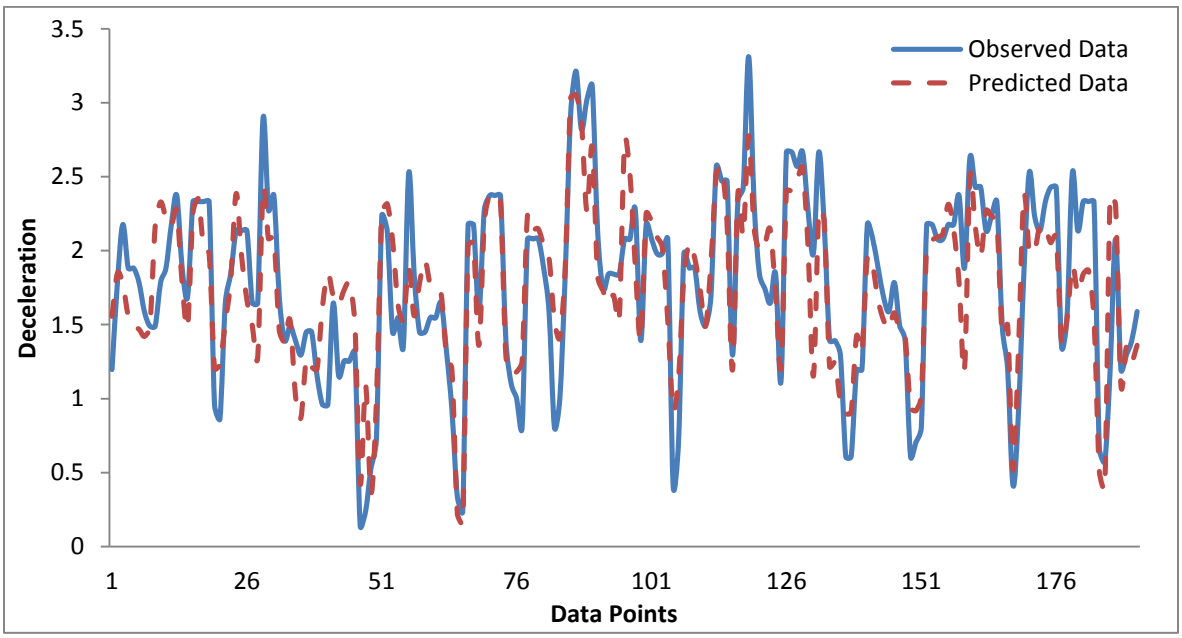

Figure 3.8 Validation of Calibrated Equation

Table 3-5 Statistical Analysis of the Validation Results

ANOVA					
	df	*SS*	*MS*	*F*	*Significance F*
Regression	1	952.200	952.200	8564.822	0
Residual	256	28.461	0.111		
Total	257	980.661			

Using the Boeing 737-700 deceleration model, the entire landing process (from aircraft touchdown to the aircraft decelerates to 15m/s) can be simulated.

Figure 3.9 is a time-speed diagram of real flight data and simulated results comparison; more results are attached in Appendix A. The two curves show small bias between the observed data and the predicted values. The simulated results indicate the model is realistic and can provide a precise landing deceleration prediction.

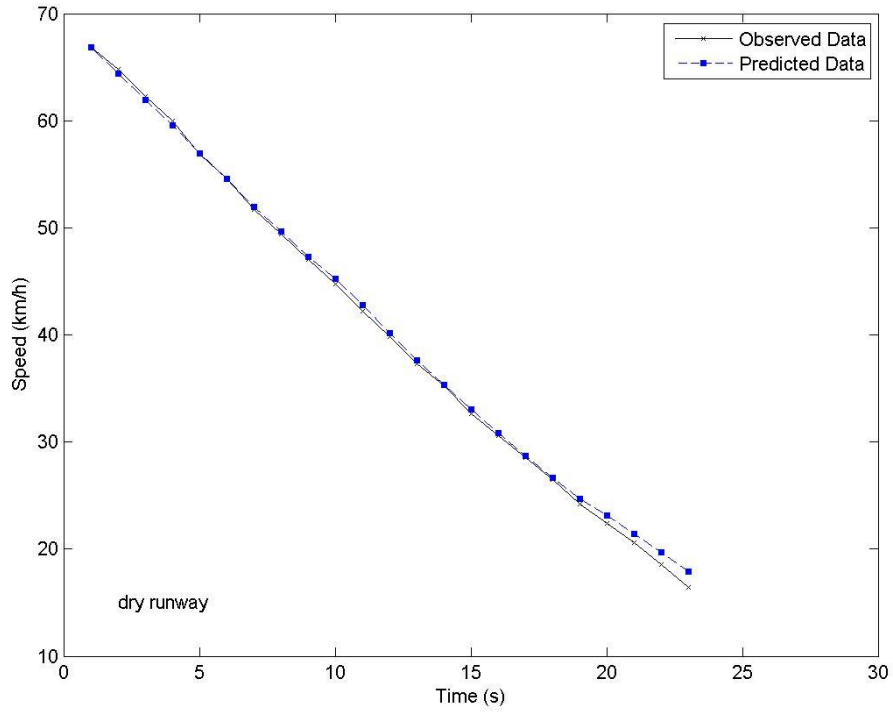

Figure 3.9 Time-Speed Diagram Validation

3.5 Summary

In order to model aircraft braking performance and predict aircraft landing deceleration, an M-E deceleration equation was developed in this chapter. The key features of this chapter are summarized as follows:

- M-E deceleration equation incorporates mechanistic force and moment analysis and real data calibration.
- Validation of the model indicates that the M-E deceleration equation provides an accurate prediction of the aircraft landing deceleration.

The M-E deceleration equation offers the potential to analyze aircraft braking performance based on digital flight data, which is discussed in Chapter 4.

In addition, using the deceleration equation, the entire landing process can be simulated and the landing distance can be computed, which is conducted in Chapter 5.

Chapter 4
Wet and Contaminated Runways Braking Analysis

Available runway friction has a significant impact on aircraft landing performance. This is especially noted when aircrafts are landing on wet or otherwise contaminated runways due to the reduced braking action, which has been well documented since the dawn of the jet aircraft age. In order to prevent runway landing excursion accidents and incidents, and enhance airport and airline operation safety, available runway friction is discussed in details in this chapter.

This chapter is based on a paper accepted by the 2014 FAA Worldwide Airport Technology Transfer Conference: Innovations in Airport Safety and Pavement, Galloway (Oceanville), New Jersey, USA, August 5-7, 2014 (Zhang & Tighe, 2014).

4.1 Introduction

A certain amount of available runway friction is required for aircraft landing operations (Klein-Paste, Sinha, Løset, & Norheim, 2007). With the presence of water film, snow, and ice, the available runway friction changes rapidly, and different measurement devices provide results with a large variance on a uniform runway condition (Klein-Paste et al., 2007). According to the results of a survey of Canadian airline pilots in the JWRFMP, "Pilots indicated that the quality of runway friction information provided by airports varies between airports. Generally the quality is better at large airports, but each airport differs depending on various factors" (Biggs & Hamilton, 2002). Because of the inconsistency of runway friction measuring devices, it is better to analysis available runway friction based on aircraft measurements.

This chapter focuses on aircraft landing performance, and the purposes of this chapter are:

- Providing background knowledge regarding wet and contaminated runway aircraft braking;
- Analyzing aircraft braking performance on wet and contaminated runways using the built M-E aircraft landing deceleration equation; and
- Studying runway available braking friction coefficients under different conditions.

4.2 Methodology

In Chapter 3, an M-E aircraft landing deceleration equation has been built to model an aircraft's real landing performance. This equation contains all major forces that contribute to aircraft braking, including aerodynamic drag force, engine thrust/reverse thrust, slope deceleration/acceleration, and friction force. As a result, the braking friction can be back calculated from the developed equation. In this way, braking friction coefficient under different runway conditions can be calculated. By comparing dry runway, wet runway, and contaminated runway braking performances, aircraft landing braking actions under different runway conditions are analyzed.

The overall methodology of this chapter is shown in Figure 4.1. First, digital flight data, airport runway condition monitoring data, and weather data are collected. The data are introduced in Chapter 3.4.1. According to the airport runway condition monitoring data and weather data, all the data are classified into three categories: dry runway data, wet runway data, and contaminated runway data. Dry runway data from 28 landings is used to calibrate M-E aircraft deceleration equations and the remaining dry runway data, wet runway data, and contaminated runway data is used to analyze the braking performance.

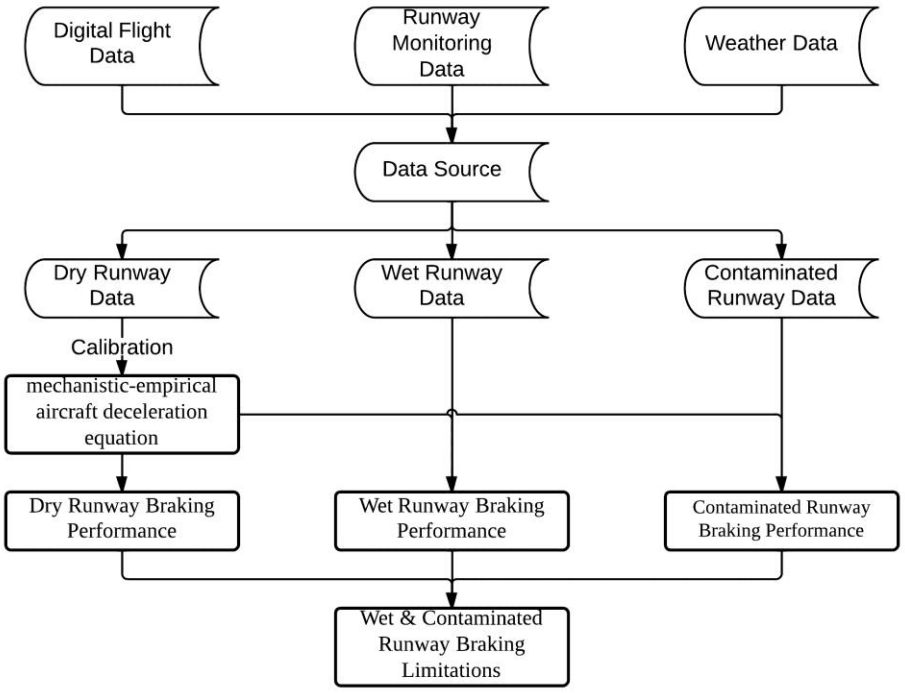

Figure 4.1 Research Methodology

4.3 Factors Affecting Runway Friction

Friction force is influenced by a combination of aircraft characteristics and airport runway pavement surface characteristics (Leland et al., 1968). Studies on these aspects have been reviewed in Chapter 2.

The following listed factors are the main factors affecting runway friction (Comfort, 2001):

- Tire texture and inflation pressure;
- Pavement texture;
- Slip Ratio;
- Ground Speed; and
- Water or contaminations.

In this research, the aircraft friction force adjustment coefficient for each landing gear is calibrated. The tire texture and inflation pressure are landing gear characteristics, and their adjustments are included in the aircraft friction force adjustment coefficient. Since all the collected data is from an asphalt runway pavement at Waterloo International Airport, the pavement texture is not studied in this research. Slip ratio is not measured in the WestJet Boeing 737-800 model; instead, braking pressure that controls slip ratio is analyzed. In this analysis, aircraft braking performance is studied regarding the relationship between braking pressure and braking friction coefficient as well as the relationship between aircraft ground speed and braking friction coefficient.

4.4 Braking Performance

When the tire is free rolling, a rolling resistance force is applied on the wheel. As braking is applied, a slip occurs between the tire and the pavement surface. As shown in Figure 4.2, the tire proceeds from free rolling to fully locked, and the coefficient of friction varies with the change of the tire slip (Hall et al., 2009). The coefficient of friction increases rapidly from a certain value near zero, which is referred as free rolling resistance coefficient, to a peak friction value and then it decreases to another certain value, which is referred to as full sliding resistance coefficient (Hall et al., 2009; Henry, 2000). The peak friction usually occurs with a 10% to 20% tire slip, which is known as the critical slip. When the slip proceeds to 100% slip, which means the wheel is fully locked, the coefficient decreases to a full sliding resistance friction coefficient. The full sliding resistance friction is lower

than the peak friction, and is much lower for wet and contaminated pavements than dry pavements. (Hall et al., 2009).

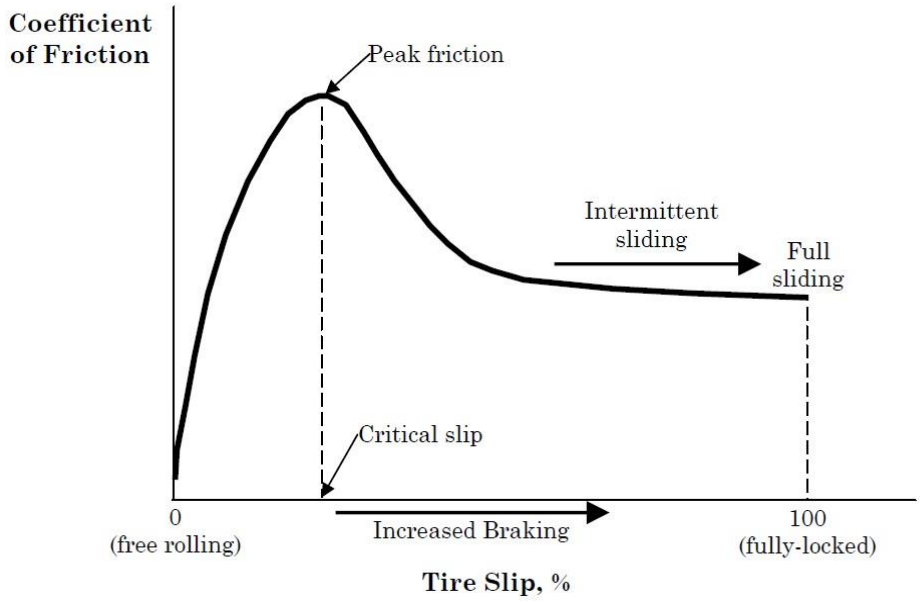

Figure 4.2 Pavement Friction vs Tire Slip (Hall et al., 2009)

Originally, antiskid braking systems are designed to prevent aircraft wheel from locking during braking. However, with the development of the antiskid braking system, current systems also have the function of achieving a maximum braking performance from different runway conditions (Horne, McCarty, & Tanner, 1976). A sensor is installed in each braking wheel of an aircraft to determine ground speed and wheel angular velocity, and hydraulic pressure is controlled by a servo control valve. The system measures the slip ratios and determines if an excessive skid occurs. If the ABS system applied braking pressure exceeds the maximum available friction, the wheel decelerates rapidly to a locked wheel. In this case, the system will release braking pressure to ensure the wheels spin up (Horne et al., 1976). The relationship between coefficient of friction and tire slip is the basic mechanism of an antiskid braking system. The antiskid braking system aims to take the most advantage of the tire-pavement friction, which means it takes the advantage of the left side of the curve shown in Figure 4.2 (Hall et al., 2009). An antiskid braking system controls the braking pressure to control the slip of the tire to achieve a peak friction. When peak friction is achieved, the antiskid brake systems will not increase braking pressure, or release the brake for a short time. More braking pressure will be applied when peak friction is not reached (Hall et al., 2009; Henry, 2000).

The relationship between braking friction coefficient and braking pressure can be described as Figure 4.3. It is assumed that for a certain landing gear, the achieved braking friction coefficient is a linear function of braking pressures before peak friction is reached (red dashed line in Figure 4.3), and the coefficient is a unique value for a specific landing gear. In addition, the relationship is under the assumption that when the tire is free rolling, the rolling resistance is negligible.

For different runway pavement conditions, the peak friction is different. In general, the peak friction of a wet or contaminated runway is smaller than a dry runway. Under wet or contaminated conditions, a lower braking pressure will result in a locked wheel.

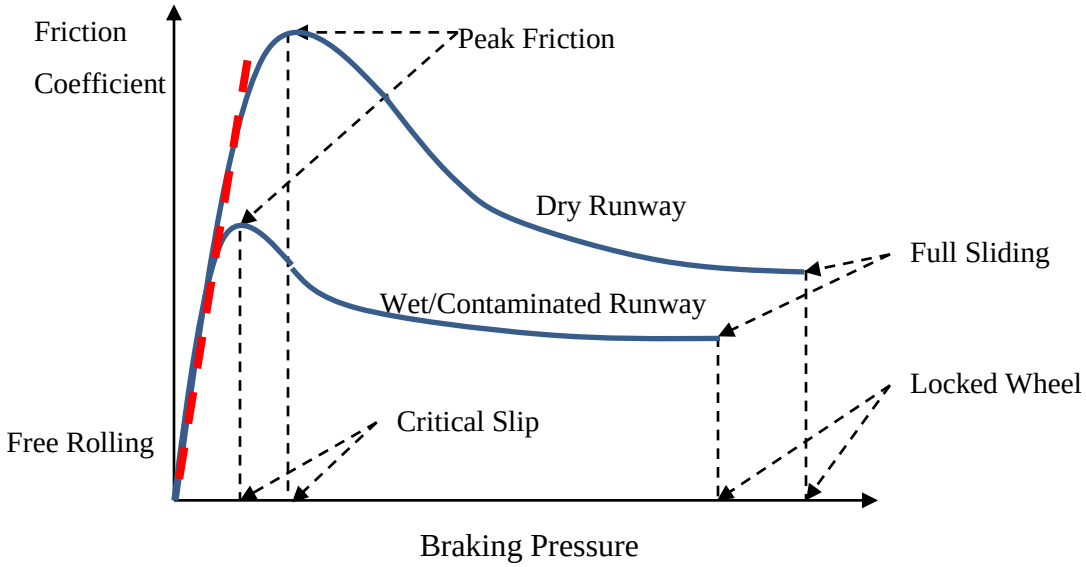

Figure 4.3 Braking Friction Coefficient vs Braking Pressure

Equation (4-1) is derived from the M-E aircraft friction equation with the input of aircraft characteristic adjustment coefficient and the braking pressure, which represents the red dashed line in Figure 4.3. Equation (4-1) is referred to as the M-E aircraft friction equation.

The M-E aircraft deceleration equation assumed a linear relation between applied braking pressure, a known value, and friction, unknown, to model the frictional forces (before it researches the peak friction). As a result, it is able to back calculate friction. Equation (4-2) and (4-3) are derived from the M-E aircraft deceleration equation. Equation (4-2) and (4-3) are used to back calculate the friction and braking friction coefficient by digital flight data. According to Equation (4-3), the braking

friction coefficient is a function of the entire deceleration, air density, velocity, TLA setting, weight of the aircraft, and the slope of the runway pavement.

$$\mu = a_3 \frac{BP}{mg} n_W \tag{4-1}$$

$$F = am - a_1 \cdot \rho_{air} V^2 - a_2 \cdot f(TLA_1) - g \cdot sin\,\varphi \tag{4-2}$$

$$\mu = \frac{am - a_1 \cdot \rho_{air} V^2 - a_2 \cdot f(TLA_1) - g \cdot sin\,\varphi}{mg} \tag{4-3}$$

4.5 Braking Limitations

4.5.1 Dry Runway Analysis

In Figure 4.4, the Y-axis is the braking friction coefficient, and the X-axis is the braking pressure. Figure 4.4 is the plot of the results of all 28 dry runway landings. Each blue point represents a back-calculated braking friction coefficient of a data point. The red centre line is the calibrated M-E aircraft friction equation, which also represents the red dashed line in Figure 4.3. It can be seen that the blue points locate along the red centre line. The location and distribution of the points are influenced by the pavement conditions.

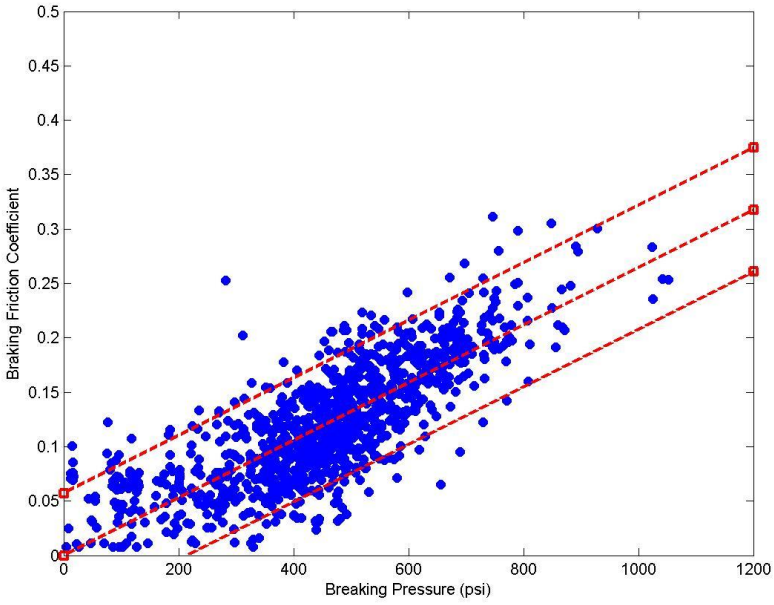

Figure 4.4 Braking Friction Coefficient vs Braking Pressure, Dry Runway

Due to the non-uniform pavement surface texture and property, the points could deviate from the red centre line. Although the pavement surface texture and its property may cause deviations, the deviations should remain in a certain range of value.

Figure 4.5 is the histogram of the deviations between the back-calculated braking friction coefficient and calibrated M-E aircraft friction equation for the dry runway data, and Figure 4.6 is the normal probability plot. Both of the figures indicate the deviations follow normal distribution. The mean value of the distribution is 0, and the standard error is 0.03. Therefore, the 90% confidence interval is -0.057 to 0.057. The upper and lower 90% confidence interval boundaries are also depicted in Figure 4.4.

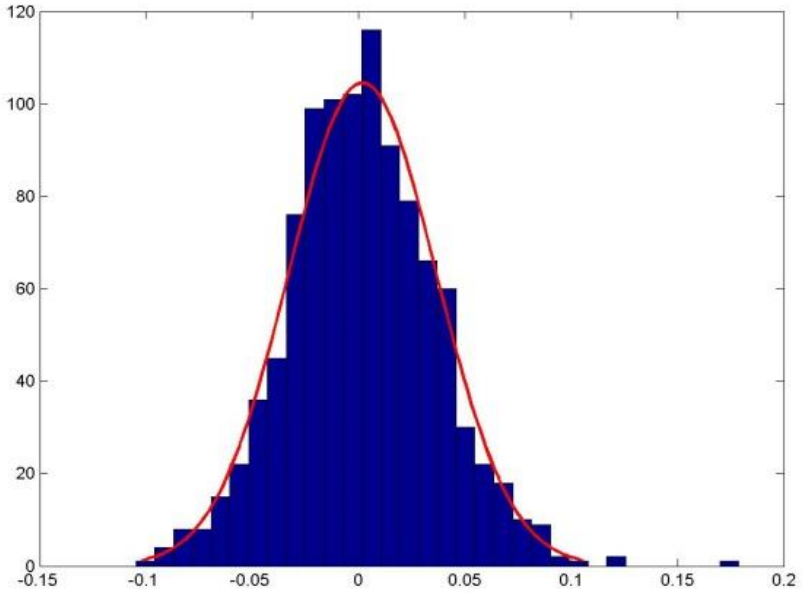

Figure 4.5 Histogram Plot

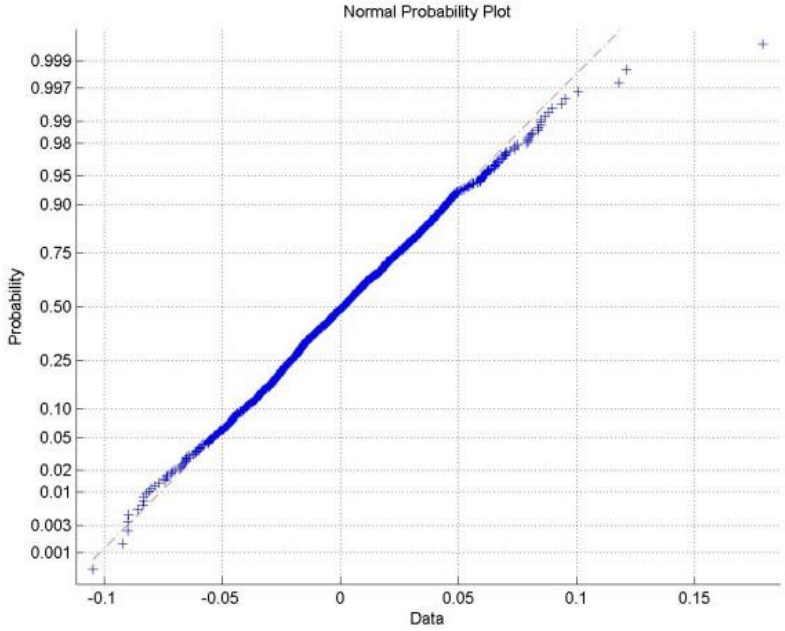

Figure 4.6 Normal Probability Plot

Figure 4.7 (a) and (b) show the results of two dry runway landings. Each red point represents a back-calculated braking friction coefficient using a data point during a given landing. The centre red line is the calibrated M-E aircraft friction equation and the top and bottom red lines are the 90% confidence boundaries. More results are attached in Appendix B. Figure 4.7 (a) indicates that for the given flight, the runway condition was good and could provide sufficient friction for braking. Figure 4.7 (b) indicates that for the second given flight, at some location, the runway could not provide expected friction for braking. The possible reasons for these occurrences are standing dust on the runway surface or rubber deposits. Among 28 dry runway landings, Figure 4.7 (b) is the worst case.

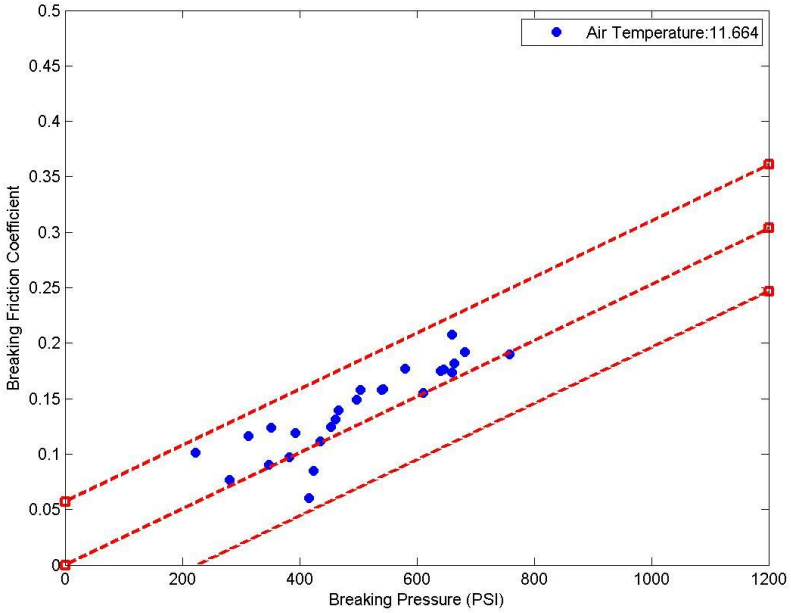

(a)

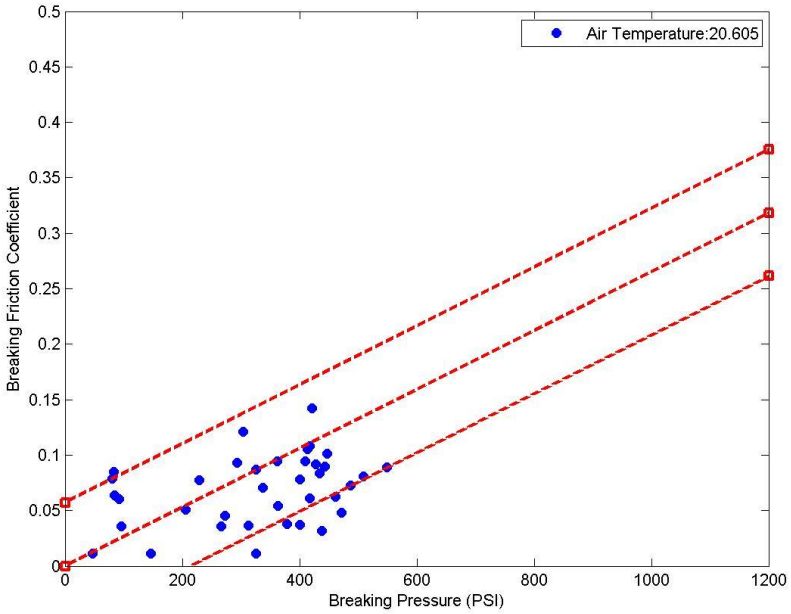

(b)

Figure 4.7 Dry Runway Sample Results

4.5.2 Wet Runway Analysis

The water on the pavement will reduce the frictional property of the runway. In addition, a water layer, which lies between the aircraft tire and the landing pavement surface, will generate a lift force. When the lift force equals to the weight of the aircraft, hydroplaning will happen. If hydroplaning happens, the aircraft is lifted and there is little friction between the aircraft tire and the runway surface. In this case, the landing gear is locked due to inefficient friction. Figure 4.8 is a free body diagram of a landing gear wheel on wet runway pavement when hydroplaning happens (Van Es, 2001).

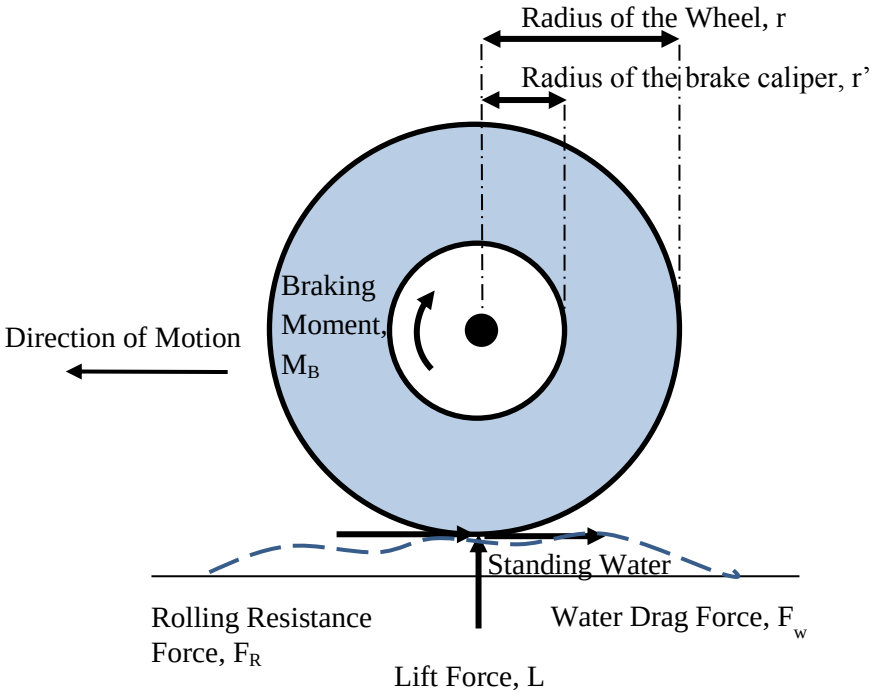

Figure 4.8 Landing Gear Wheel on Wet Runway Pavement

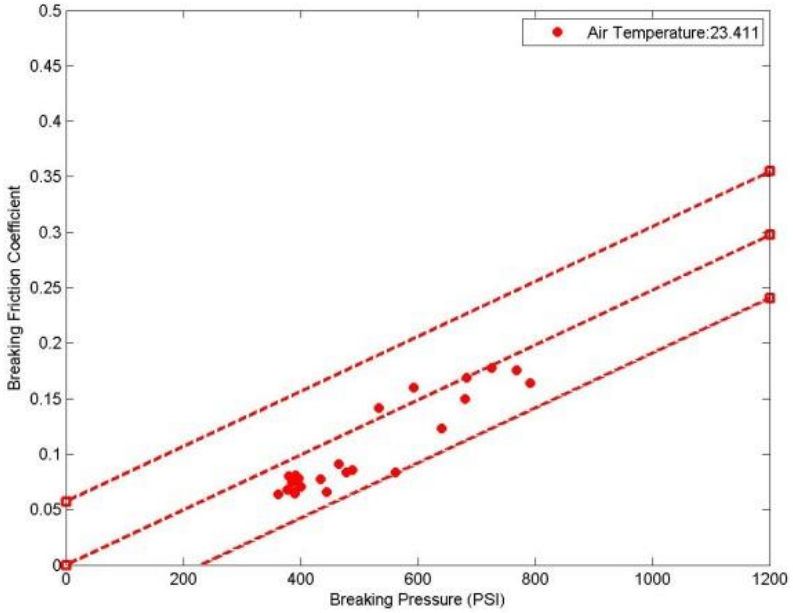

(a)

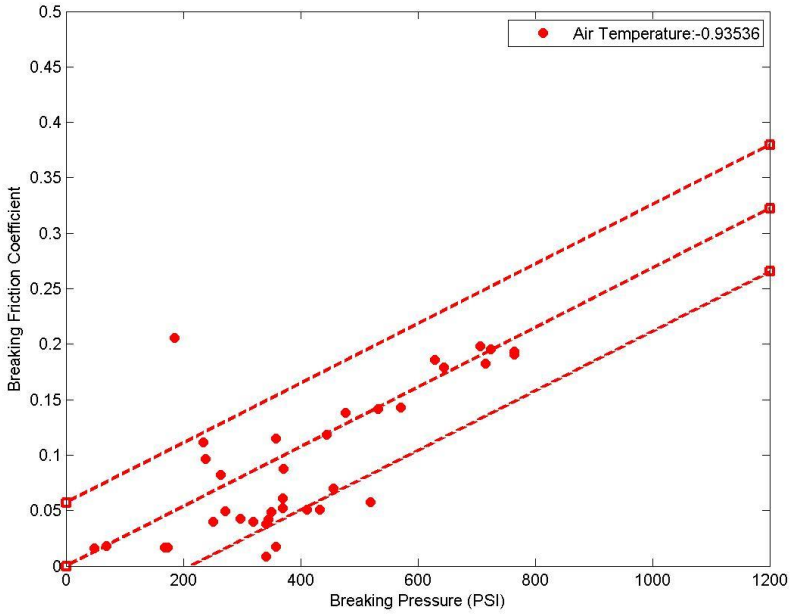

(b)

Figure 4.9 Wet Runway Sample Results

Figure 4.9 (a) and (b) provide the results of two wet runway landings. The centre red line in Figure 4.9 is the calibrated M-E aircraft friction equation and the top and bottom red lines are the 90% confidence boundaries. More results are attached in Appendix C. The red points below the bottom red line represent that at those locations the tire does not achieve the expected friction forces. The possible reasons for this are listed as follows:

- Hydroplaning. When hydroplaning happens, the aircraft is lifted and cannot touch the pavement, so the braking friction is almost zero. Hydroplaning can happen only for a very short time slot, because of the aircraft antiskid braking system.
- Poor frictional prosperity area. Some poor frictional prosperity area may exist for the reasons including poor pavement surface texture, dust on the pavement surface, rubber deposits, and standing water.
- Error data points. Error data might be recorded due to system accuracy and lags.

Figure 4.10 shows the results of all of the 21 wet runway landings. Most of the points locate within the 90% confidence interval, which indicates that during these 21 flights, wet runway remains a good runway friction condition similar to a dry runway pavement. This is most likely related to the fact that the Waterloo International Airport ensured the runway is maintained to a high level of service.

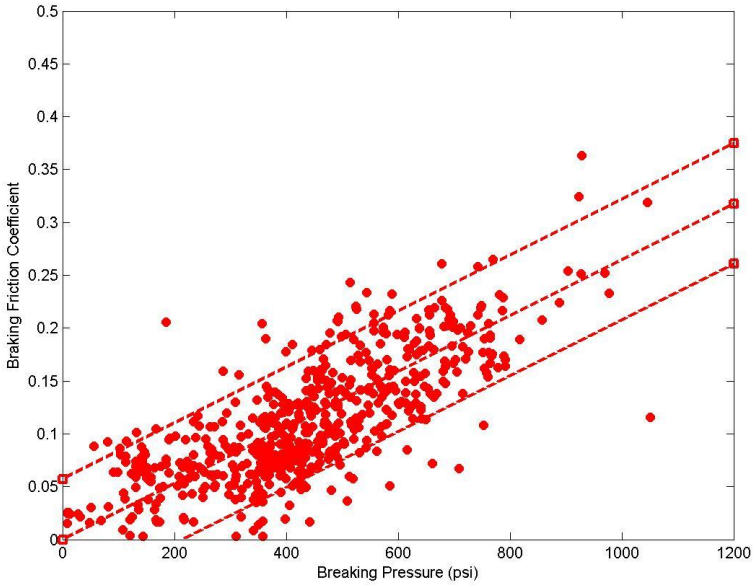

Figure 4.10 Braking Friction Coefficient vs Braking Pressure, Wet Runway

4.5.3 Contaminated Runway Analysis

A contaminated runway is a runway with "standing water, slush, snow, compacted snow, ice or frost covering more than 25% of the required length and width of its surface (Transport Canada, 1999a)". The presence of contaminations on the runway reduces the friction between the tires and runway surface. The reduction is a function of several factors including the tire-pavement interaction, the antiskid system performance, and type of runway pavement. The contaminants can contribute to aircraft deceleration by applying a drag force against the motion of moment. However, the drag is very small compared to the reduction of friction between the tire and runway surface. Also, the contaminants may cause damage to the landing gear wheel.

Figure 4.11 (a) is the back-calculated data from a landing on a runway with a condition of "95 PERCENT BARE AND DRY, 5 PERCENT COMPACTED SNOW" and Figure 4.11 (b) is from a runway of "40 PERCENT BARE AND DRY, 60 PERCENT DRY SNOW TRACE. RMK: SNOW REMOVAL IN PROGRESS". The circled points in Figure 4.11 (b) represent the situation that the aircraft achieved a friction that is below the average friction value. The comparison between Figure 4.11 (a) and (b) indicates that the contaminants have a significant influence on aircraft braking and the more contaminates on the runway, the greater reduction in friction is. However, it should be noted that a small amount of contaminant on the runway can still result in a good frictional value. Figure 4.11 (b) is the worst case in the collected data. The possible reason for the occurrence of the circled points in Figure 4.11 (b) is the fact that the snow on the pavement reduced the frictional property of the pavement or separated the tire and pavement surface.

Figure 4.12 shows the results of 11 contaminated runway landings. Most of the points locate within the 90% confidence interval. This is most likely related to the fact that the Waterloo International Airport ensured the runway is maintained to a high level of service. The runway condition is good, so insufficient friction braking landing did not occur in the collected data.

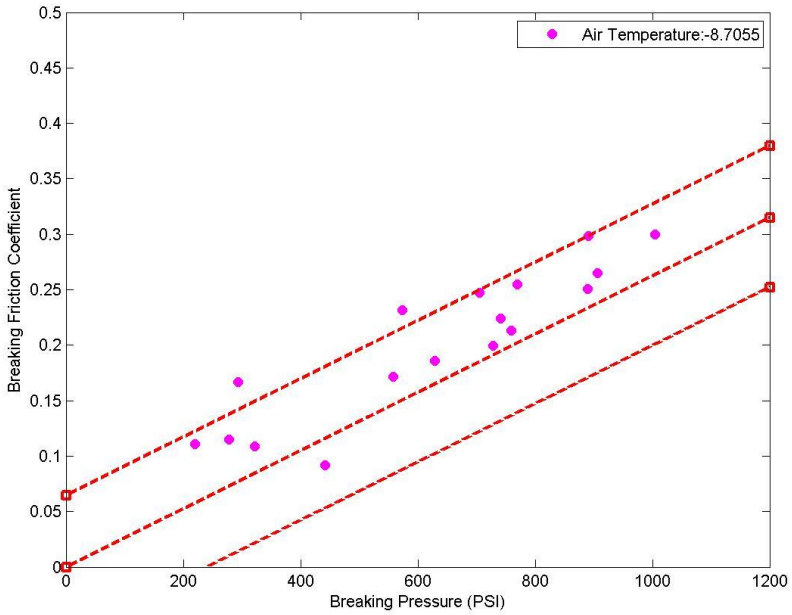

(a)

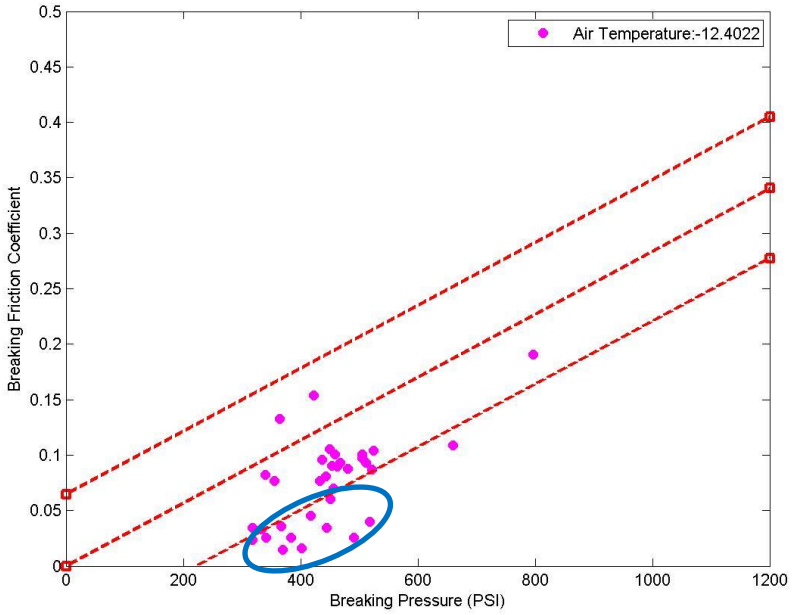

(b)

Figure 4.11 Contaminated Runway Sample Results

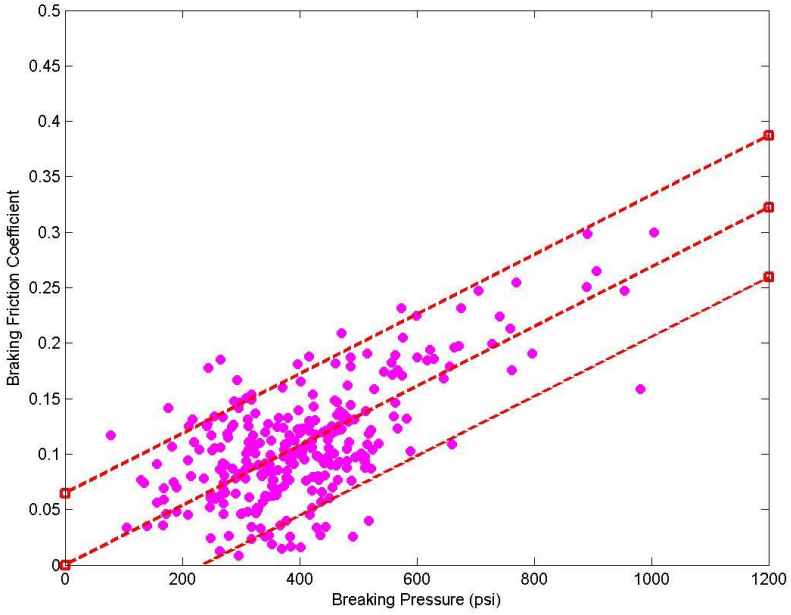

Figure 4.12 Braking Friction Coefficient vs Braking Pressure, Contaminated Runway

4.6 Speed vs Braking Friction Coefficient

The relationship between braking friction coefficient and aircraft ground speed is shown in Figure 4.13. Since all data is from a commercial aircraft, maximum braking is not used for all the collected flights. It is assured the highest back-calculated braking friction coefficient value for each speed is the maximum available braking friction coefficient under that speed. Due to the variances, some of the data points are considered as error points or outliers. The blue points in Figure 11 (a) are the back-calculated braking friction coefficient when the runway is "Bare and Dry 100%"; the red points in Figure 11 (b) are the back-calculated braking friction coefficient when the runway is wet; the pink points in Figure 11 (b) are the back-calculated braking friction coefficient when the runway is winter contaminated. The speed of analyzed data is in the range of 30 knots to 135 knots. The results indicate that when the speed is low, the wet runway has a maximum available braking friction that is nearly the same as the dry runway. When the speed increases, the maximum available braking friction decreases for both wet runways and dry runways. However, a bigger drop in maximum available braking friction occurs when the runway is wet. The results for contaminated runway landings are of big variance. The available braking friction coefficient can be as high as a clean dry runway; however, the distribution of the majority of the collected data indicates there is a big drop in braking

friction coefficient. The reason for this variance is likely related to the uniform contaminant distribution on the runway.

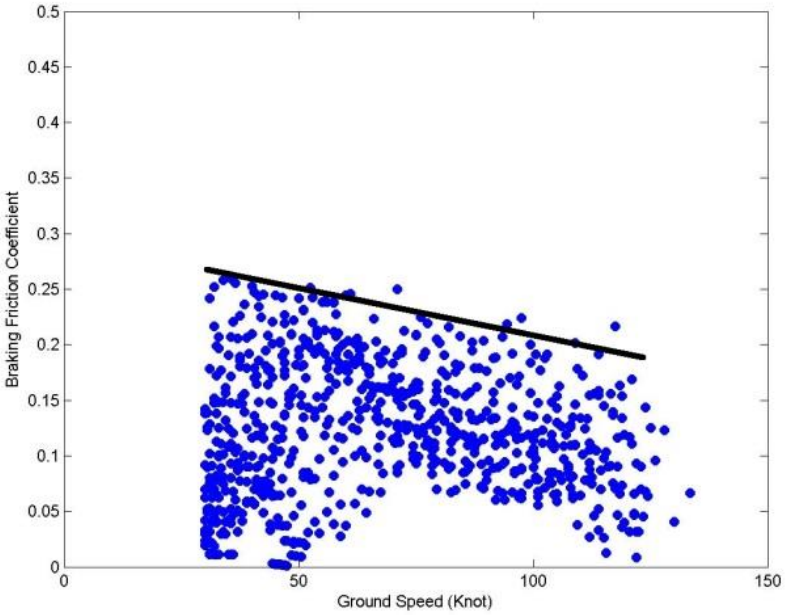

(a) Dry Runway

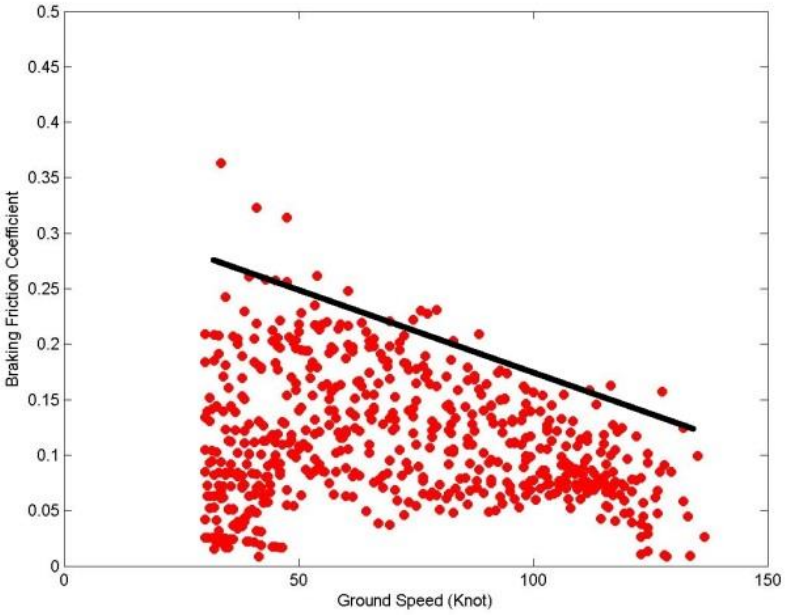

(b) Wet Runway

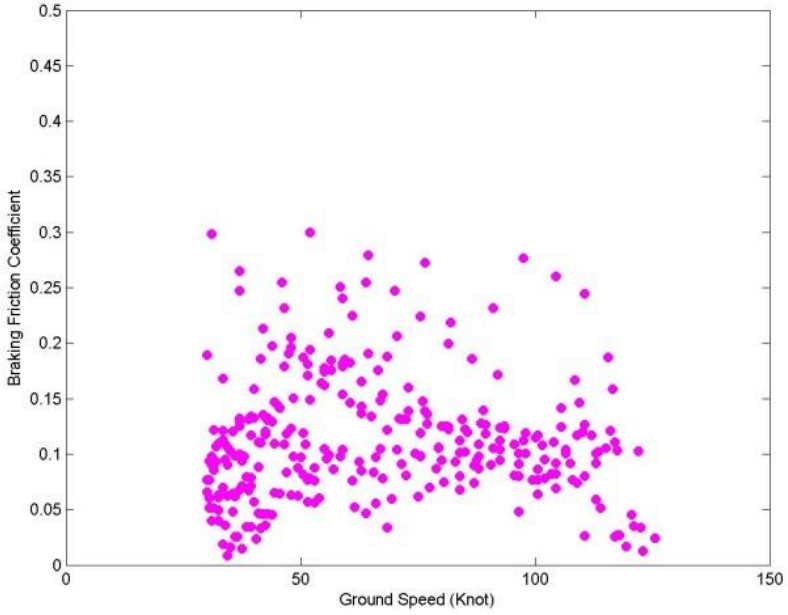

(c) Contaminated Runway

Figure 4.13 Braking Friction Coefficient vs Speed

4.7 Summary

In this chapter, a method to analyze aircraft braking on wet and contaminated runways using the developed M-E aircraft landing deceleration equation was introduced. A study of a Boeing 737-700 aircraft landing on dry and wet runways was conducted. The key findings of this chapter are summarized as follows:

- If well maintained, a wet runway does not reduce braking performance significantly.
- Available braking friction coefficient is ground speed dependent. When the speed increases, the available braking friction coefficient decreases. Wet runway available braking friction coefficient is more dependent on speed and decreases faster than dry runways.
- Contaminated runways have a larger impact on braking performance than wet runways; however, a reliable runway with a small amount of winter contaminants can still satisfy landing requirements approaching a dry runway.

Chapter 5
Landing Distance Model

The M-E aircraft deceleration equation provides the opportunity to simulate the landing performance by estimating deceleration for each short time slot. An M-E landing distance model, which incorporates a variety of influence factors, parameters of pilot settings (TLA, spoiler position, and flap position, settings), runway condition, aircraft operational characteristics (touchdown speed and weight), and aircraft braking system characteristics, is introduced in this chapter.

This chapter is based on a paper presented at the 94th Transportation Research Board Annual Meeting, Washington D.C., U.S.A., 12-16 January, 2014 (Zhang et al., 2014).

5.1 Landing Distance Model

5.1.1 Aircraft Landing Distance Equations

Aircraft landing has three segments: approaching, flaring, and braking (ground rolling). This research focuses on aircraft braking and is conducted under the assumption that the aircraft applies braking actions, both aerodynamic braking and landing gear braking, immediately after touchdown. The entire landing distance is regarded as a sum of the braking distance and the distance from the runway threshold to aircraft touchdown location. The equations related to aircraft landing distance and braking distance are given as follows:

$$S = S_0 + S_1 = S_0 + \int_{t_0}^{t_n} v(t)dt = S_0 + \sum_{i=1}^{n} (\, v(t_i) \cdot \Delta t) \quad \textbf{(5-1)}$$

$$v(t) = v(t_0) + \int_{t_0}^{t_n} a(t)dt = v(t_0) + \sum_{i=1}^{n} (\, a(t_i) \cdot \Delta t) \quad \textbf{(5-2)}$$

$$v(t_n) = v(t_{n-1}) + \, a(t_{n-1}) \cdot \Delta \mathrm{t} \quad \textbf{(5-3)}$$

where:

S: Landing distance, m;

S_1: Braking distance, m;

S_0: Distance from the runway threshold to aircraft touchdown location, m;

L: The entire runway length, m;

$L_{touchdown}$: the distance from the runway threshold to aircraft touchdown location, m;

t_0: Aircraft touchdown time, s;

t_n: Time when the aircraft decelerate to a lower safe-turnoff speed (10 m/s), s;

t_i: Time when the aircraft decelerates, s;

Δt: Time slot between two time points, s;

v: The aircraft ground speed, m/s; and

a: The deceleration/acceleration of the aircraft, m/s^2 (Zhang et al., 2014).

5.1.2 Aircraft Braking System Characteristics

Aircraft braking system is a deceleration rate controlled system (Moir & Seabridge, 2008). During landing, a deceleration rate is selected by setting an automatic braking level. The automatic brake system applies braking pressure to achieve the programmed rate. If aerodynamic braking applications (flap, spoilers, and reverse thrust) are used, the automatic brake system reduces braking pressure to achieve the programmed deceleration rate. Anti-skid brake systems prevent the wheel from locking by releasing braking for a short time when peak friction is achieved, and applying braking when peak friction is not reached (Hall et al., 2009; Henry, 2000).

As discussed in Chapter 4.4, a maximum friction coefficient exists, and it varies from one pavement to another. Even for the same pavement, the peak friction value differs from one certain condition to another (Hall et al., 2009). According to Chapter 4, a maximum available braking pressure exists and can be calculated using the given equations:

$$F = a_3 \cdot BP \tag{5-4}$$

$$\mu_{max} = \frac{F_{max}}{F_R} = \frac{a_3 \cdot BP_{max}}{W - L} \tag{5-5}$$

$$L = \frac{1}{2}\rho S V^2 C_L \tag{5-6}$$

$$BP_{max} = \frac{\mu_{max} \cdot (W - L)}{a_3} \tag{5-7}$$

where:

F: Friction force, N;

BP: Braking pressure, psi;

L: Aerodynamic lift force, N;

W: Gravity of the aircraft, N;

ρ: Air density, kg/m3;

S: The aircraft reference area, m^2;

V: Aircraft velocity in the freestream, m/s

a_3: Aircraft friction force adjustment coefficients for each landing gear calipers;

μ_{max}: Maximum braking coefficient; and

C_L: Aircraft lift coefficient (Zhang et al., 2014).

5.1.3 Landing Distance Model

The aircraft landing distance model is shown in Figure 5.1. Runway condition, pilot configurations, and aircraft operational characteristics are taken into consideration and are the three inputs in the model. The equations for D, T, and F in Equation (3-9) are referred as the M-E aerodynamic drag force deceleration equation, the M-E engine thrust/reverse thrust deceleration equation, and the M-E friction deceleration equation.

First, according to the runway slope information, the slope deceleration or acceleration is identified. In addition, runway friction data is used to determine the maximum available braking pressure based on Equation (5-7).

Then, pilot configurations are taken into consideration. First, auto braking level selection is used to determine the deceleration rate to achieve. This deceleration rate is identified based on the aircraft characteristics. For instance, for a Boeing 737, if auto braking level 1 is selected, the deceleration rate to achieve is $1.22 m/s^2$; if auto braking level MAX is selected, the deceleration rate to achieve is $4.27 m/s^2$ when the speed is greater than 41.2m/s and $3.66 m/s^2$ when the speed is lower than 41.2m/s (Christ, 2013). As discussed before, spoiler and flap positions have a significant impact on aerodynamic drag force, so spoiler and flap positions are used to determine the amount of drag force

applied to the aircraft body. The real-time aerodynamic drag deceleration is identified by the M-E aerodynamic drag force deceleration equation using the spoiler and flap configurations. In addition, according to the TLA configuration and the M-E engine thrust/reverse thrust deceleration equation, the real-time thrust/reverse deceleration rate is determined. The aerodynamic deceleration rate, which is a part of the entire deceleration, is a sum of both the real-time aerodynamic drag deceleration rate and the real-time thrust/reverse deceleration rate. The friction deceleration to achieve is determined by the deceleration rate to achieve and the aerodynamic deceleration rate. For example, if the real-time aerodynamic deceleration is $1m/s^2$ and the deceleration rate to achieve is $1.22m/s^2$ (auto braking level 1); the friction deceleration to achieve from the runway pavement is $0.22m/s^2$. According to the friction deceleration to achieve we can calculate the braking pressure needed. Aircrafts have limits for braking pressure for each auto braking level, and the limits vary from one aircraft type to another. For instance, the maximum aircraft system braking pressure for a Boeing 737-700, when auto braking level 2 is selected, is 10335kPa. The final applied braking pressure is determined based on the braking pressure needed; however, final applied braking pressure cannot exceed the maximum available braking pressure and the maximum aircraft system braking pressure. Once the applied braking pressure is selected, the final pavement friction deceleration rate can be calculated using the M-E friction deceleration equation.

The final achieved deceleration rate of the aircraft is a sum of the slope deceleration/acceleration, pavement friction deceleration rate, and the aerodynamic deceleration rate. The entire landing distance model is a dynamic model. The aircraft speed and weight are significant parameters in the process. The initial speed of the aircraft is determined by the aircraft touchdown speed. Finally, the aircraft deceleration rate for each time point can be calculated. The entire braking process can be simulated, which will provide speed and deceleration information to calculate the braking distance. The entire landing distance is a combination of braking distance and the distance from the runway threshold to the touchdown point.

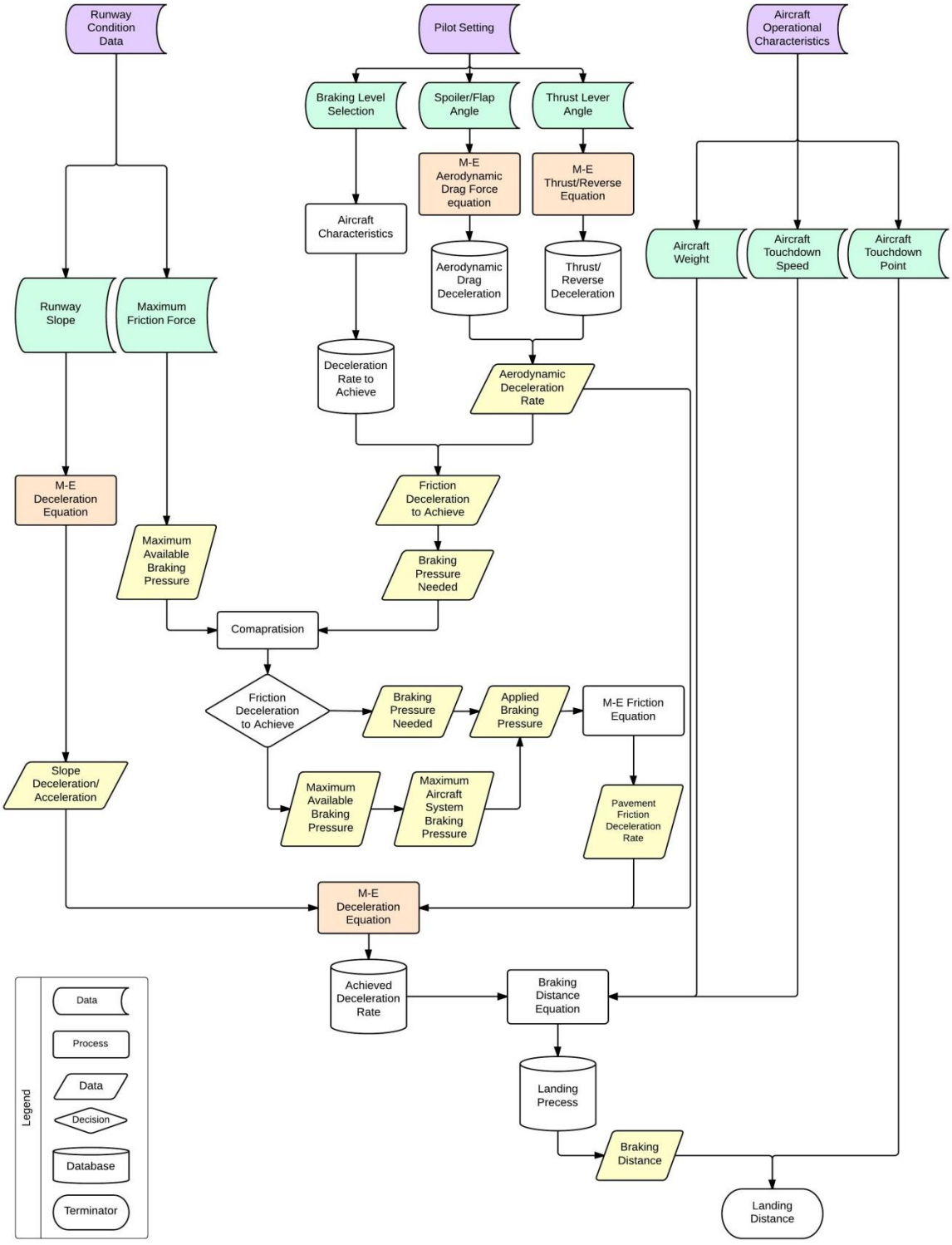

Figure 5.1 M-E Aircraft Landing Distance Model

5.2 Boeing 737-700 Real Data Case Study

5.2.1 Boeing 737-700 Landing Distance Prediction Study

This case study uses the same data as Chapter 3.4.1. The Boeing 737-700 aircraft programmed deceleration rate associated with each auto braking level is provided in Table 5-1 (Christ, 2013). Four auto braking levels are available for landing: 1, 2, 3, and MAX. Each level has a programmed deceleration rate as well as a maximum aircraft braking pressure.

Table 5-1 737 NG Airplanes Deceleration Rate (Christ, 2013)

AUTO BRAKE Selection	Deceleration Rate (m/s^2)	Pressure (kPa)
1	1.22	8853
2	1.52	10335
3	2.19	13780
Max	4.27(>41.2m/s) 3.66(<41.2m/s)	20670

The Angle of Attack (AOA) is an important factor in aircraft aerodynamic forces. AOA is the angle between the chord line of the airfoil and the relative motion vector between the aircraft and the fluid (Dole & Lewis, 2000). The lift coefficient increases with the increase of the AOA until it reaches a peak value. The relationship between the lift coefficient increases and AOA is linear before the maximum lift coefficient is achieved (Dole & Lewis, 2000).

According to the collected data, flap position 30 degree was selected, and ground spoiler position 40 degree was selected. Under this flap and spoiler configuration, the average AOA of the aircraft during braking, between aircraft touchdown and aircraft reducing to a lower safe speed, is -2.71. According to the Boeing 737 airfoil geometric shape, the relationship between AOA and lift coefficient is presented in Figure 5.2 (AirfoilTools.com, 2014; UIUC Applied Aerodynamics Group, 2014). The lift coefficient is negative and close to zero when the AOA is -2.21. The negative value means instead of generating a lift force, the aircraft airfoil generate a down force. Since the coefficient is relative small and close to zero, the force is assumed to be negligible in this research.

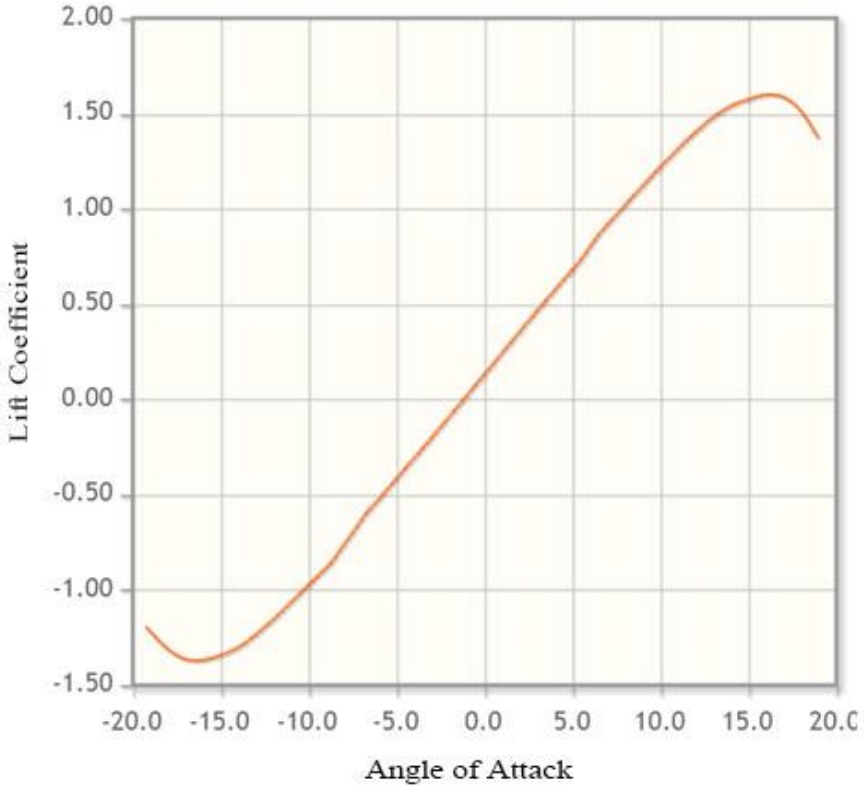

Figure 5.2 Boeing 737 Lift Coefficient vs AOA (AirfoilTools.com, 2014)

A comparison between the established M-E landing distance model and the 737 Quick Reference Handbook (737 QRH) reference landing distance is made to validate the model. The maximum braking coefficients of 0.05, 0.1, 0.2, and 0.3 are selected. Simulations are made with the input parameters displayed in Table 5-2.

Table 5-2 Simulation Parameters Information

No Reverse Thrust Aircraft Information	
TLA IDLE-Engine 1	35 deg
TLA IDLE-Engine 2	35 deg
Touchdown Speed	60 m/s
Air Density	1.3 kg/m3
Weight	60,000 kg
Flap Position	30 deg
Spoiler Position	40 deg
Angle of Attack	-3.2 deg
Reverse Thrust Aircraft Information	
Reverse Thrust Start Speed	60 m/s
Reverse Thrust End Speed	20 m/s
TLA IDLE-Engine 1	35 deg
TLA Reverse Thrust-Engine 1	10 deg
TLA IDLE-Engine 2	35 deg
TLA Reverse Thrust-Engine 2	10 deg
Touchdown Speed	70 m/s
Weight	60,000 kg
Flap Position	30 deg
Spoiler Position	40 deg
Angle of Attack	-3.2 deg
Airport Information	
Airport Altitude	321.6 m above sea level
Runway Length	3000 m
Runway Slope	0%
Weather Information	
Air Density	1.3 kg/m3

5.2.2 Results and Findings

Figure 5.3 and Figure 5.4 are the results of no reverse thrust landing distance and reverse thrust landing distance prediction, respectively, using the method in this thesis. Figure 5.5 and Figure 5.6 are the required landing distance provided by 737QRH Normal Configuration Landing Distance

Chart (NCLDC) with reverse thrust and without reverse thrust, respectively, with altitude adjustment conducted.

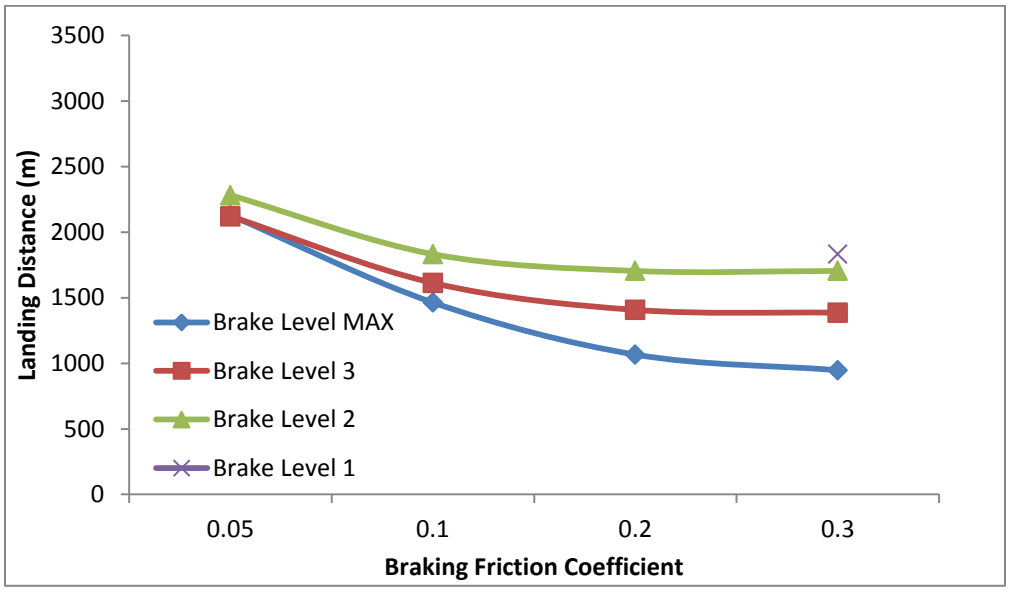

Figure 5.3 Landing Distance, Landing Distance Model, Reverse

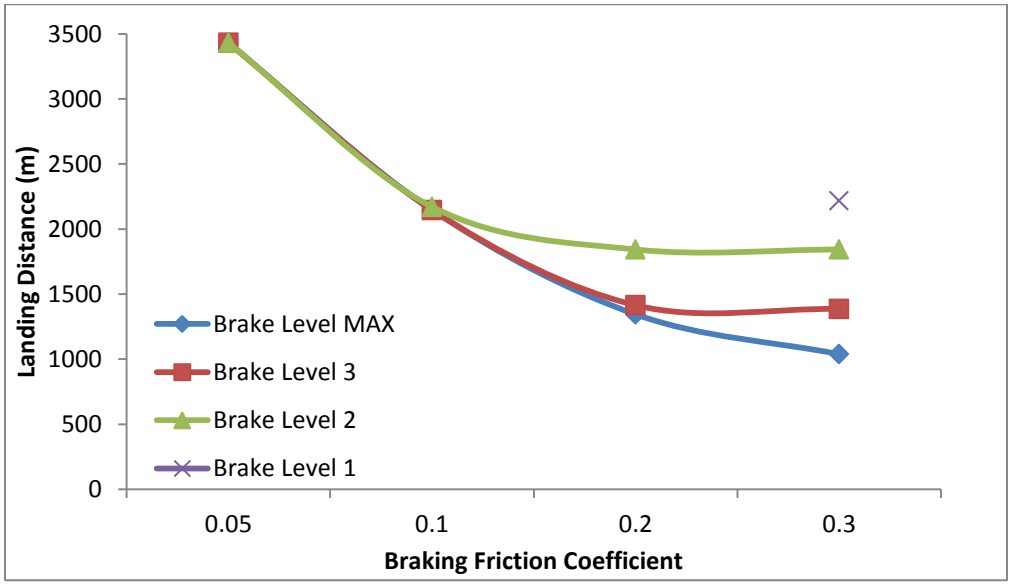

Figure 5.4 Landing Distance, Landing Distance Model, No Reverse

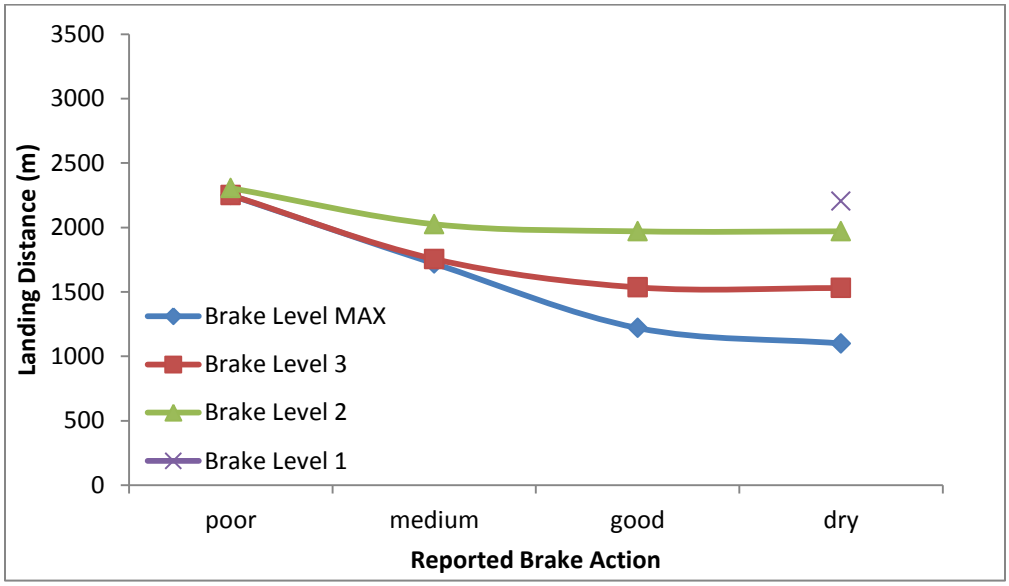

Figure 5.5 Reference Landing Distance, 737 QRH, Reverse (The Boeing Company, 2013)

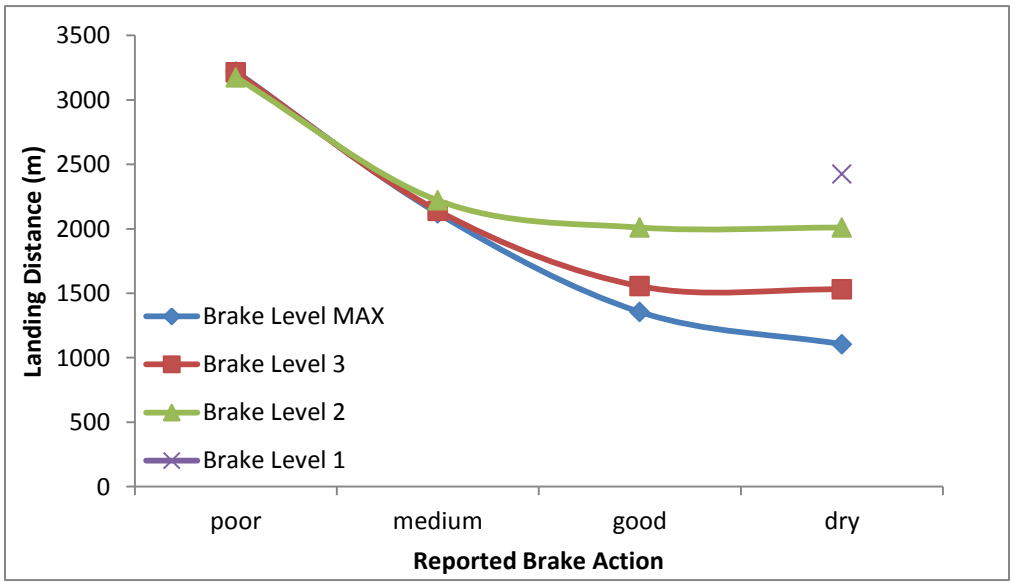

Figure 5.6 Reference Landing Distance, 737 QRH, No Reverse (The Boeing Company, 2013)

The two methods have similar results in landing distance. For reverse landing, the maximum difference between the two methods is 13%; and for no reverse landing, the maximum difference is 9%. The results indicate that the M-E landing distance model can provide an accurate prediction of landing distance.

When the runway pavement condition is poor, either the reported braking action is poor or the braking friction coefficient is 0.05, the landing distance is approximate 3500m when reverse thrust is not use and 2250m when reverse is used. Braking level 1, 2, 3, and MAX landing have similar landing distance. This fact indicates that when the runway condition is poor, changes in auto braking level will not influence much on landing distance. The reason is that the combination of runway surface braking and aerodynamic braking cannot generate enough deceleration to meet any auto braking level programmed deceleration rate for both reverse thrust landing and no reverse thrust landing. No reverse thrust landing takes 50% longer for the aircraft to stop, which demonstrates the importance of reverse thrust under severe runway conditions.

As the runway pavement friction increases, the landing distance decreases. A big drop in landing distance occurs when runway braking action turns from poor to medium and runway braking friction increases from 0.05 to 0.1 for no reverse landing, but for reverse landing, the decrease in landing distance is much smaller under the same condition. It indicates when the runway friction condition is very poor, reverse thrust is the main aircraft decelerating contributor.

For all the results, the differences of the landing distances between different levels become greater with the friction condition improves. As the runway pavement friction increases, the difference between no reverse landing and reverse landing for each level becomes smaller. The figures indicate that when the runway is dry or reported braking action is good, braking level 2, 3 have the same landing distance. The reason is that the runway friction is enough to achieve the programmed deceleration rate. But for braking level MAX landing, the landing distance is still decreasing with the runway friction increases. The reason is because the programmed deceleration rate for level MAX is excessively high and needs a very good runway surface friction condition to meet the requirement.

The time-speed diagrams of the results are given in Figure 5.7 and Figure 5.8. The findings are summarized as follows.

The slopes of the curves represent the deceleration; and the larger the slope is, the greater the deceleration is. The time-speed curves are not straight lines or straight polylines. The slope of the curves becomes smaller with the decrease of the speed. The reason is that the aerodynamic drag force is a function of speed square. As time goes on, the speed decreases, resulting in a decrease in aerodynamic drag force.

In Figure 5.7 (a), (c), (e), and (g), big changes in slope occur when the speed is 65m/s and 30 m/s. The reason is that during speed decreasing from 65 m/s to 30m/s reverse thrust is used. The changes for the runway braking friction coefficient of 0.05 and 0.1 are more obvious than the changes for the runway braking friction coefficient of 0.2 and 0.3. This fact proves that when the runway cannot provide enough friction force, reverse thrust has a significant influence on aircraft landing deceleration as well as landing distance. As the runway frictional quality increases, the influence becomes smaller.

In Figure 5.7 (b), all the time-speed curves coincide, because during poor runway friction condition landing, the combination of aerodynamic drag force and friction force cannot provide enough deceleration for any braking level. In this case, aircraft braking system takes the most advantage of the available friction for all braking levels, therefore, they have the same deceleration.

Comparison between Figure 5.7 (b), (d), (f), and (h) indicates that the difference between different braking levels become greater as the runway available braking friction coefficient increases. This is because the runway surface can provide more friction to try to fulfill the programmed deceleration rate.

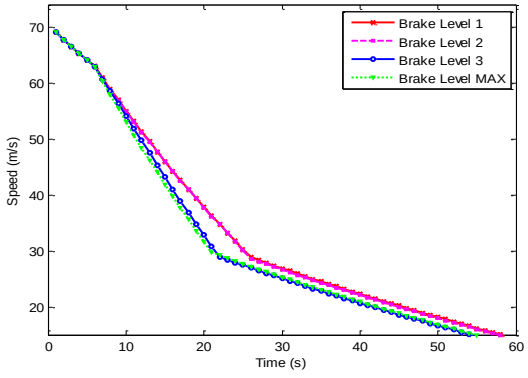

(a) Mu=0.05, Reverse Thrust

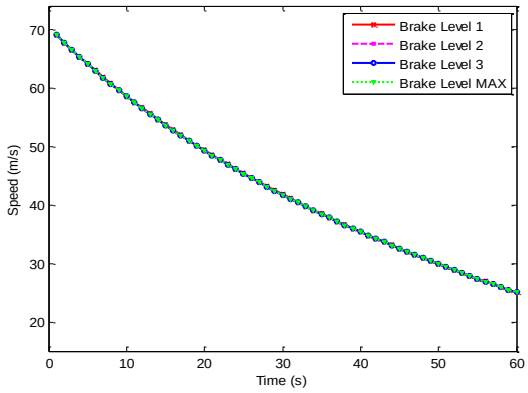

(b) Mu=0.05, No Reverse Thrust

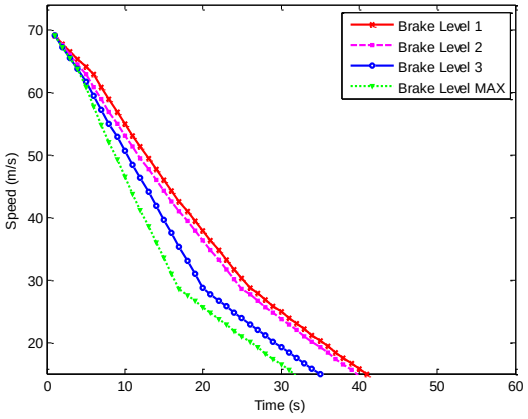

(c) Mu=0.1, Reverse Thrust

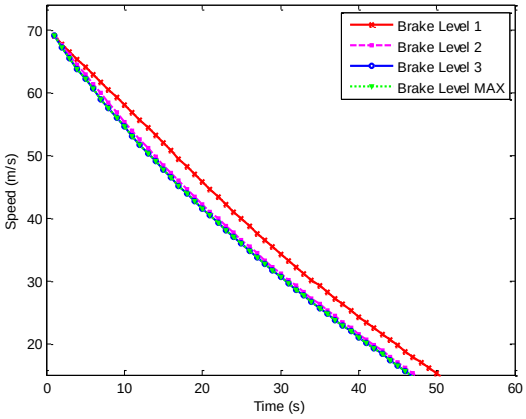

(d) Mu=0.1, No Reverse Thrust

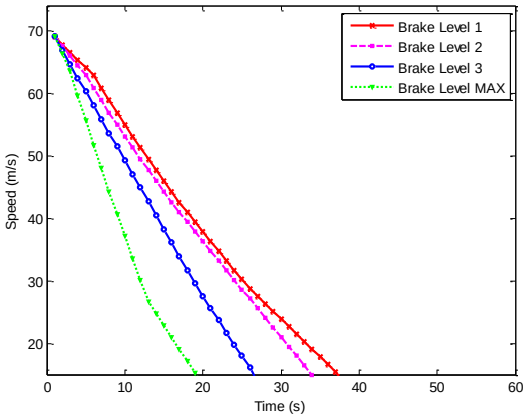

(e) Mu=0.2, Reverse Thrust

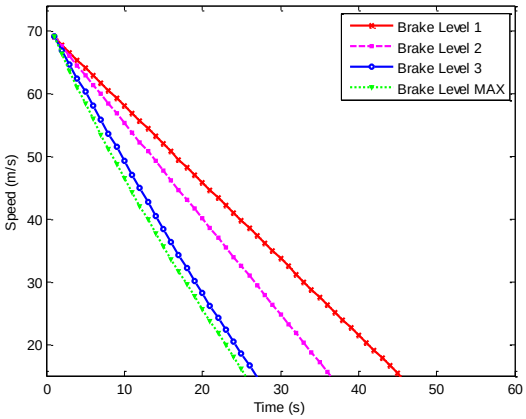

(f) Mu=0.2, No Reverse Thrust

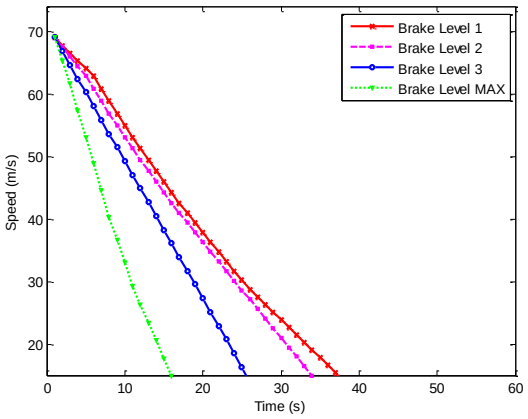

(g) Mu=0.3, Reverse Thrust

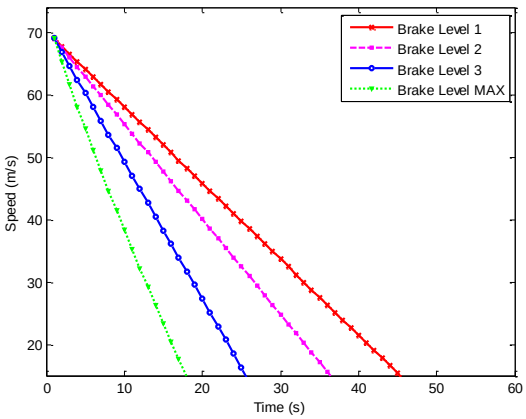

(h) Mu=0.3, No Reverse Thrust

Figure 5.7 Time-Speed Diagrams by Braking Coefficient

Figure 5.8 indicates that when reverse thrust is used, the difference between different runway pavement braking friction coefficients for the same braking level is smaller than when reverse thrust is not used. When the braking friction coefficient increases, lower braking levels start to distinguish from each other, and then the higher levels.

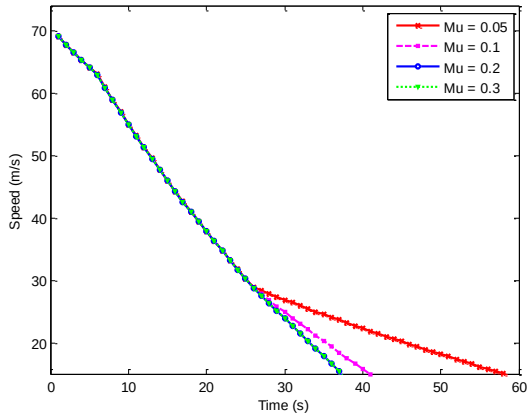

(a) Braking Level 1, Reverse Thrust

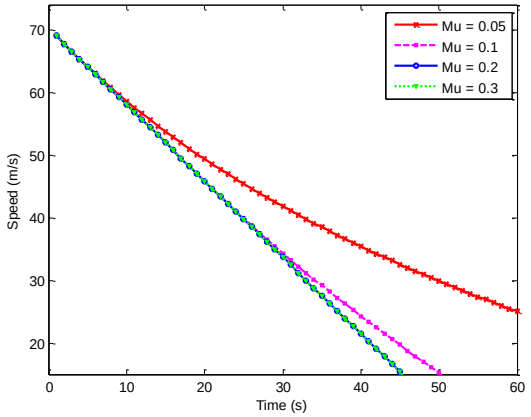

(b) Braking Level 1, No Reverse Thrust

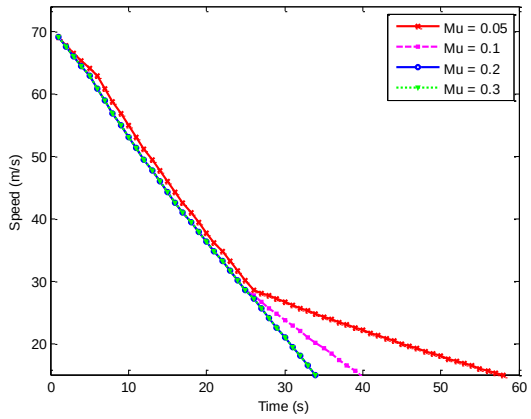

(c) Braking Level 2, Reverse Thrust

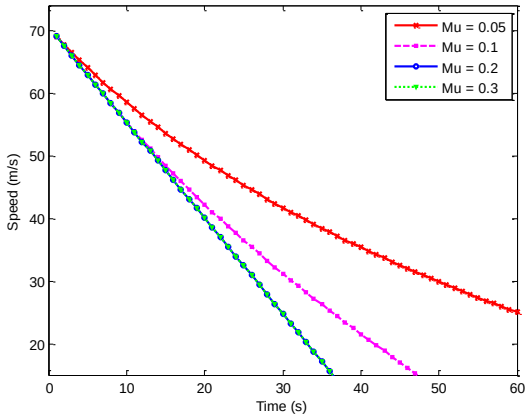

(d) Braking Level 2, No Reverse Thrust

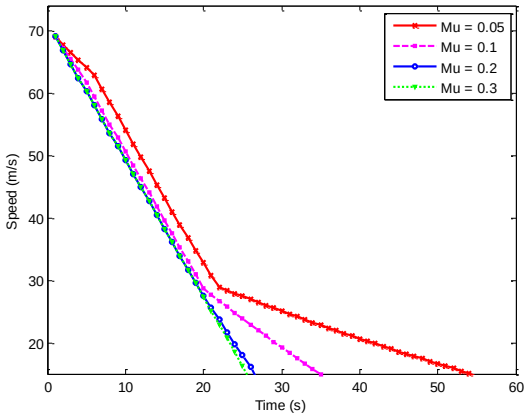

(e) Braking Level 3, Reverse Thrust

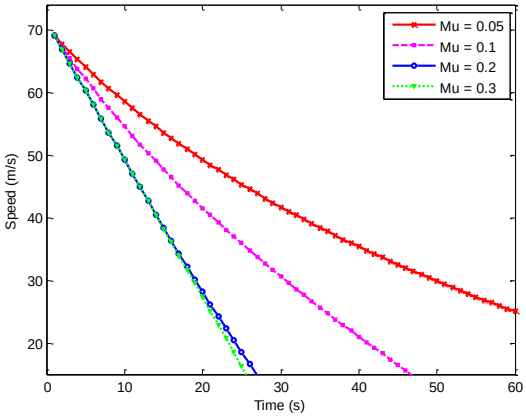

(f) Braking Level 3, No Reverse Thrust

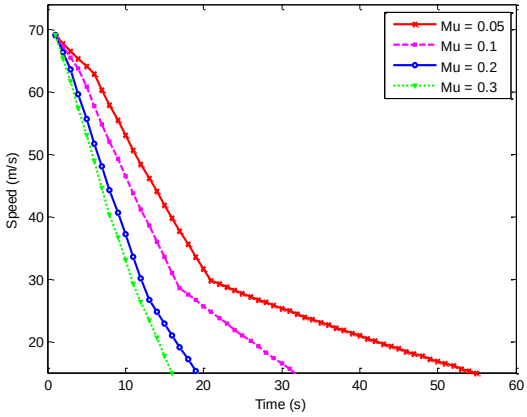

(g) Braking Level MAX, Reverse Thrust

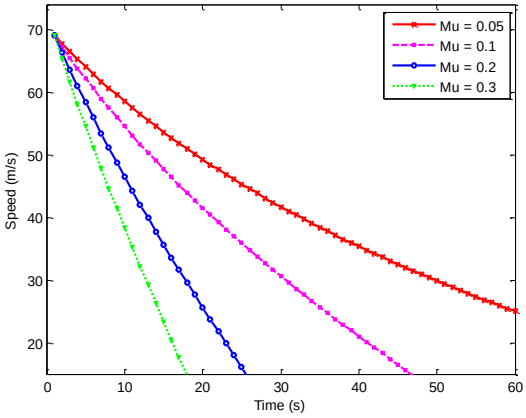

(h) Braking Level MAX, No Reverse Thrust

Figure 5.8 Time-Speed Diagrams by Braking Level

5.3 Advantages of This Method

In this chapter, a landing distance prediction method is established which incorporates a mechanistic-based analysis and an empirical real flight data calibration. The method established in this paper has several advantages over the current landing distance prediction methods. Compared to the NCLDC provided by the Boeing Company (2013), the method established in this paper uses quantified runway condition information and an accurate amount of reverse thrust applied. Compared to the ROPS provided by Airbus Company (Airbus, 2010; Chapman, 2013) and Puvrez's study (1965), the method can be applied to a wide application of aircrafts. Compared to the Transport Canada method (Transport Canada, 2014b), it can be used for both winter operation and summer operation (both

contaminated runway and wet runway) and does not need dry runway landing distance reference. Compared to Combat Traction Report (Wahi, 1977; Warren et al., 1974) and Van Es et al.'s study (2010), pilot settings are taken into consideration and more factors are studied to calculate the landing distance. Compared to Pasindu et al.'s study (2011), reverse thrust and antiskid brake system is incorporated.

5.4 Summary

A landing distance model has been established base on the M-E deceleration equation in this chapter. Parameters of pilot settings, aircraft operational characteristics, weather condition, and runway friction condition are considered in building the model.

Since the model incorporates mechanistic analysis and empirical calibrations and integrates a variety of influence factors, it has several advantages over the previous research methods:

- Incorporating pilot settings;
- Considering accurate amount of reverse thrust;
- Providing a wide application of aircrafts and airport runways; and
- Considering antiskid braking system.

A Boeing 737-700 landing distance real data case study was conducted using the landing distance prediction method established in this thesis. Simulation results indicated the model has similar results as the required landing distance provided by Boeing 737 QRH and offers an accurate prediction of aircraft landing distance.

Chapter 6
Potential Applications

Following the development of the M-E aircraft deceleration equation and landing distance model, a summary of their potential applications is presented in this chapter.

6.1 Introduction

Since the M-E aircraft deceleration equation and braking analysis are based on aircraft measurements, a uniform runway assessment, evaluation, and reporting framework can be built based on this study. Aircraft runway overrun is a major airline and airport safety concern, especially for airports located in Canada with diverse weather conditions. Therefore, the landing distance model can be applied to calculate required landing distances before landing to mitigate the risk of runway overrun. Because of the accurate prediction of landing distance model, it can potentially be applied to optimize quick exit taxiway design and airport operation. Considering pilot settings and accurate amount of reverse thrust are incorporated, the landing distance model also has the potential to help airlines control and reduce fuel consumption. Finally, a braking availability tester and an associated study of wet and contaminated runway aircraft landing performance will be discussed.

6.2 Runway Assessment, Evaluation, and Reporting Framework

It should be noted that different airports use different runway friction measurement devices. The devices may be produced by different manufacturers and provide testing results inconsistently. The aviation industry and aviation authorities have realized this inconsistency. FAA and ICAO developed friction level classification for runway pavement surfaces based on different friction measurement devices. In addition, the pilots have realized that the runway friction information varies between different airports (Biggs & Hamilton, 2002). The reported friction assessment should be converted to a standard braking friction value. Figure 6.1 is a runway assessment, evaluation, and reporting framework, which is based on the developed M-E aircraft deceleration equation, the braking friction coefficient, and the M-E landing distance model.

In this framework, airports can use their own local friction measurement device and convert the testing result to a braking friction coefficient value that can be directly related to an aircraft braking performance through the M-E aircraft deceleration equation.

One friction measure device should be selected as the standard friction measurement device. Data from the standard friction device and different friction measurement devices are collected and retrieved into a ground device databases. As a result, the results from different friction devices can be converted to the standard device results, which are reported as braking friction coefficient values. Digital flight data from different types of aircrafts are collected and retrieved into an aircraft database. Based on the digital flight data, M-E deceleration equation for each type aircraft can be developed. A relationship between the aircraft braking performance and the standard friction measurement device test results can be built. In this way, airports can develop the relationship between their local devices and the landing aircraft. The M-E deceleration equation and the calibrated aircraft braking friction coefficient should be reported to the authority and provided to the pilots. With the help of the landing distance model, the pilot can calculate the required landing distance prior to landing.

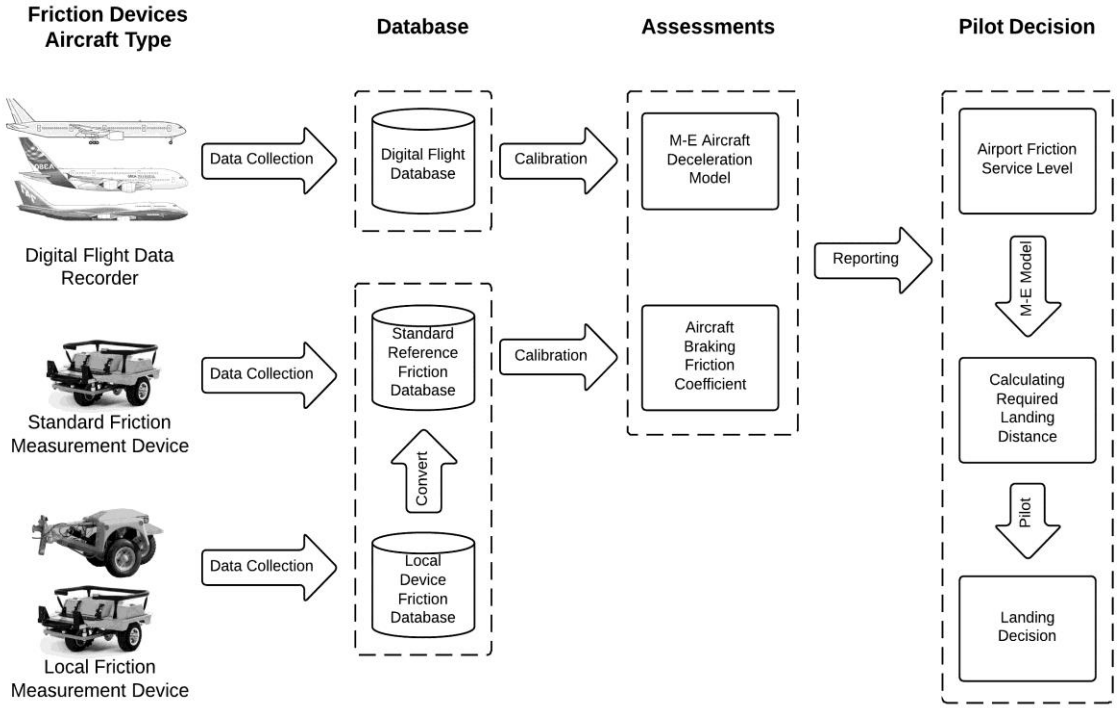

Figure 6.1 Runway Assessment, Evaluation, and Reporting Framework

6.2.1 Improvement over Current Framework

One of the distinguishing features of this framework is that the framework can provide uniform information with small variance because all the local testing results are converted to standard braking friction coefficient values, which can be related directly to an aircraft braking performance. The current reported friction coefficient represents the friction condition of the runway surface but cannot reflect the aircraft braking performance accurately. In addition, the other distinguishing feature is that in this framework, different devices and aircrafts are calibrated respectively, which contributes a good correlation between the braking friction coefficient and a given aircraft's landing performance.

6.3 On-Board Landing Distance Calculation

The M-E landing distance model can be applied in airlines for routine safety management. The airlines can collect flight data from the Quick Access Recorder or the Flight Data Recorder on their aircraft and reserve them into a database. Then deceleration equations for each aircraft can be calibrated based on the flight data. Then the airline can use the landing distance prediction model to calculate the landing distance for a specific airport runway under different runway friction conditions. In this way, the airline can have an accurate prediction of the required landing distance. Therefore, aircraft overrun accidents can be prevented and airline operation safety can be improved. A program has been developed based on the M-E aircraft landing distance prediction method. Figure 6.2 demonstrates the user interface of the program.

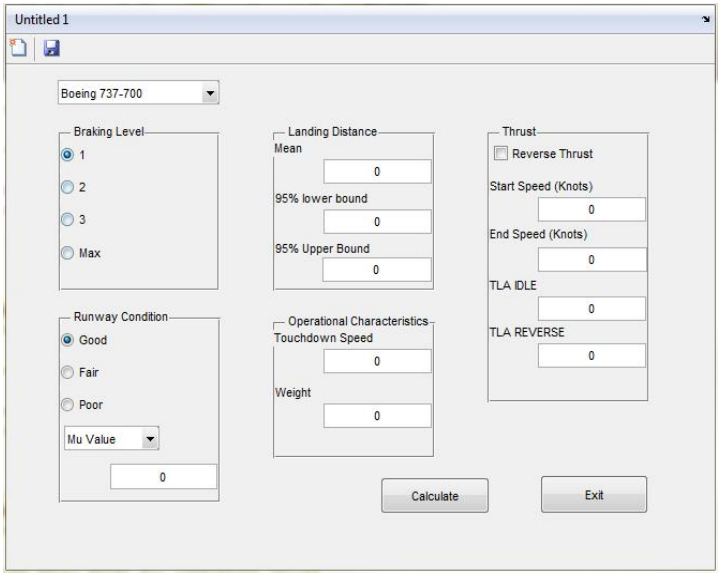

Figure 6.2 M-E Aircraft Landing Distance Prediction Program

6.4 Quick Exit Taxiway Design and Airport Operation Optimization

When designing the airport, aircraft demands are predicted. With the prediction of different type of aircrafts, associated landing processes can be simulated. As a result, quick exit taxiway can be designed at the location where most aircrafts stop to a lower safe turn-off speed.

The airport and air traffic control can use the landing distance model to calculate the landing distance and landing time needed. In this way, better decision of taxiway selection can be made and runway occupation time can be determined more accurately.

6.5 Fuel Consumption Reduction

The M-E aircraft landing distance model considers an accurate amount of reverse thrust, and reverse thrust is one of the main fuel consumptions during landing. Therefore, the M-E aircraft landing distance model has the potential to help airlines reduce fuel consumption. An example is given below.

Example: a Boeing 737-700 aircraft is going to land on a runway at sea level 0 ft with a runway length of 3400m. The air density is 1.3kg/m^3, and the wind is heading 30 degree off the runway with a headwind component of 8.5 knots and a crosswind component of 5 knots. The runway condition is 100 percent bare and dry with good frictional prosperity. The available braking friction coefficient of the given runway is 0.45. The aircraft is approaching using standard technique which includes a stable approach and flare, and a firm touch down. The weight of the aircraft is 60t and the touchdown speed of the aircraft is 125 knots (65 m/s).

With the given information, M-E aircraft landing distance model is used to calculate the required landing distance. Four options are given in Table 6-1. For a 3400m runway, the safety factor is determined to be 1.5. With the given four landing thrust configurations, all landings can provide enough safety margins. The first three options have similar landing distance with the same braking level, but the reverse thrust time is significantly different. Compared to Option 1, Option 3 has approximately the same landing distance; however, saves fuel of 23 seconds reverse thrust.

Table 6-1 Landing Setting Options

	Option 1	Option 2	Option 3	Option 4
Reverse Thrust Use	Yes	Yes	No	No
Flap Position (Degree)	30	30	30	30
Spoiler Use	Yes	Yes	Yes	Yes
Braking Level	2	2	2	1
Reverse Thrust Start Speed (m/s)	65	65	N/A	N/A
Reverse End Start Speed (m/s)	30	45	N/A	N/A
Reverse Thrust Time (s)	**23**	**13**	**0**	**0**
Predicted Landing Distance (m)	1732	1748	1843	2217
Runway Required Length (m)	**2598**	**2662**	**2764**	**3325**
Runway Length Adequate (m)	Yes	Yes	Yes	Yes

6.6 Braking Availability Tester

6.6.1 Introduction

The Braking Availability Tester (BAT) was developed in partnership with the University of Waterloo and Team Eagle Ltd. The objective of the BAT project is to design a runway pavement measurement device that can provide pilots with real time runway braking availability, especially for landing at airports with wet or contaminated runways. The provided braking availability information can help pilots make better landing decisions.

The distinguishing feature of the BAT is that it simulates an aircraft's real braking performance. This is done by installing an aircraft landing gear wheel and brake with an Antiskid Braking System (ABS) algorithm controlling them in the bank of a F350 (Figure 6.3). The BAT can provide loading of nearly 10% of a Boeing 737 aircraft, which provides a relative accurate simulation of a real aircraft braking performance (Joshi, Jeon, Kwon, & Tighe, 2013). Several sensors are embedded and measure torque load, speed, braking pressure, wheel speed, drag force, temperature, etc. This allows the BAT to monitor all aspects of braking performance of the landing gear wheel. During testing, the pickup truck accelerates to a certain speed with embedded landing gear wheel raised. After the certain speed is reached, the hydraulic system power down the landing gear wheel, this process can simulate the touchdown process of an aircraft. As soon as the landing gear touches the pavement surface, braking pressure can be applied to the wheel. During the testing, the drag force from the pavement surface is measured by the horizontal load cell; braking torque is measured by the torque load cell.

(a) BAT Braking Landing Gear Wheel (MME, UW)

(b) Overall View of BAT (MME, UW)

Figure 6.3 BAT

6.6.2 Anticipated Significance and Future Works

The BAT has the potential to be the standard friction measurement device in the runway assessment, evaluation, and reporting framework. Additionally, by combining the M-E aircraft landing distance prediction method and the BAT, this project is able to provide the aviation industry a better understanding of the effects of contaminated runways regarding aircraft braking performance as well

as an accurate prediction of aircraft braking performance and its required landing distance. For example, since the BAT simulates the landing performance of an aircraft, it has the potential to measure the braking friction coefficient of the pavement. With the help of the real-time braking friction coefficient measured by BAT, the aircraft braking performance can be analyzed and its required landing distance can be calculated by the M-E landing distance model.

Chapter 7
Conclusions and Recommendations

7.1 Conclusions

The purpose of this research is to produce a comparative new method of analyzing airport runway pavement braking performance through innovative modeling. The objectives stated in Chapter 1 of this thesis have been successfully achieved in this research.

First, the establishment of the M-E deceleration equation was conducted. The equation was developed based on aircraft force and moment analysis and is calibrated by digital flight data and weather data. A WestJet Boeing 737-700 case study is conducted. According to the equations, digital flight data, weather data, and pavement data were collected and used to calibrate the aircraft characteristic adjustment coefficients. The validation results indicated that the equation provides an accurate prediction of the aircraft landing deceleration.

Then, the braking analysis is done based on the developed M-E deceleration equation. A study of a Boeing 737-700 aircraft landing on dry, wet, and contaminated runways is conducted. The final conclusions from the study can be summarized as follows:

- A wet runway can have a similar runway frictional condition as a dry runway if the runway pavement is well maintained.
- Compared to wet runways, contaminated runways have a larger impact on aircraft braking performance. However, a small amount of contaminant on a reliable runway will not decrease runway braking friction considerably; instead, the runway will perform similar to a clean dry runway.
- Available braking friction coefficient decreases with the increase of the ground speed. The available braking friction coefficient of a wet runway is more dependent on speed and decreases faster than that of a dry runway.

An M-E landing distance model is developed based on the M-E deceleration equation, aircraft braking system characteristics, and pilot configurations. In addition, weather conditions and aircraft operational characteristics are incorporated in this model. Therefore, the model has several distinguishing features including: incorporating a variety of influence factors, considering an accurate amount of reverse thrust, providing wide application of aircrafts and airport runways, and

incorporating antiskid braking system. A Boeing 737-700 case study is conducted using the developed model and the Boeing 737 QRH. The results can be concluded as:

- The M-E landing distance model can offer an accurate prediction of the required landing distance.
- Reverse thrust is a significant landing distance influence factor when the runway is in severe condition; however, with the runway fictional condition increases, the contribution of reverse thrust decreases.

Finally, potential application of this research is discussed and summarized as follows:

- Development of a Runway Assessment, Evaluation, and Reporting Framework
- On-Board Landing Distance Calculation,
- Quick Exit Taxiway Design and Airport Operation Optimization
- Fuel Consumption Reduction
- Development of the Braking Availability Tester

7.2 Major Contributions

The major contributions of this thesis are listed as the following points:

- This thesis developed a novel M-E deceleration equation to model aircraft braking performance during landing. The equation is calibrated using flight data, which provides a more precise prediction of aircraft deceleration.
- This thesis presents a new method of analyzing aircraft braking performance with the developed M-E deceleration equation which addresses the issue of friction measurement devices' inconsistences. Braking friction coefficient is studied in detail, which provides a deep understanding of aircraft braking performance based on aircraft measurements.
- This thesis introduces an M-E aircraft landing distance model. The M-E aircraft landing distance model integrated a variety of influence factors such as pilot settings, accurate amount of reverse thrust, antiskid braking system performance, and provided a wide application of aircrafts and airport runways. There characteristics have not been

incorporated together in a current existing method. In addition, the M-E aircraft landing distance model is proved to offer an accurate prediction of the required landing distance.

7.3 Recommendations and Future Work

All of the collected data in this research is from a commercial aircraft that did not use full braking for all the flights. In addition, Waterloo International Airport maintained its runway in a good condition with high level of services. Therefore, hydroplaning and insufficient friction braking due to wet and contaminated runways did not occur in the collected data. The following points are recommended for future research.

- Testing of aircraft landing on runways with more severe wet and contaminated conditions are recommended.
- Full braking or max braking landing testing is recommended to analyze the available braking friction.
- Runway roughness influence on runway braking should be conducted in the future study.

References

Airbus. (2010). Runway Overrun Protection System. *Third Meeting of the Regional Aviation Safety Group – Pan America,*

AirfoilTools.com. (2014). Boeing 737 Midspan Airfoil - Boeing Commercial Airplane Company Model 737 Airfoils. Retrieved 05/19, 2014, from http://airfoiltools.com/airfoil/details?airfoil=b737b-il

Anderson, J. D. (2001). *Fundamentals of Aerodynamics* (3rd ed.). New York: McGraw-Hill.

Andresen, A., & Wambold, J. (1999). *Friction Fundamentals, Concepts and Methodology (Prepared for Transportation Development Centre Transport Canada).* (No. TP 13837E). Montreal, Quebec, Canada: Transport Canada.

Biggs, D. C., & Hamilton, G. (2002). *Runway Friction Accountability Risk Assessment, Results of a Survey of Canadian Airline Pilots.* (No. TP 13941E). Montreal: Transportation Development Centre: Transport Canada.

Chapman, F. (2013). A380 & A380 On Board Technology Support for Ground Manoeuvering. *Airfield Action Forum 2013: Optimising Airport Capacity,*

Christ, B. (2013). The Boeing 737 Technical Site-Landing Gear, Updated 24 Feb 2013. Retrieved 07/13, 2013, from http://www.b737.org.uk/landinggear.htm

Comfort, G. (2001). *Wet Runway Friction: Literature and Information Review.* (Final No. TP 14002E). Transportation Development Centre, Montréal: BMT Fleet Technology Limited.

Croll, J., Bastuan, M., Martin, J. C. T., & Carson, P. (2002). *Evaluation of Aircraft Braking Performance on Winter Contaminated Runways and Prediction of Aircraft Landing Distance Using the Canadian Runway Friction Index.* (Final No. TP 13943E). Ottawa, Ontario, Canada: Transport Canada.

Dole, C. E., & Lewis, J. E. (2000). *Flight Theory and Aerodynamics: A Practical Guide for Operational Safety* (2nd Edition). U.S.A.: John Wiley & Sons. DOI: TL570.D56

Environment Canada. (2014). Canadian Historical Weather Radar - Exeter (near London). Retrieved 05/09, 2014, from http://climate.weather.gc.ca/radar/index_e.html?RadarSite=WSO

FAA. (1997). *Measurement, Construction, and Maintenance of Skid-Resistant Airport Pavement Surfaces.* (Advisory Circular No. 150/5320-12C). U.S.: U.S. Department of Transportation.

Joshi, K., Jeon, S., Kwon, H., & Tighe, S. (2013). Braking Availability Tester (BAT) for Realistic Assessment of Aircraft Landing Distance on Winter Runways. *Journal of Aerospace Engineering*, doi:10.1061/(ASCE)AS.1943-5525.0000395

Hall, J. W., Smith, K. L., Titus-Glover, L., Wambold, J. C., Yager, T. J., & Rado, Z. (2009). *Guide for Pavement Friction.* (No. NCHRP Web-Only Document 108). U.S.: National Cooperative Highway Research Program, Transportation Research Board of the National Academies.

Henry, J. (2000). *Evaluation of Pavement Friction Characteristics, A Synthesis of Highway Practice. NCHRP Synthesis no. 291*. Washington D.C.: National Cooperative Highway Research Program.

Horne, W. B. (1975). *Wet runways.* (Technical Memorandum No. TM-X-72650). NASA Langley Research Center, Hampton, VA 23665: NASA.

Horne, W. B., McCarty, J. L., & Tanner, J. A. (1976). *Some Effect of Adverse Weather Conditions on Performance of Airplane Antiskid Braking Systems.* (Technical Note No. NASA TN D-8202). Washington, D.C.: NASA.

Horne, W. B., & Dreher, R. C. (1963). *Phenomena of Pneumatic Tire Hydroplaning* National Aeronautics and Space Administration.

IATA. (2009). *Annual report - 2009.* (Annual Report). Kuala Lumpur: International Air Transport Association.

IATA. (2011). *Annual report - 2011.* (Annual Report). Singapore: International Air Transport Association.

IATA. (2012a). *Annual review - 2012*. Beijing: International Air Transport Association.

IATA. (2012b). Global Accident Rate Reaches New Low - Regional Challenges Remain. Retrieved 02/21, 2014, from http://www.iata.org/pressroom/pr/pages/2012-03-06-01.aspx

ICAO. (2002). *Airport Service Manual, Part 2: Pavement Surface Conditions,* (4th ed.) International Civil Aviation Organization.

ICAO. (2004). *Annex 14 Aerodromes, Volume I, Aerodrome Design and Operations.* International Civil Aviation Organization:

Klein-Paste, A., Huseby, A. B., Anderson, J. D., Giesman, P., Bugge, H. J., & Langedahl, T. (2012). Braking Performance of Commercial Airplanes During Operation on Winter Contaminated Runways. *Cold Regions Science and Technology, 79*, 29-37.

Klein-Paste, A., Sinha, N. K., Løset, S., & Norheim, A. (2007). Microstructural Analytical Techniques for Snow Compacted by an Aircraft Tire. *Tribology International, 40*(2), 412-417.

Leland, T. J. (1965). *An Investigation of The Influence of Aircraft Tire-Tread Wear on Wet-Runway Braking.* (NASA Technical Note No. NASA-TN-D-2770). WASHINGTON, D. C.: National Aeronautics and Space Administration.

Leland, T. J., Yager, T. J., & Joyner, U. T. (1968). *Effects of Pavement Texture on Wet-Runway Braking Performance.* (No. NASA-TN-D-4323). NASA, Washington D.C.: National Aeronautics and Space Administration.

Moir, I., & Seabridge, A. (2008). *Aircraft Systems: Mechanical, Electrical and Avionics Subsystems Integration* (3rd ed.). England: John Wiley & Sons.

NTSB. (2007). *Aircraft Accident Report：Runway Overrun and Collision Southwest Airlines Flight 1248.* (Aircraft Accident Report No. NTSB/AAR-07/06). Washington, D.C.: National Transportation Safety Board.

NTSB. (2008). *Aircraft Accident Report: Runway Overrun During Landing Pinnacle Airlines Flight 4712.* (Aircraft Accident Report No. NTSB/AAR-08/02). Washington, D.C.: National Transportation Safety Board.

Pasindu, H., Fwa, T., & Ong, G. P. (2011). Computation of Aircraft Braking Distances. *Transportation Research Record: Journal of the Transportation Research Board, 2214,* 126-135. doi:10.3141/2214-16

Puvrez, P. A. (1965). Variations of Landing Distance of Fixed-Wing Aircraft in STOL Operations. *Journal of Aircraft, 2*(4), 288-296.

Shepler, A. J. (2010). *Turbine Engine Thrust Scheduling* U.S. Patent Application,12/775,586.

TAC. (2013). *Pavement Asset Design and Management Guide*. Canada: Transportation Association of Canada.

Tanner, J. A., & Stubbs, S. M. (1977). *Behavior of Aircraft Antiskid Braking Systems on Dry and Wet Runway Surfaces: A Slip-Ratio-Controlled System with Ground Speed Reference from Unbraked Nose Wheel.* (No. NASA TN D-8455). Washington D.C.: NASA Langley Research Center.

The Boeing Company. (2013). *737 Flight Crew Operations Manual-737 Quick Reference Handbook.* (No. D6-27370-7Q8-SHA). Seattle, Washington, U.S.: The Boeing Company;.

Transport Canada. (1989). *Runway Rubber Removal Requirements Study.* (No. AK-67-09-370). Canada:

Transport Canada. (1999a). *Commercial and Business Aviation Advisory Circular*. (Aviation Advisory Circular No. No. 0164). Canada: Transport Canada.

Transport Canada. (1999b). *Overview of The Joint Winter Runway Friction Measurement Program* (No. 2450-B-14). Montreal, Quebec, Canada: Transport Canada.

Transport Canada. (2004). *Guidelines Respecting the Measurement, Evaluation and Maintenance of Airfield Pavement Surface Friction.* (Aerodrome Safety Circular No. ASC 2004-024). Canada: Transport Canada.

Transport Canada. (2012). *Glossary for Pilots and Air Traffic Services Personnel (REVISION no. 21).* (No. TC-1004759). Ottawa: Transport Canada.

Transport Canada. (2014a). *Airport Winter Maintenance and Planning.* (Advisory Circular No. AC 302-013). Canada: Transport Canada.

Transport Canada. (2014b). *TP 14371 - Transport Canada Aeronautical Information Manual (TC AIM) : AIR - Airmanship*. Canada: Transport Canada.

UIUC Applied Aerodynamics Group. (2014). UIUC Airfoil Coordinates Database. Retrieved 05/19, 2014, from http://www.ae.illinois.edu/m-selig/ads/coord_database.html

Van Es, G. W. H. (2005). *Running Out of Runway: Analysis of 35 Years of Landing Overrun Accidents.* (No. NLR-TP-2005-498). Amsterdam: National Aerospace Laboratory.

Van Es, G. W. H., Van der Geest, Peter J, Cheng, A., & Hackler, L. (2010). *Estimation of Landing Stopping Distances from Flight Data.* (No. DOT/FAA/AR-09/46). Washington, DC: U.S. Department of Transportation, Federal Aviation Administration.

Van Es, G. (2001). Hydroplaning of Modern Aircraft Tires. (No. NLR-TP-2001-242).National Aerospace Laboratory NLR.

Van Es, G., Roelen, A., Kruijsen, E., & Giesberts, M. (2001). *Safety Aspects of Aircraft Performance on Wet and Contaminated Runways.* (No. NLR-TP-2001-216).National Aerospace Laboratory NLR.

Wahi, M. K. (1977). Application of Dimensional Analysis to Predict Airplane Stopping Distance. *Journal of Aircraft, 14*(2), 209-214.

Warren, S., Wahi, M., Amberg, R., Straub, H., & Attri, N. (1974). *Combat Traction II, Phase II, Volume I, Narrative.* (No. ASD-TR-74-41 FAA-RD-74-221). U.S.: DTIC Document.

WestJet. (2014). Media and Investor Relations-Our fleet. Retrieved 05/05, 2014, from http://www.westjet.com/guest/en/media-investors/fleet.shtml

Xiaoyan, L. (2009). Statistical Analysis of Global Runway Excursion Accidents of Commercial Jets in the Last Decade. *China Civil Aviation, 9*, 37-39.

Yager, T. (1983). Factors Affecting Aircraft Ground Handling Performance. *NASA Technical Memorandum, 85652*

YKF. (2014). The Region of Waterloo International Airport-Airport Specifications. Retrieved 06/01, 2014, from http://www.waterlooairport.ca/en/pilotinformation/airportspecifications.asp

Zhang, C., Tighe, S. L., Jeon, S., & Kwon, H. J. (2014). A Mechanistic-Empirical Aircraft Landing Distance Prediction Method. *Transportation Research Board 93rd Annual Meeting,* Washington D.C. (Development of Database Applications for Airport Planning and Design)

Zhang, C., & Tighe, S. L. (2014). Improving Runway Pavement Friction Analysis through Innovative Modeling. *2014 FAA Worldwide Airport Technology Transfer Conference,* New Jersey, USA. (Innovations in Airport Safety and Pavement)

Appendix A

Speed-Time Diagrams

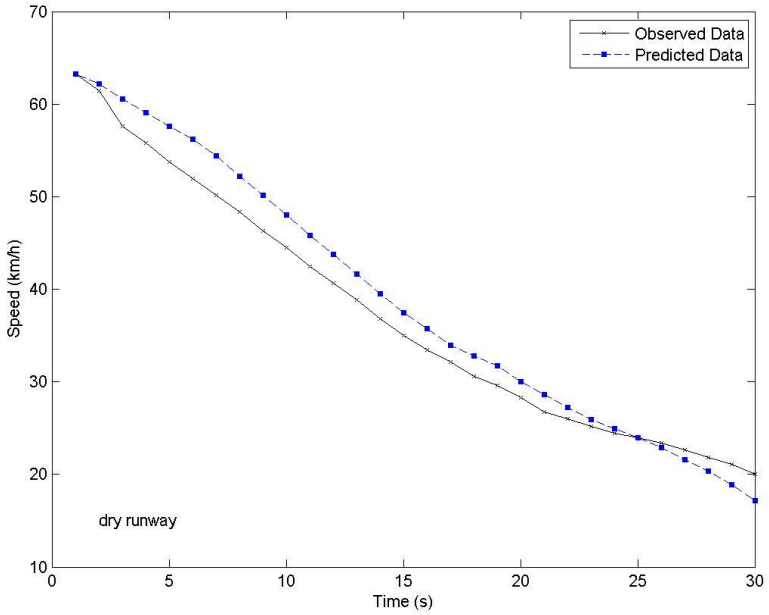

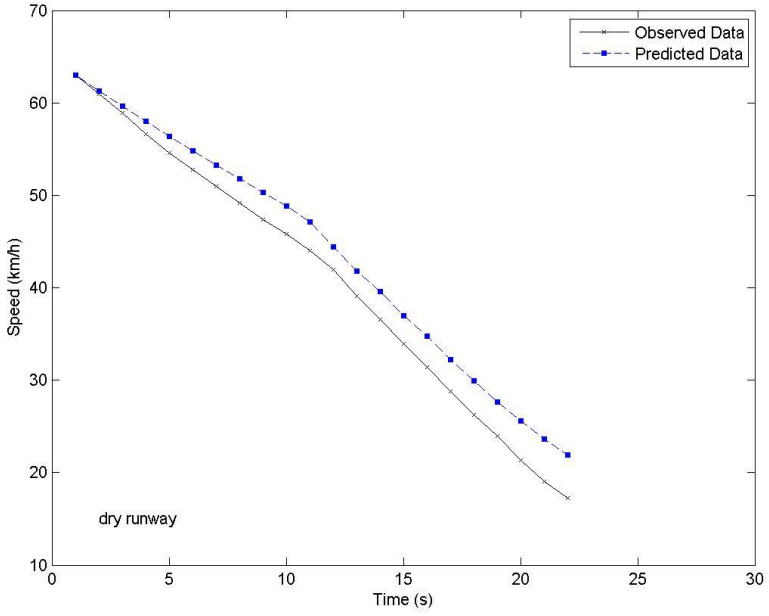

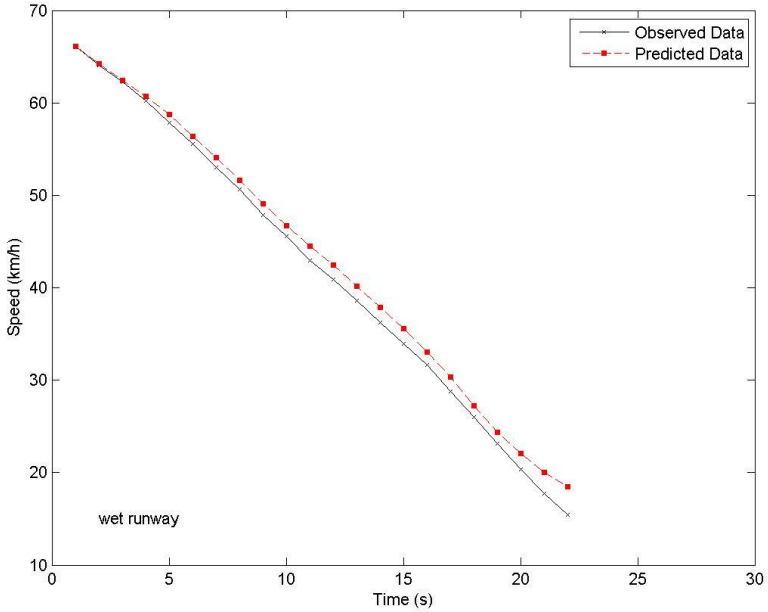
Observed Data
Predicted Data
Speed (km/h)
Time (s)
wet runway
70
60
50
40
30
20
10
0
5
10
15
20
25
30

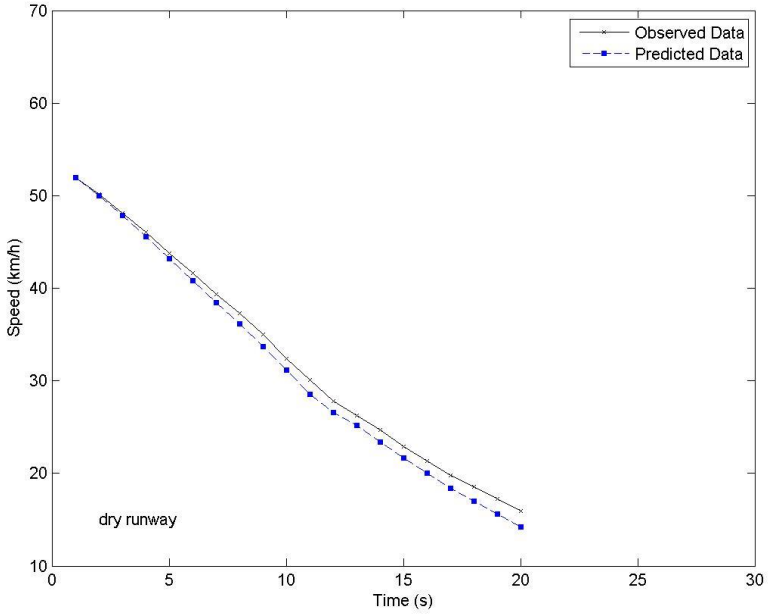
Observed Data
Predicted Data
Speed (km/h)
Time (s)
dry runway
70
60
50
40
30
20
10
0
5
10
15
20
25
30

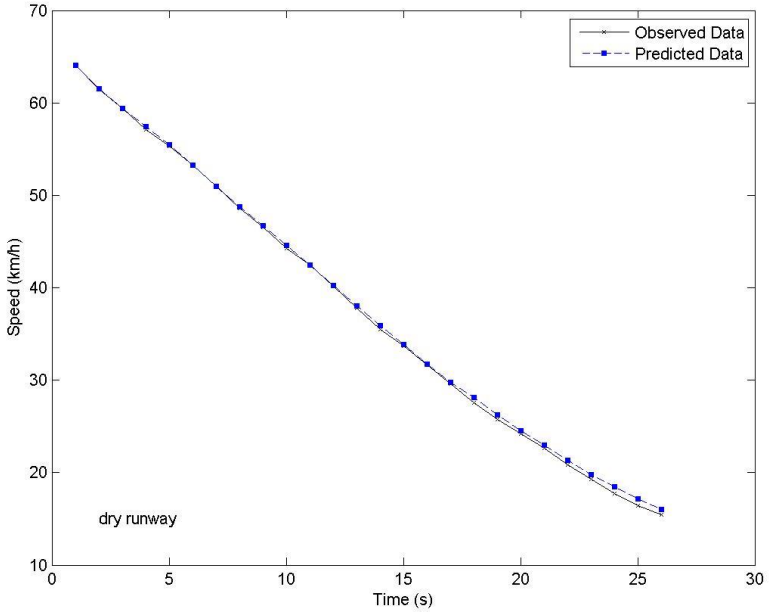
Observed Data
Predicted Data
Speed (km/h)
Time (s)
dry runway
70
60
50
40
30
20
10
0
5
10
15
20
25
30

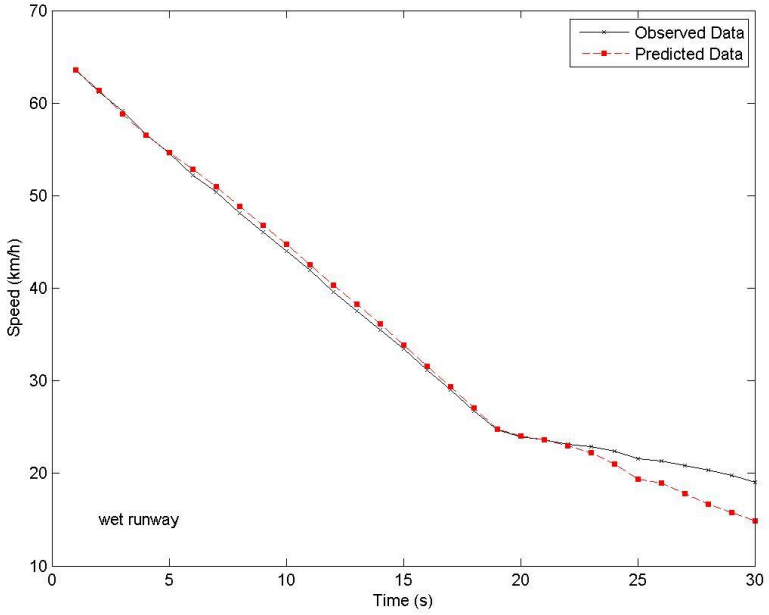
Observed Data
Predicted Data
Speed (km/h)
Time (s)
wet runway
70
60
50
40
30
20
10
0
5
10
15
20
25
30

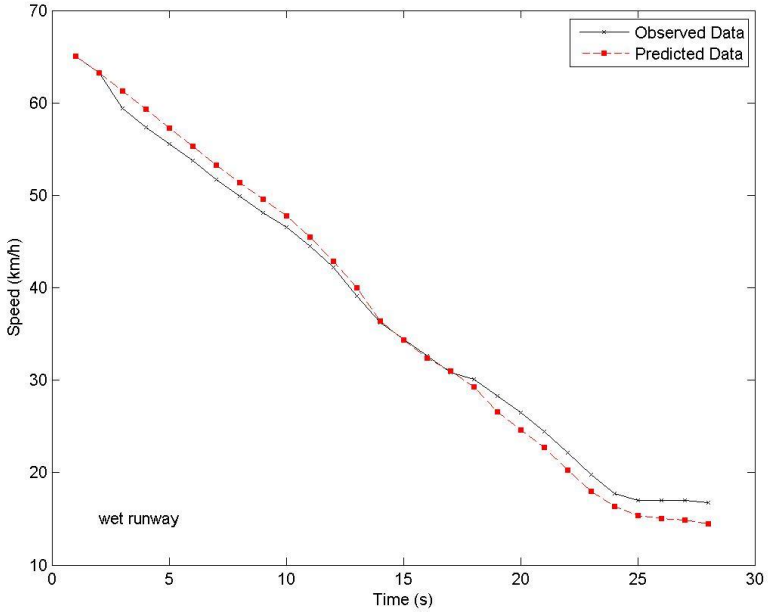
Observed Data
Predicted Data
Speed (km/h)
Time (s)
wet runway
70
60
50
40
30
20
10
0
5
10
15
20
25
30

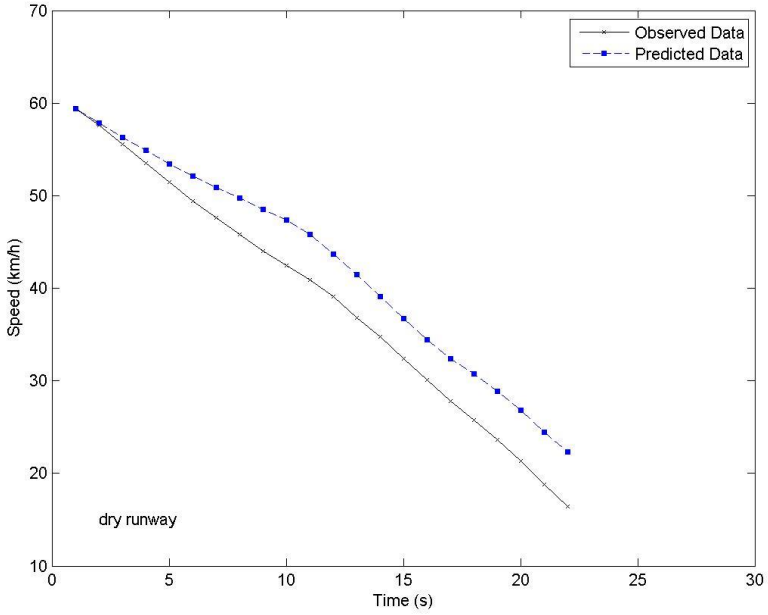
Observed Data
Predicted Data
Speed (km/h)
Time (s)
dry runway
70
60
50
40
30
20
10
0
5
10
15
20
25
30

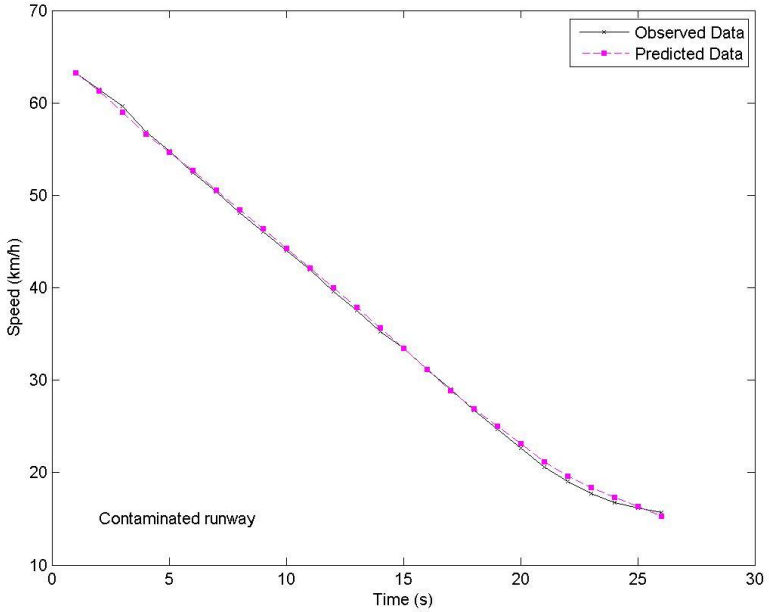
Observed Data
Predicted Data
Speed (km/h)
Time (s)
Contaminated runway
70
60
50
40
30
20
10
0
5
10
15
20
25
30

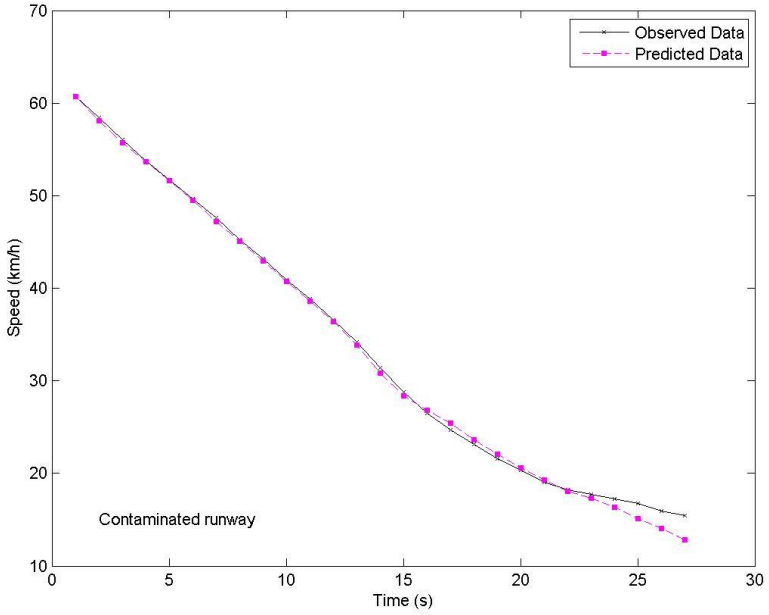
Observed Data
Predicted Data
Speed (km/h)
Time (s)
Contaminated runway
70
60
50
40
30
20
10
0
5
10
15
20
25
30

Appendix B

Dry Runway Braking Analysis

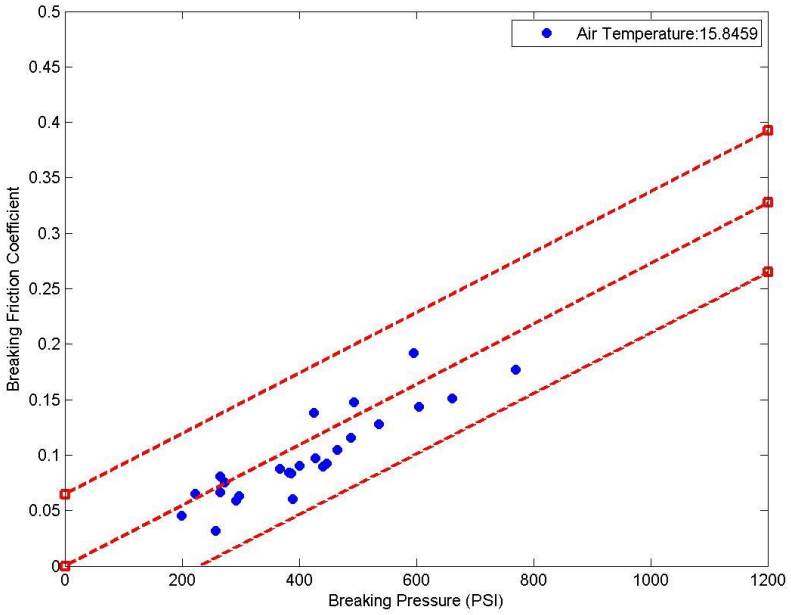

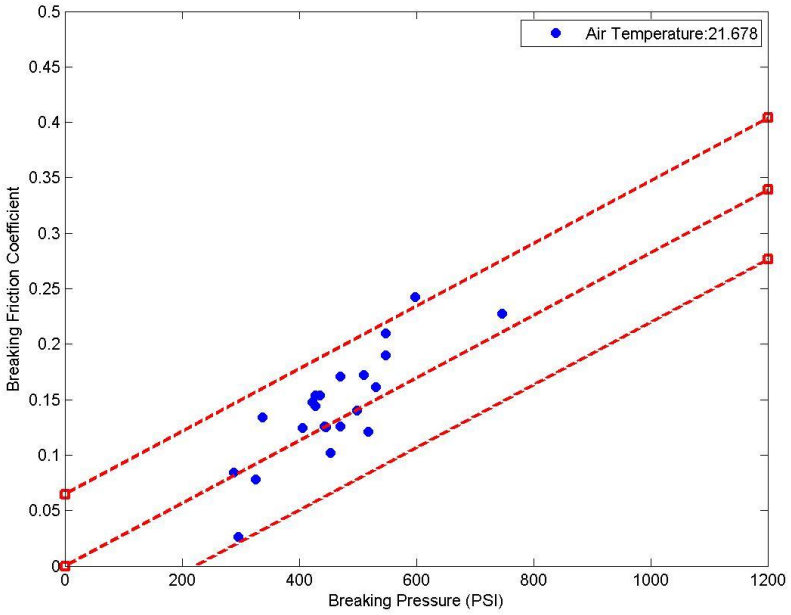

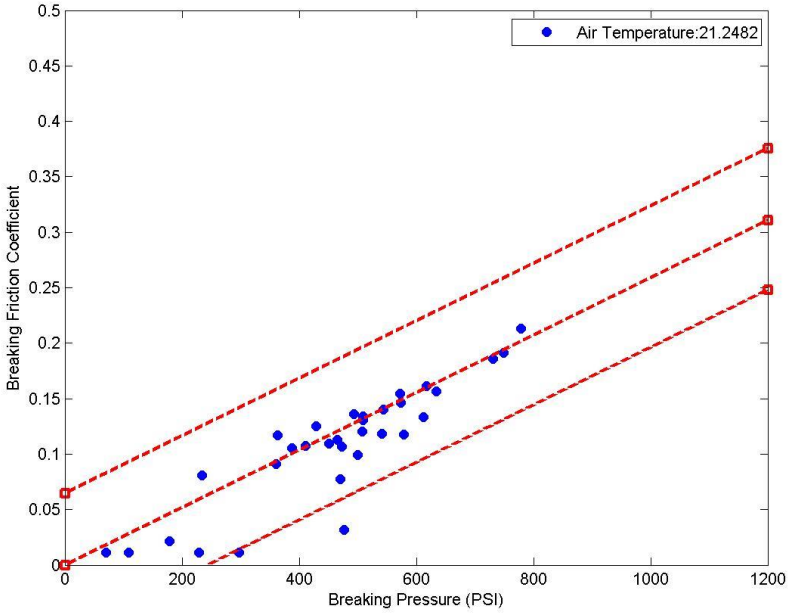
Air Temperature:21.2482
Breaking Friction Coefficient
Breaking Pressure (PSI)
0
0.05
0.1
0.15
0.2
0.25
0.3
0.35
0.4
0.45
0.5
0
200
400
600
800
1000
1200

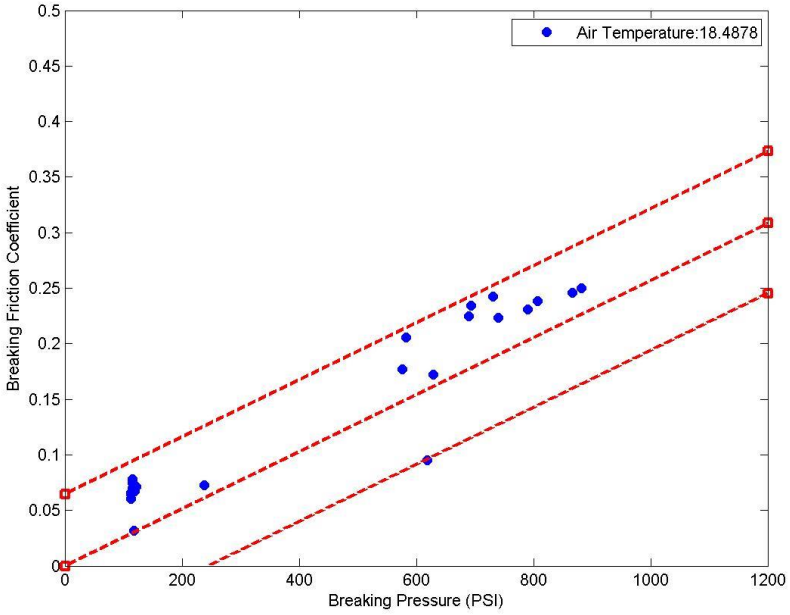
Air Temperature:18.4878
Breaking Friction Coefficient
Breaking Pressure (PSI)
0
0.05
0.1
0.15
0.2
0.25
0.3
0.35
0.4
0.45
0.5
0
200
400
600
800
1000
1200

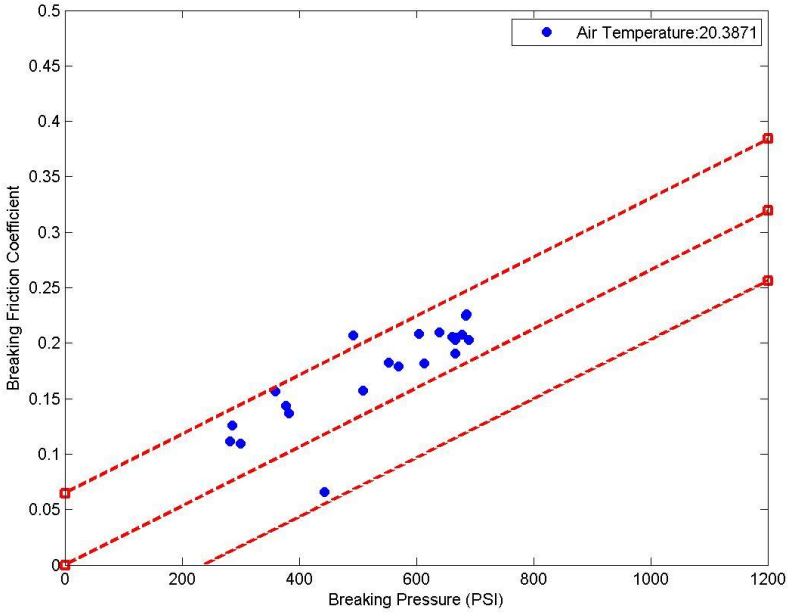
Air Temperature:20.3871
Breaking Friction Coefficient
Breaking Pressure (PSI)
0
0.05
0.1
0.15
0.2
0.25
0.3
0.35
0.4
0.45
0.5
0
200
400
600
800
1000
1200

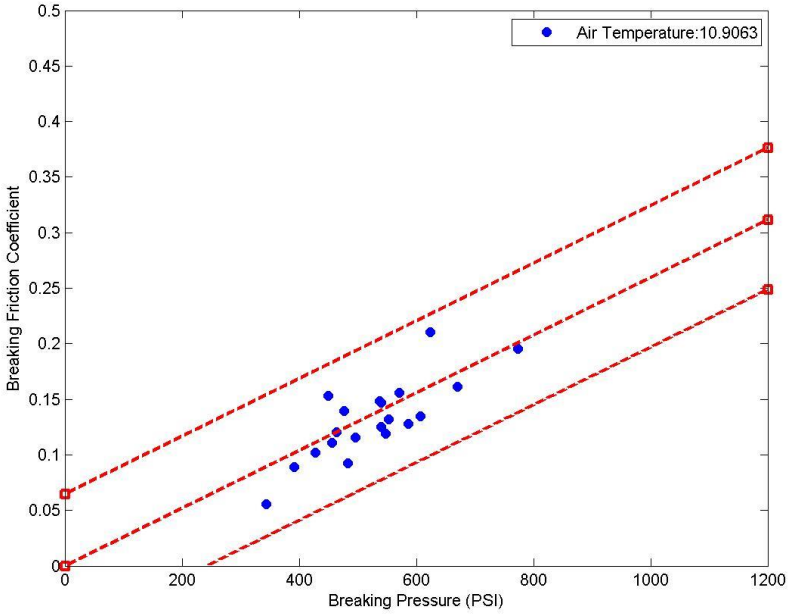
Air Temperature:10.9063
Breaking Friction Coefficient
Breaking Pressure (PSI)
0
0.05
0.1
0.15
0.2
0.25
0.3
0.35
0.4
0.45
0.5
0
200
400
600
800
1000
1200

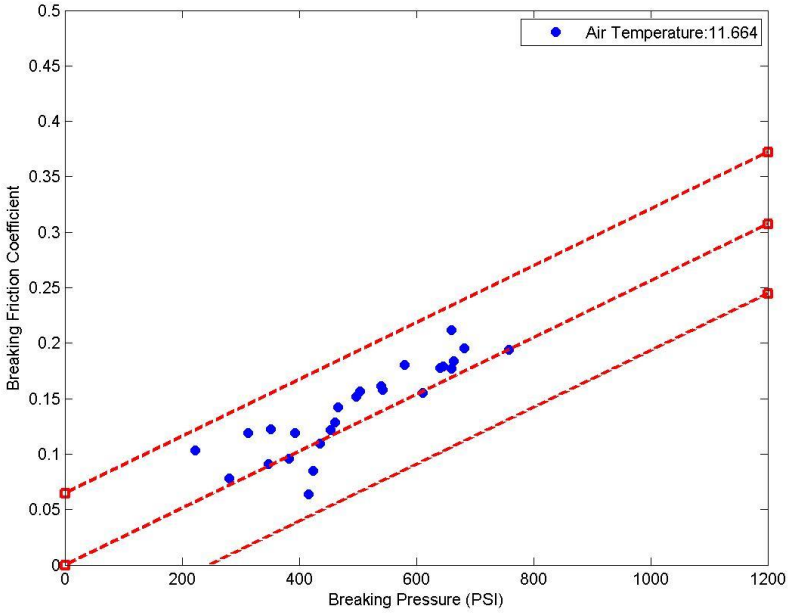
Air Temperature:11.664
Breaking Friction Coefficient
Breaking Pressure (PSI)
0
0.05
0.1
0.15
0.2
0.25
0.3
0.35
0.4
0.45
0.5
0
200
400
600
800
1000
1200

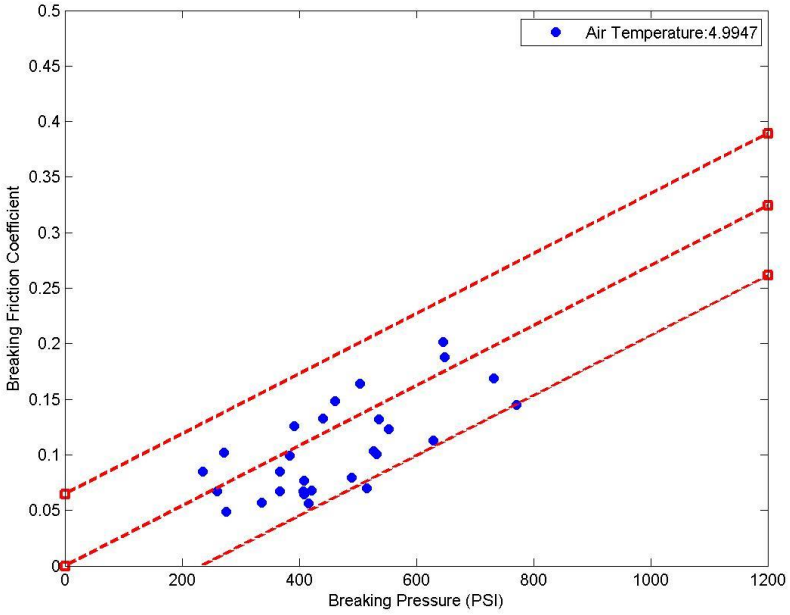
Air Temperature:4.9947
Breaking Friction Coefficient
Breaking Pressure (PSI)
0
0.05
0.1
0.15
0.2
0.25
0.3
0.35
0.4
0.45
0.5
0
200
400
600
800
1000
1200

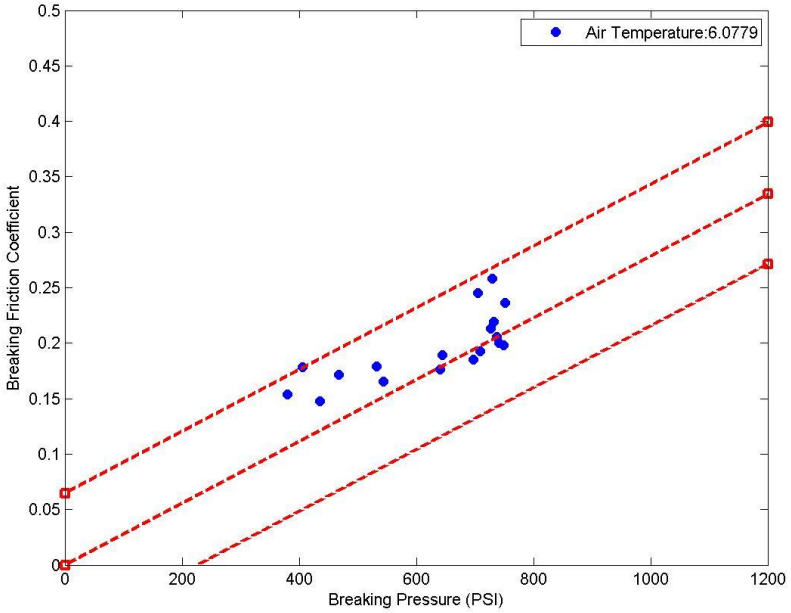
Air Temperature:6.0779
Breaking Friction Coefficient
Breaking Pressure (PSI)
0.5
0.45
0.4
0.35
0.3
0.25
0.2
0.15
0.1
0.05
0
0
200
400
600
800
1000
1200

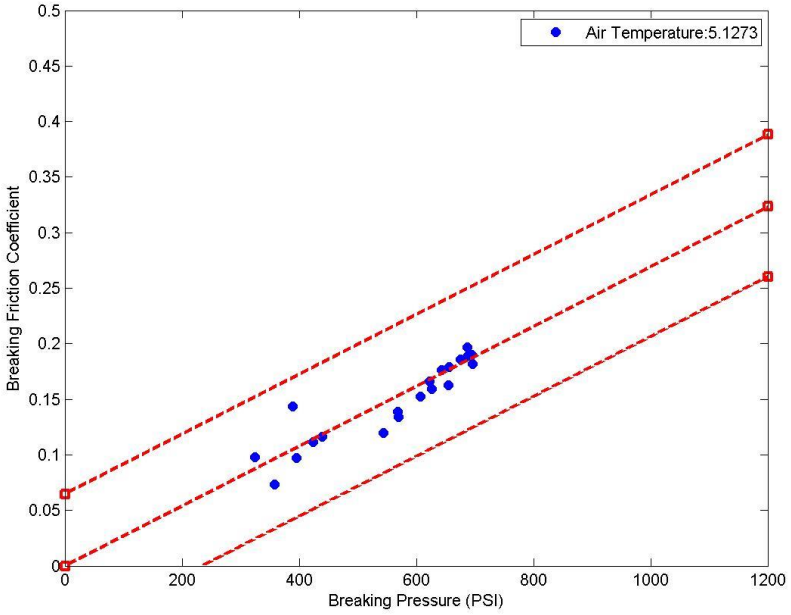
Air Temperature:5.1273
Breaking Friction Coefficient
Breaking Pressure (PSI)
0.5
0.45
0.4
0.35
0.3
0.25
0.2
0.15
0.1
0.05
0
0
200
400
600
800
1000
1200

Appendix C

Wet Runway Braking Analysis

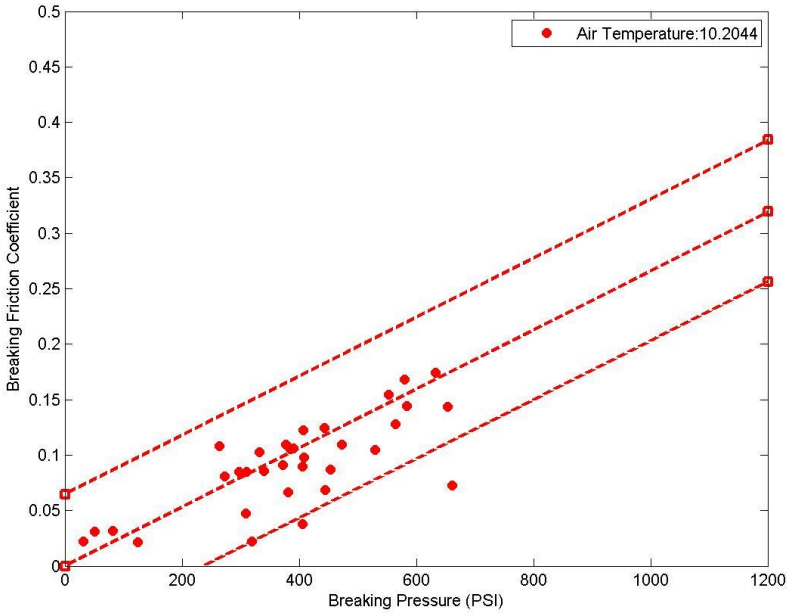

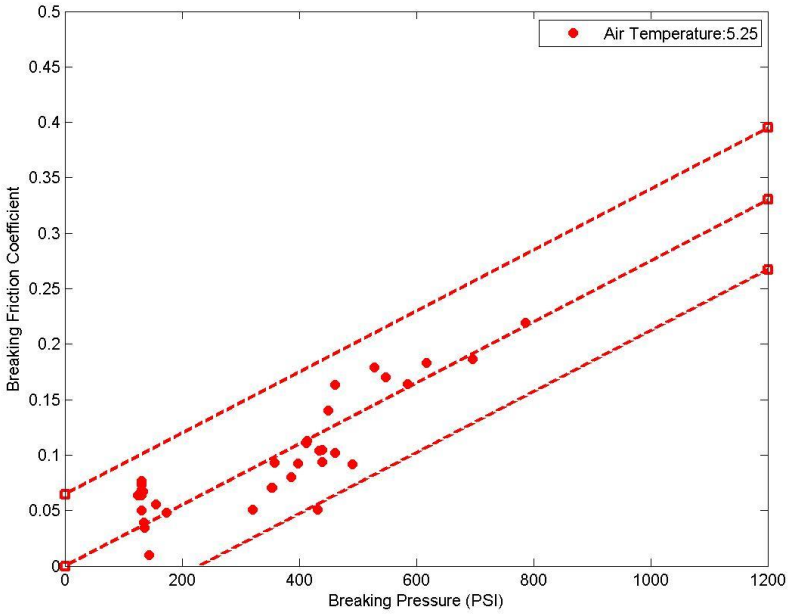

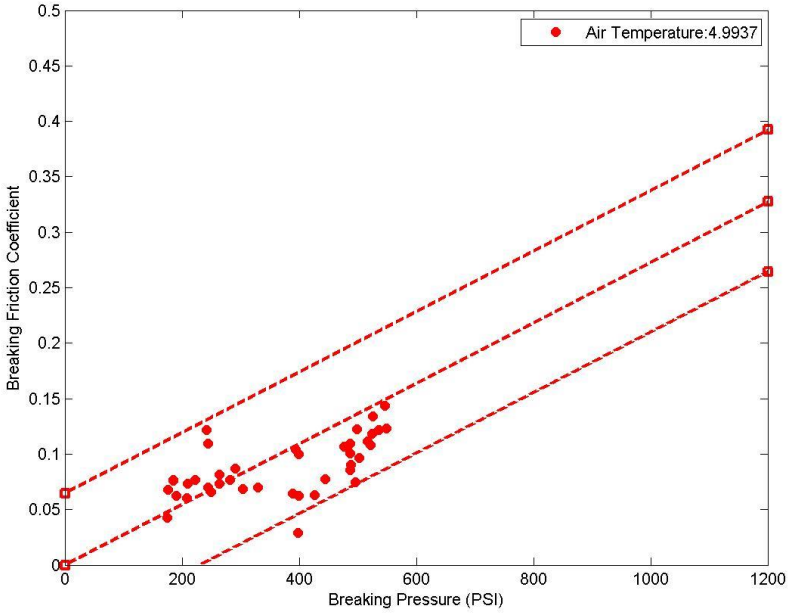
Air Temperature:4.9937
Breaking Friction Coefficient
Breaking Pressure (PSI)
0
0.05
0.1
0.15
0.2
0.25
0.3
0.35
0.4
0.45
0.5
0
200
400
600
800
1000
1200

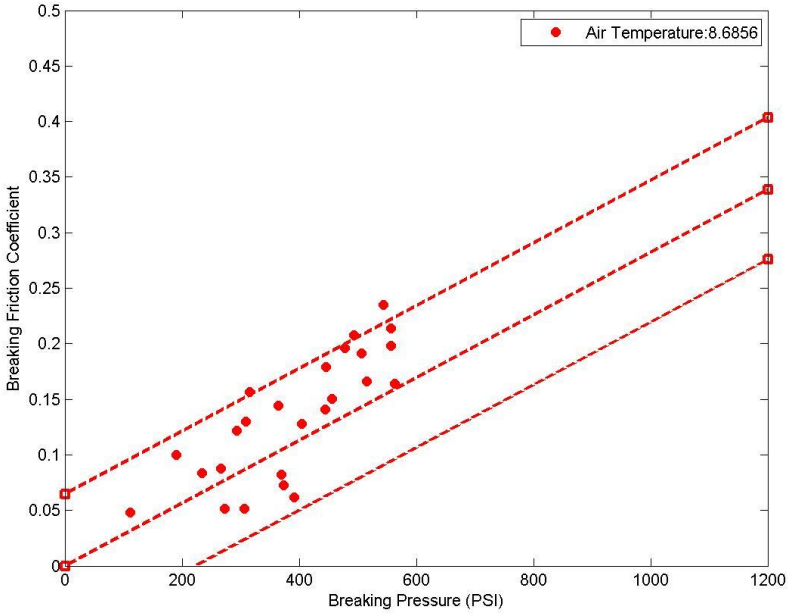
Air Temperature:8.6856
Breaking Friction Coefficient
Breaking Pressure (PSI)
0
0.05
0.1
0.15
0.2
0.25
0.3
0.35
0.4
0.45
0.5
0
200
400
600
800
1000
1200

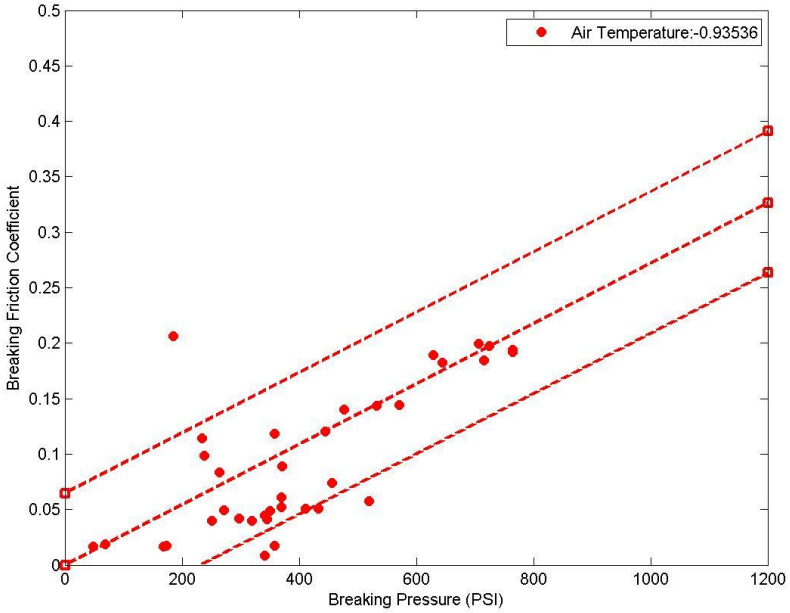
Air Temperature:-0.93536
Breaking Friction Coefficient
Breaking Pressure (PSI)
0
0.05
0.1
0.15
0.2
0.25
0.3
0.35
0.4
0.45
0.5
0
200
400
600
800
1000
1200

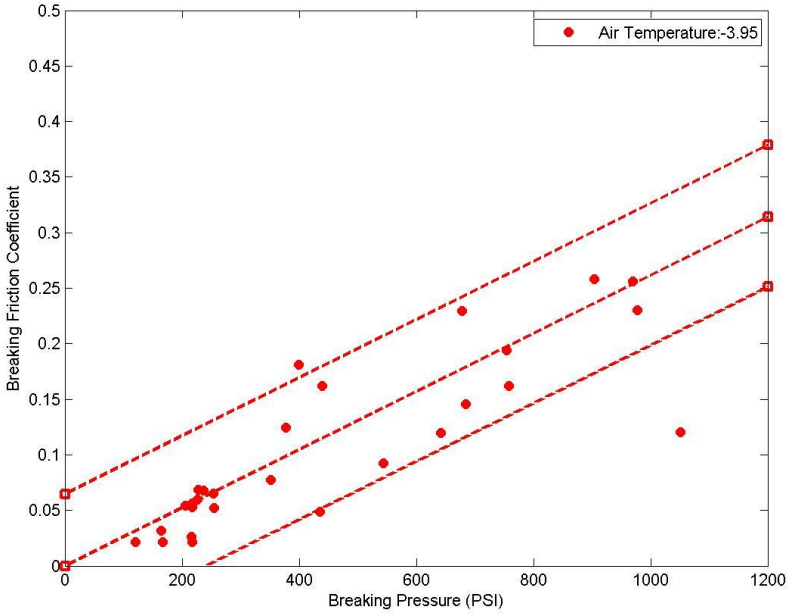
Air Temperature:-3.95
Breaking Friction Coefficient
Breaking Pressure (PSI)
0
0.05
0.1
0.15
0.2
0.25
0.3
0.35
0.4
0.45
0.5
0
200
400
600
800
1000
1200

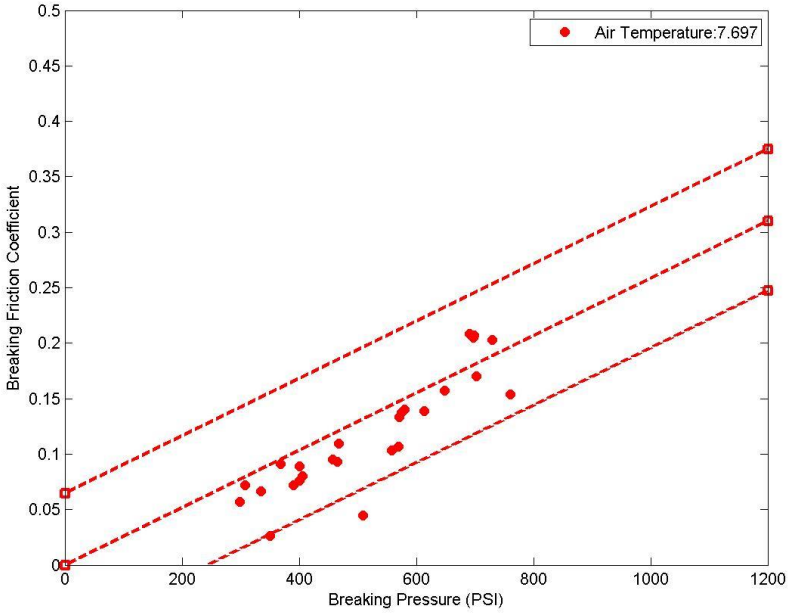
Air Temperature:7.697
Breaking Friction Coefficient
Breaking Pressure (PSI)
0
0.05
0.1
0.15
0.2
0.25
0.3
0.35
0.4
0.45
0.5
0
200
400
600
800
1000
1200

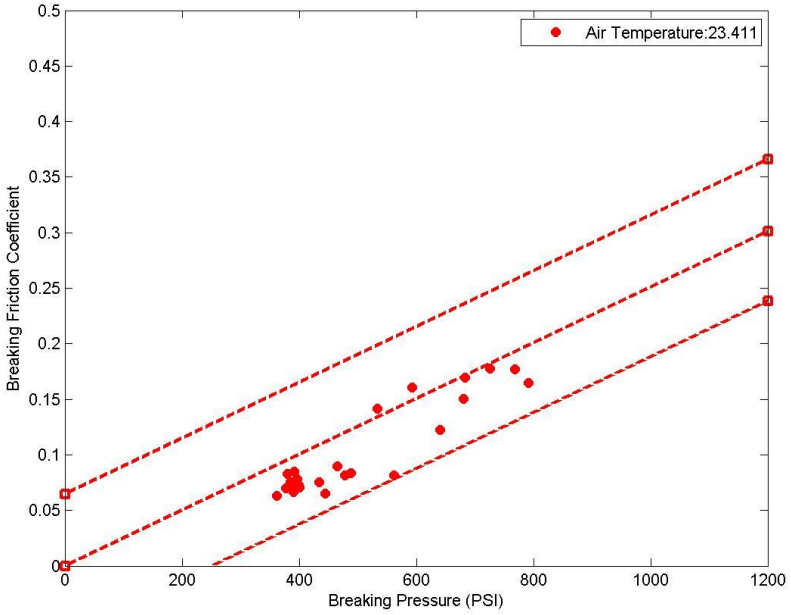
Air Temperature:23.411
Breaking Friction Coefficient
Breaking Pressure (PSI)
0
0.05
0.1
0.15
0.2
0.25
0.3
0.35
0.4
0.45
0.5
0
200
400
600
800
1000
1200

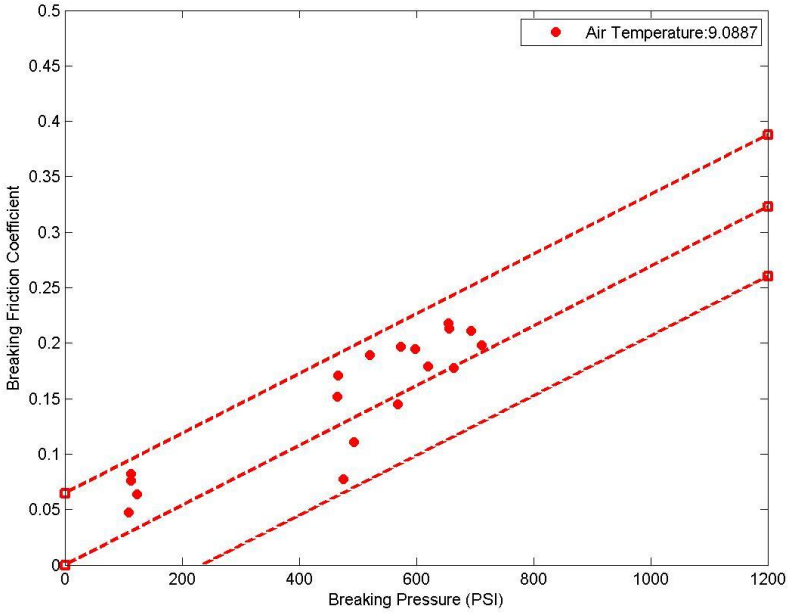
Air Temperature:9.0887
Breaking Friction Coefficient
Breaking Pressure (PSI)
0
0.05
0.1
0.15
0.2
0.25
0.3
0.35
0.4
0.45
0.5
0
200
400
600
800
1000
1200

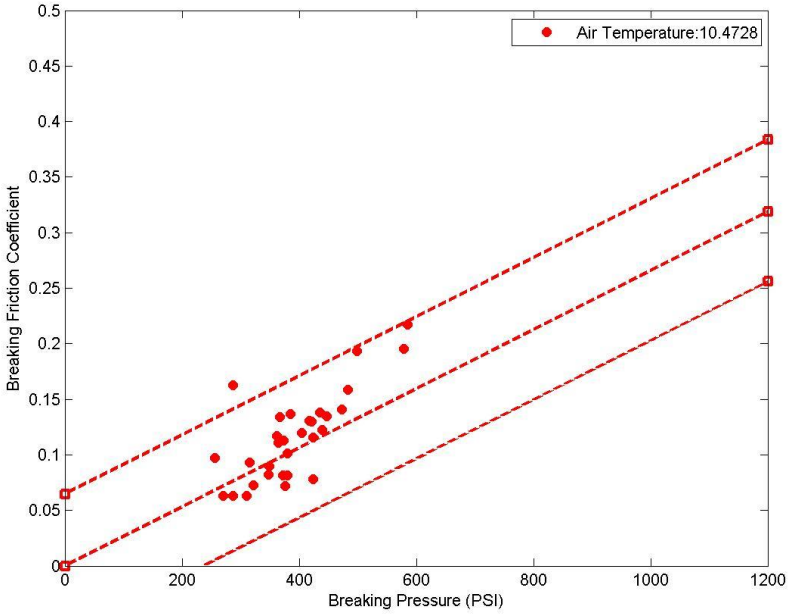
Air Temperature:10.4728
Breaking Friction Coefficient
Breaking Pressure (PSI)
0
0.05
0.1
0.15
0.2
0.25
0.3
0.35
0.4
0.45
0.5
0
200
400
600
800
1000
1200

Appendix D

Contaminated Runway Braking Analysis

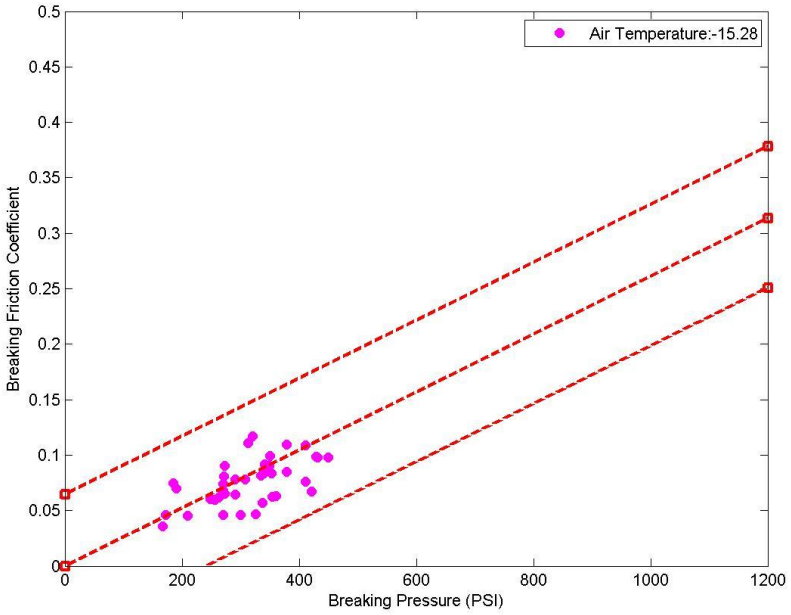

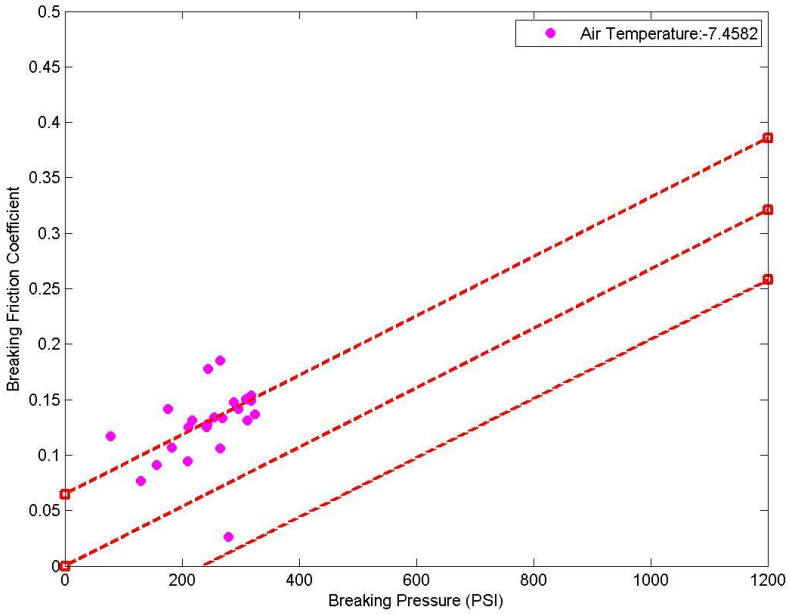

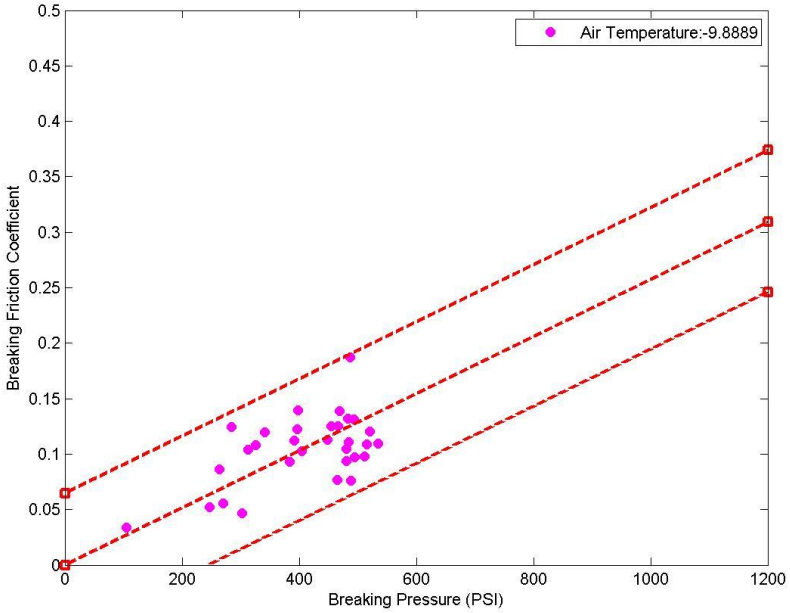
Air Temperature:-9.8889
Breaking Friction Coefficient
Breaking Pressure (PSI)
0
0.05
0.1
0.15
0.2
0.25
0.3
0.35
0.4
0.45
0.5
0
200
400
600
800
1000
1200

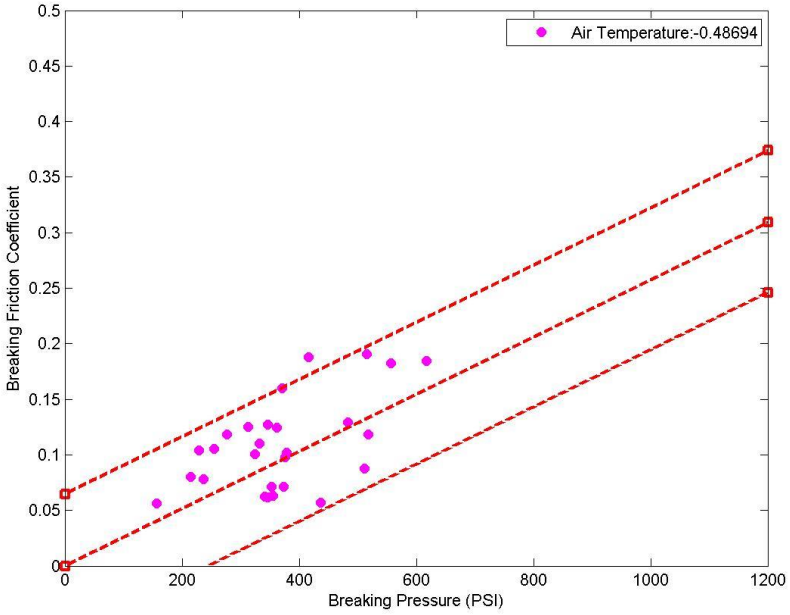
Air Temperature:-0.48694
Breaking Friction Coefficient
Breaking Pressure (PSI)
0
0.05
0.1
0.15
0.2
0.25
0.3
0.35
0.4
0.45
0.5
0
200
400
600
800
1000
1200

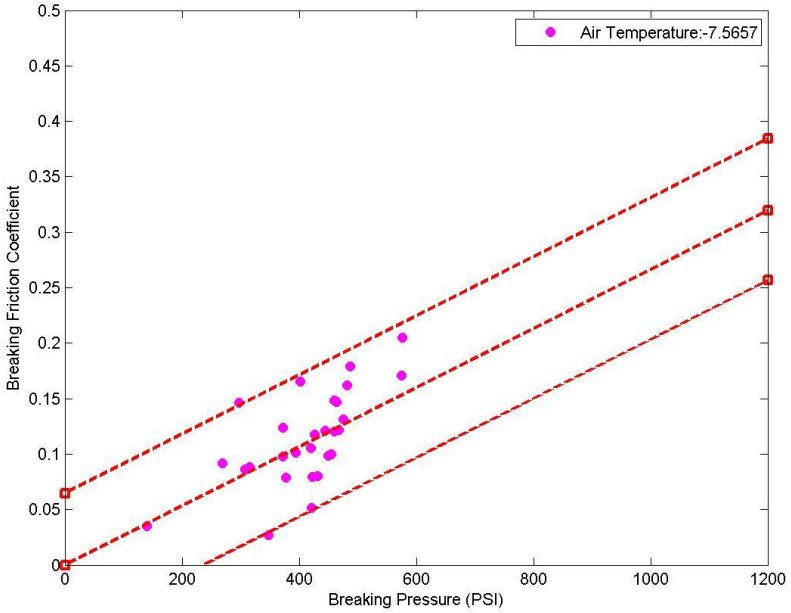
Air Temperature:-7.5657
Breaking Friction Coefficient
Breaking Pressure (PSI)
0
0.05
0.1
0.15
0.2
0.25
0.3
0.35
0.4
0.45
0.5
0
200
400
600
800
1000
1200

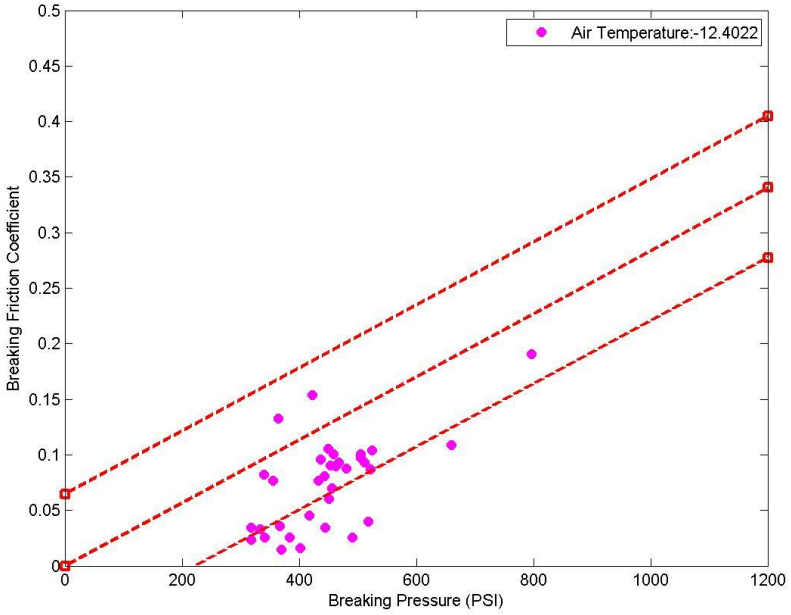
Air Temperature:-12.4022
Breaking Friction Coefficient
Breaking Pressure (PSI)
0
0.05
0.1
0.15
0.2
0.25
0.3
0.35
0.4
0.45
0.5
0
200
400
600
800
1000
1200

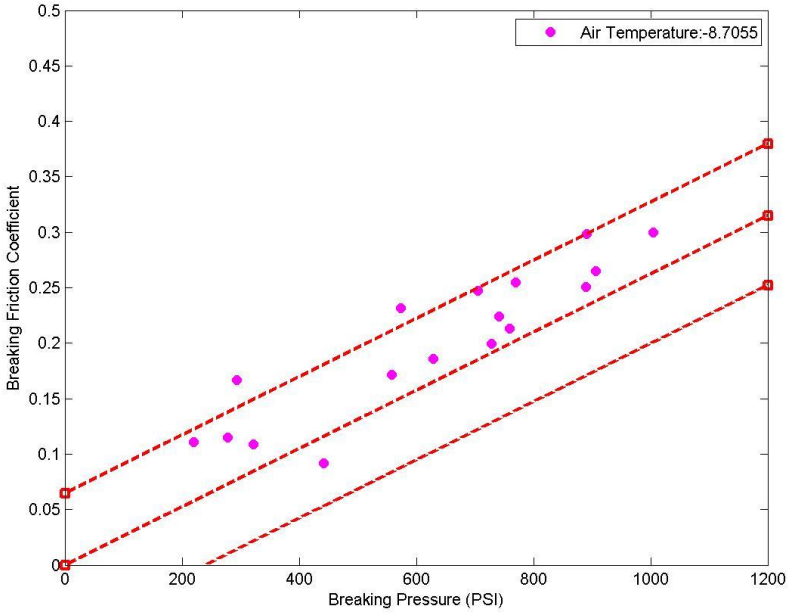
Air Temperature:-8.7055
Breaking Friction Coefficient
Breaking Pressure (PSI)
0
0.05
0.1
0.15
0.2
0.25
0.3
0.35
0.4
0.45
0.5
0
200
400
600
800
1000
1200

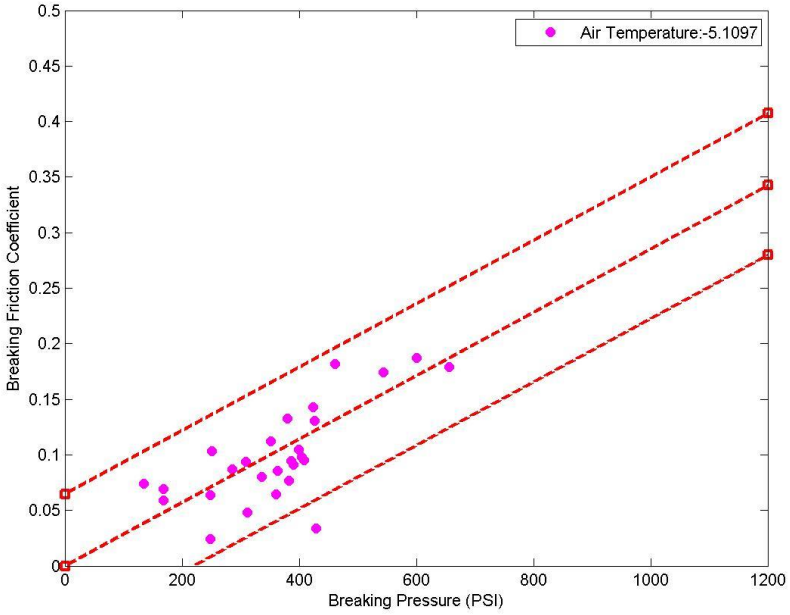
Air Temperature:-5.1097
Breaking Friction Coefficient
Breaking Pressure (PSI)
0
0.05
0.1
0.15
0.2
0.25
0.3
0.35
0.4
0.45
0.5
0
200
400
600
800
1000
1200

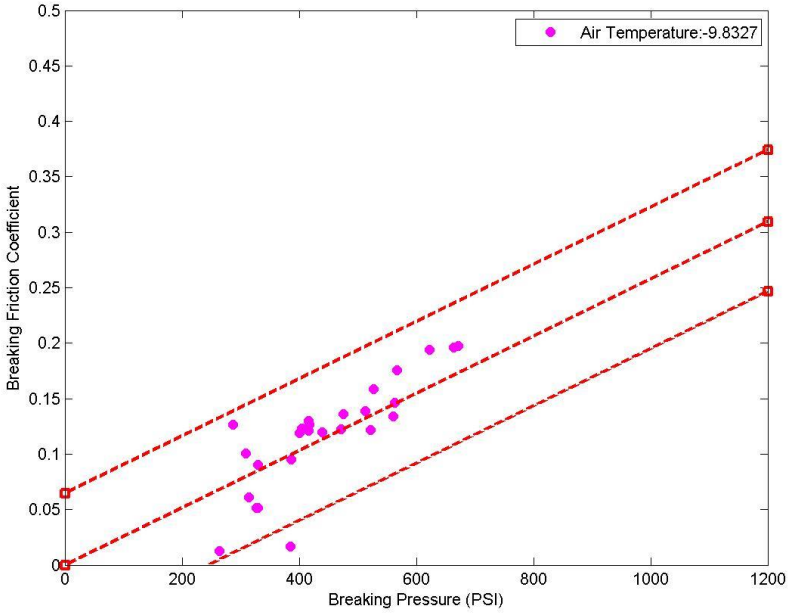
Air Temperature:-9.8327
Breaking Friction Coefficient
Breaking Pressure (PSI)
0
0.05
0.1
0.15
0.2
0.25
0.3
0.35
0.4
0.45
0.5
0
200
400
600
800
1000
1200

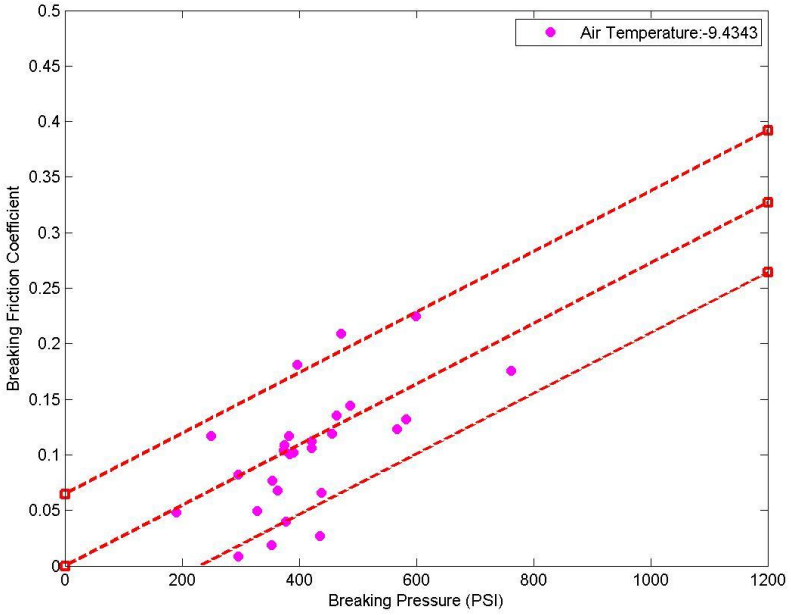
Air Temperature:-9.4343
Breaking Friction Coefficient
Breaking Pressure (PSI)
0
0.05
0.1
0.15
0.2
0.25
0.3
0.35
0.4
0.45
0.5
0
200
400
600
800
1000
1200